

Autofluorescence of Intact Food
- An Exploratory Multi-way Study

PhD thesis by
Jakob Christensen

Autofluorescence of Intact Food - An Exploratory Multi-way Study

PhD thesis by
Jakob Christensen, 2005

Supervisors:
Associate Professor Lars Nørgaard
and Professor Søren Balling Engelsen
Quality and Technology, Department of Food Science
The Royal Veterinary and Agricultural University, Denmark

Cover illustration by Mie Damgaard
Title: Autofluorescence of Intact Food – An Exploratory Multi-way Study
2005 © Jakob Christensen
ISBN: 87-7611-088-5
Printed by Samfundslitteratur Grafik, Frederiksberg C, Denmark

Preface

This PhD thesis is written to fulfil the requirements for obtaining a PhD degree at the Royal Veterinary and Agricultural University (KVL). The presented work has been carried out at the Food Technology Group at KVL under the supervision of Associate Professor Lars Nørgaard and Professor Søren Balling Engelsen.

I am grateful to my supervisors for their inspiring guidance and for giving me the opportunity to complete this PhD by the back door. I am indebted to Lars Nørgaard for introducing me to the world of spectroscopy and chemometrics. With his open mind, analytical skills and everlasting positivity he has been a great mentor to me. Also my colleagues at the Food Technology Group have been of great inspiration by creating a unique working atmosphere. Especially, I wish to thank Elisabeth, Åsmund, Vibeke, Erik, Christian, Frans, Lisbeth, Jesper, Henrik, Dorthe, Rasmus and Lars Munck for all the joyful moments and experiences during my stay in the group.

The presented publications involved several co-authors, to whom I am grateful for their contribution and cooperation. Carsten Lindemann and the people at Delta are acknowledged for the close cooperation in the OPUS project. Lisbeth Hansen is acknowledged for her unremitting efforts in the lab, performing the fluorescence measurements presented in the thesis. The work to complete this PhD study has been performed parallel to several project employments at KVL. Fundings by the European Commission and the Ministry of Food, Agriculture and Fisheries are acknowledged.

Jakob Christensen
Frederiksberg, March 2005

Summary

Fluorescence measurements of a broad variety of food samples make up the experimental benchmark of this thesis. The presented experimental food fluorescence gives an overview of the intrinsic fluorescence of intact food systems and highlights the most common fluorescence characteristics of food products.

Apart from the experimental overview of food fluorescence, the thesis consists of a literature survey on autofluorescence of intact food and five papers. The papers represent examples of applications of the described techniques to intact food systems in the form of beer (Paper I), yogurt (Paper II and Paper IV), various dry food products (Paper III) and cheese (Paper V).

The possibility to perform rapid non-destructive fluorescence analyses in combination with the high sensitivity and specificity makes fluorescence spectroscopy a potential screening method of food products, both in food production and in regulatory affairs. Autofluorescence can in some cases compete with time-consuming analyses of trace elements based on high resolution chromatography or tedious extraction steps, as exemplified in Paper I and Paper IV. New methods based on autofluorescence are suggested for determination of bitterness in beer (Paper I) as well as riboflavin in yogurt (Paper IV).

It is shown that the two-dimensional nature (excitation + emission) of fluorescence spectroscopy can improve the selectivity of the method. With the application of multi-way chemometrics this inherent data structure of the technique can be utilized in the development of fluorescence sensors and analyses. In Paper II and Paper IV multi-way analysis of fluorescence measurements of dairy products revealed detailed information about the oxidation throughout storage. Assignment of the inherent fluorophores and the understanding of the chemical/physical system were facilitated by the multi-way data approach.

Resumé

Fluorescensmålinger af en lang række fødevarer udgør omdrejningspunktet for denne afhandling. De præsenterede målinger af fødevarefluorescens giver et overblik over naturligt forekommende fluorescence og dens karakteristika i intakte fødevarer. Afhandlingen består desuden af en litteraturgennemgang af artikler om autofluorescens af intakte fødevarer samt 5 forskningspublikationer, der repræsenterer eksempler på anvendelse af de beskrevne analysemetoder på intakte fødevaresystemer i form af øl (Paper I), yoghurt (Paper II og IV), diverse tørrede produkter (Paper III) og ost (Paper V).

Muligheden for at udføre hurtige ikke-destruktive analyser kombineret med den høje følsomhed og specificitet, gør fluorescensspektroskopi til en potentiel screeningsmetode af fødevarer, både i forbindelse med produktion og kontrol. Autofluorescens kan i visse sammenhænge erstatte langsommelige analyser af sporstoffer baseret på kromatografi eller besværlige ekstraktionstrin. Eksempler på dette er givet i Paper I og Paper IV, hvor nye analysemetoder baseret på autofluorescens bliver foreslået til bestemmelse af indholdet af bitterstof i øl (Paper I) og riboflavin i yoghurt (Paper IV).

Den todimensionelle data struktur af fluorescensspektroskopi (excitation + emission) giver muligheden for en høj selektivitet for analysemetoden. Ved hjælp af multivejs kemometri kan denne data struktur udnyttes i udviklingen af fluorescens sensorer og – analyser. I Paper II og Paper V giver fluorescensmålinger på mejeriprodukter detaljeret information om de oxidative processer under lagring. Anvendelsen af multivejs data analyse letter identifikationen af de forekommende fluorescerende forbindelser og forståelsen af det kemisk-fysiske system.

List of Publications

Paper I

Jakob Christensen, Anne Marie Ladefoged and Lars Nørgaard: Determination of bitterness in beer using fluorescence spectroscopy and chemometrics. *Journal of the Institute of Brewing* 111 (1), 2005, in press.

Paper II

Jakob Christensen, Eleonora Miquel Becker and Charlotte S. Frederiksen: Fluorescence spectroscopy and PARAFAC in the analysis of yogurt. *Chemometrics and Intelligent Laboratory* 75 (2), 201-208, 2005.

Paper III

Pernille N. Jensen, Jakob Christensen and Søren B. Engelsen: Oxidative changes in pork scratchings, peanuts, oatmeal and muesli viewed by fluorescence, near-infrared and infrared spectroscopy. *European Food Research and Technology* 219 (3), 294-304, 2004

Paper IV

Eleonora Miquel Becker, Jakob Christensen, Charlotte S. Frederiksen and Vibeke K. Haugaard: Front-Face Fluorescence Spectroscopy and Chemometrics for Analysis of Yogurt –Rapid Analysis of Riboflavin. *Journal of Dairy Science* 86 (8), 2508-2515, 2003.

Paper V

Jakob Christensen, Vibeke T. Povlsen and John Sørensen: Application of Fluorescence Spectroscopy and Chemometrics in the Evaluation of Processed Cheese During Storage. *Journal of Dairy Science* 86 (4), 1101-1107, 2003.

Additional Publications

Erik Tønning, Svetlana Sapelnikova, Jakob Christensen, Charlotte Carlsson, Margrethe Winther-Nielsen, Eva Dock, Renata Solna, Petr Skladal, Lars Nørgaard, Tautgirdas Ruzgas and Jenny Emneus: Chemometric exploration of an amperometric biosensor array for fast determination of wastewater quality. *Biosensors and Bioelectronics*, 2005, in press.

Sandra Casani, Tina Hansen, Jakob Christensen and Susanne Knöchel: Comparison of methods for assessing reverse osmosis membrane treatment of shrimp process water. *Journal of Food Protection*, 2005, in press.

Eva Dock, Jakob Christensen, Mattias Olsson, Erik Tønning, Tautgirdas Ruzgas and Jenny Emnéus: Multivariate data analysis of dynamic amperometric biosensor responses from binary analyte mixtures - application of sensitivity correction algorithms. *Talanta* 65 (2), 298-305, 2005.

Catalin Nistor, Jakob Christensen, Natalia Ocio, Lars Nørgaard and Jenny Emnéus: Multivariate analysis to resolve the signal given by cross-reactants in immunoassay with sample matrix dilution. *Analytical and Bioanalytical Chemistry* 380 (7-8), 898-907, 2004.

Jakob Christensen, Lars Nørgaard, Joan Grønkjær Pedersen, Hanne Heimdal and Søren Balling Engelsen: Rapid Spectroscopic Analysis of Marzipan - Comparative instrumentation. *Journal of Near Infrared Spectroscopy* 12 (1), 63-75, 2004.

Jens K.S. Møller, Giovanni Parolari, Laura Gabba, Jakob Christensen and Leif H. Skibsted: Monitoring Chemical Changes of Dry-Cured Parma Ham during Processing by Surface Autofluorescence Spectroscopy. *Journal of Agricultural and Food Chemistry* 51 (5), 1224-1230, 2003.

Romas Baronas, Jakob Christensen, Feliksas Ivanauskas and Jouzas Kulys: Computer Simulation of Amperometric Biosensor Response to Mixtures of Compounds. *Nonlinear Analysis: Modelling and Control* 7 (2), 3-14, 2002.

-

Jakob Christensen, Lars Nørgaard, Anne Marie Ladefoged and Lars Munck: Improved method and apparatus for measuring bitterness in beer and brewing samples. *Patent application*, priority date November 5, 2003.

Table of Contents

Preface	
Summary	
Resumé	
List of publications	
Additional Publications	
0. Introduction.....	11
Content outline	12
1. Fluorescence Spectroscopy	15
Basic Principles	15
<i>Molecular luminescence spectroscopy</i>	15
<i>Fluorescence spectroscopy</i>	16
<i>Stoke's shift</i>	17
<i>Fluorescence measurements</i>	18
<i>Instrumentation</i>	19
<i>Fluorophores</i>	20
Factors affecting fluorescence intensity.....	21
<i>Quenching</i>	22
<i>Concentration and inner filter effect</i>	22
<i>Solvent effect</i>	25
<i>Macromolecules</i>	26
<i>pH</i>	27
<i>Scatter</i>	28
2. Chemometrics	31
Introduction.....	31
<i>What's chemometrics?</i>	31
<i>Multivariate Data Analysis</i>	32
Bilinear models	32
<i>PCA</i>	32
<i>PLS</i>	33
<i>Applications of PCA and PLS to fluorescence spectroscopy</i>	34
Multi-way analysis	36
<i>PARAFAC</i>	36
<i>PARAFAC and Fluorescence spectroscopy</i>	38

<i>Applications of PARAFAC to fluorescence spectroscopy</i>	40
3. Literature Food Fluorescence	43
Meat	43
<i>Multi-way studies</i>	46
Fish.....	46
Dairy products	47
<i>Normalized tryptophan emission spectra</i>	47
<i>Vitamin A</i>	47
<i>Heat treatment of milk</i>	48
<i>Riboflavin</i>	48
<i>Multi-way studies</i>	49
Edible Oils.....	49
<i>Multi-way studies</i>	50
Cereals	51
<i>Flour</i>	51
Beer	52
Fruit	52
Sugar.....	53
<i>Multi-way studies</i>	54
Biotechnology	54
<i>Multi-way studies</i>	55
4. Experimental Food Fluorescence	57
Food fluorophores	57
Fluorescence of intact food samples.....	59
<i>Fluorescence landscapes of food products</i>	60
Global PARAFAC of all food products	63
<i>PARAFAC loadings</i>	63
<i>PARAFAC scores and loadings</i>	66
<i>Overview of PARAFAC result</i>	69
Notes on the presented models	71
5. Conclusions and Perspectives	73
Challenges.....	73
Technical trends and options	74
Prospective applications	75
References	78
Appendix A: List of Fluorophores	97
Appendix B: Fluorescence landscapes of food products	101

Paper I-V

0. Introduction

Public interest in food quality and production has increased in recent decades, probably related to changes in eating habits, consumer behaviour, and the development and increased industrialisation of the food supplying chains. The growing demand for high quality and safety in food production obviously calls for high standards for quality and process control, which in turn require appropriate analytical tools for investigation of food. In this context, fluorescence spectroscopy is an interesting analytical method to explore and it forms the basis of the present work. Several fluorescent substances are indigenous in food systems in the form of proteins, vitamins, secondary metabolites and various sorts of flavouring compounds and pigments.

Fluorescence spectroscopy is an analytical technique widely used in biological sciences and known for its high sensitivity and specificity. The main research and applications in the field are normally carried out using a univariate approach, with development of fluorescence probes, sensors and analyses specifically developed for certain problems based on one single or a few selected wavelengths. Typically, such analyses imply extraction or other sample pretreatment steps prior to the fluorescent measurement. In contrast, the approach used throughout this thesis is to measure the intrinsic fluorescence – also known as autofluorescence - of intact food samples. In the last few years, many examples of autofluorescence of biological samples have been reported. By measuring directly on the intact sample, the speed of analysis can be considerably increased and more or less non-destructive analyses can be performed. In this way the method holds the potential to be utilized as a screening method and to be applied for on-line purposes. Furthermore, the direct way of analysis increases the explorative dimension of the investigation, as no sample pretreatment restricts the fluorescence analysis and the effects of the sample matrix can also be assessed.

Food makes up a complex chemical and physical system, which in most cases includes several phenomena which interfere with fluorescence. In order to deal with the complex chemical/physical system in the intact food matrix, a multivariate fluorescence signal is obtained and chemometrics in the form of multivariate data analysis is applied for unentangling of the obtained multifaceted spectroscopic signals. Fluorescence spectroscopy involves two descriptive wavelength parameters – excitation and emission - in contrast to most other spectroscopic techniques, e.g. vibrational spectroscopy. By recording and utilising the two-way nature of fluorescence in the data analysis, the selectivity of the technique can be further improved.

The title of the thesis refers to the experimental benchmark of this study. Fluorescence measurements of a broad variety of food samples will be presented in order to form a general view of autofluorescence of intact food. The presented experimental food fluorescence forms a starting point from which to put the applications of autofluorescence to intact food found in literature and the presented papers into context. Three-way chemometrics in the form of Parallel Factor Analysis (PARAFAC) was applied in the evaluation of the obtained fluorescence data, rendering this work a multi-way study.

Content outline

The thesis consists of five main chapters and two appendices followed by five papers, which were published in peer-reviewed scientific journals in the period 2003-2005.

First, the employed analytical techniques, *Fluorescence Spectroscopy* and *Chemometrics*, will be introduced in Chapters 1 and 2. The basic principles of fluorescence spectroscopy are described in the first chapter, followed by an introduction to chemometrics with focus on the application of multivariate and multi-way data analysis in the evaluation of fluorescence data.

Chapter 3 (*Literature Food Fluorescence*) contains a comprehensive review of studies on autofluorescence of intact food found in literature. Fluorescence measurements of various food samples are presented in Chapter 4 (*Experimental Food Fluorescence*) in order to exemplify some of the fluorescence phenomena mentioned in the theoretical introduction in Chapter 1 and to present the common structures of fluorescence from food

products. The fluorescence landscapes will be analysed with PARAFAC for a further investigation of the common structures and as an example of the data analytical tools described in Chapter 2. The results from this exploratory multi-way study of autofluorescence from intact food will be compared to the presented papers and the findings in literature, as summarized in Chapter 3. The documentation on the presented experiments can be found in the two appendices. Some concluding remarks on the presented study will be given in Chapter 5 (*Conclusions and Perspectives*), including a discussion of challenges and suggestions for future applications and perspectives for fluorescence spectroscopy in analysis of food.

Five papers are included in the thesis. They represent examples of applications of the described techniques to intact food systems in the form of beer (Paper I), yogurt (Paper II and Paper IV), various dry food products (Paper III) and cheese (Paper V).

1. Fluorescence Spectroscopy

Basic Principles

Fluorescence spectroscopy is an analytical tool with high sensitivity and specificity. Fluorescence spectroscopy holds the potential as a non-destructive technique to provide information about fluorescent molecules and their environment in a wide variety of biological samples, and it is reported 100-1000 times more sensitive¹²³ than other spectrophotometric techniques.

In this chapter a short introduction to fluorescence spectroscopy will be given based on the textbooks of Lakowicz⁸⁰, Sharma and Schulman¹¹³ and Schulman¹¹⁰, in which more detailed descriptions of the principles and aspects of fluorescence spectroscopy can be found. The focus here will be on the basic principles and its application to food systems. All figures in this chapter describing fluorescence measurements are based on own data from measurements performed in the laboratory of Food Technology, using a Perkin Elmer LS50B or a Cary Varian Eclipse spectrofluorometer.

Molecular luminescence spectroscopy

Molecular luminescence spectroscopy is the overall term to describe emission of light from molecules in electronically excited states. The emission can arise from excitation by way of absorption of light (photoluminescence) or by way of a chemical reaction (chemiluminescence). Photoluminescence can further be divided into fluorescence and phosphorescence. Fluorescence arises from electrons in excited singlet state, and emission appears $10^{-11} - 10^{-7}$ seconds after excitation¹¹⁰. Phosphorescence is emission of light from electrons in triplet excited states, and will not be further discussed in this thesis. The emission rate is much slower than fluorescence, and phosphorescence lifetime is typically milliseconds to seconds⁸⁰.

Fluorescence spectroscopy

Fluorescence is the emission of light, *luminescence*, subsequent to absorption of ultraviolet (UV) or visible light of a fluorescent molecule or substructure, called a *fluorophore*. Thus, the fluorophore absorbs energy in the form of light at a specific wavelength and liberate energy in the form of emission of light at a specific higher wavelength (i.e. with lower energy). The general principles can be illustrated by a Jablonski diagram, as seen in Figure 1.

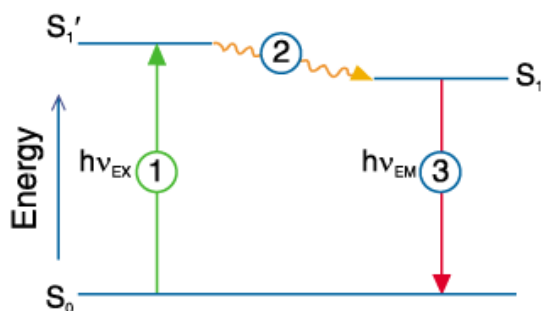


Figure 1. Jablonski diagram showing the basic principles in fluorescence spectroscopy

The first step is the *excitation*, where light is absorbed by the molecule which is transferred to an electronically excited state, meaning that an electron goes from the ground singlet states, S_0 , to an excited singlet state, S_1' . This is followed by a vibrational relaxation or internal conversion (2), where the molecule undergoes a transition from an upper electronically excited state to a lower one, S_1 , without any radiation. Finally, the *emission* occurs (3), typically 10^{-8} seconds after the excitation, when the electron returns to its more stable ground state, S_0 , emitting light at a wavelength according to the difference in energy between the two electronic states. This explanation is somewhat simplified. In molecules, each electronic state has several associated vibrational states. In the ground state, almost all molecules occupy the lowest vibrational level. By excitation with UV and visible light is it possible to promote the molecule of interest to one of several vibrational levels for the given electronically excited level. This implies that fluorescence emission does not only occur at one single wavelength, but rather over a distribution of wavelengths corresponding to several vibrational transitions as components of a single electronic transition. This is why excitation and emission spectra are obtained to describe the detailed fluorescence

characteristics of molecules. The fact that fluorescence is characterised by two wavelength parameters, significantly improves the specificity of the method, compared to spectroscopic techniques based only on absorption.

Stoke's shift

According to the Jablonski diagram, the energy of the emission is lower than that of excitation, meaning that the fluorescence emission occur at higher wavelength than the absorption (excitation). The difference between the excitation and emission wavelength is known as *Stoke's shift*, as indicated with the arrow in Figure 2, marking the difference between the excitation (full line) and the emission (dotted line) spectrum. The excitation and emission properties can also be presented as a fluorescence landscape (Figure 2) also known as an excitation-emission matrix, comprising a multiplication of the excitation and emission spectrum.

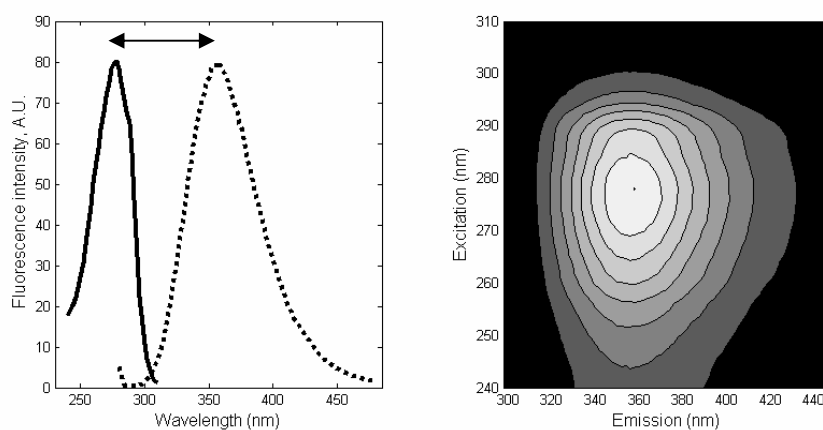


Figure 2. Fluorescence properties of tryptophan, 10^{-5} M.
Left: The excitation spectrum (full line) and emission spectrum (dotted line). Right: Contour plot of the fluorescence landscape

Normally, the emission spectrum for a given fluorophore is a mirror image of the excitation spectrum, as seen to some extent in Figure 2 for tryptophan. The general symmetric nature is a result of the same transitions being involved in both absorption and emission and the similarities of the vibrational levels of S_0 and S_1 . However, several exceptions exist; in the case where the fluorophore is excited to more electronic and vibrational levels a rapid relaxation occurs, leaving the fluorophore in the lowest vibrational

level of S_1 . Thus, several absorption bands can be observed in the excitation spectrum but only the last peak is observed in the emission spectrum, representing the transition from S_1 to S_0 . The fluorescence of riboflavin (vitamin B₂) as seen in Figure 3, is an example of this, with three absorption peaks and only one emission peak.

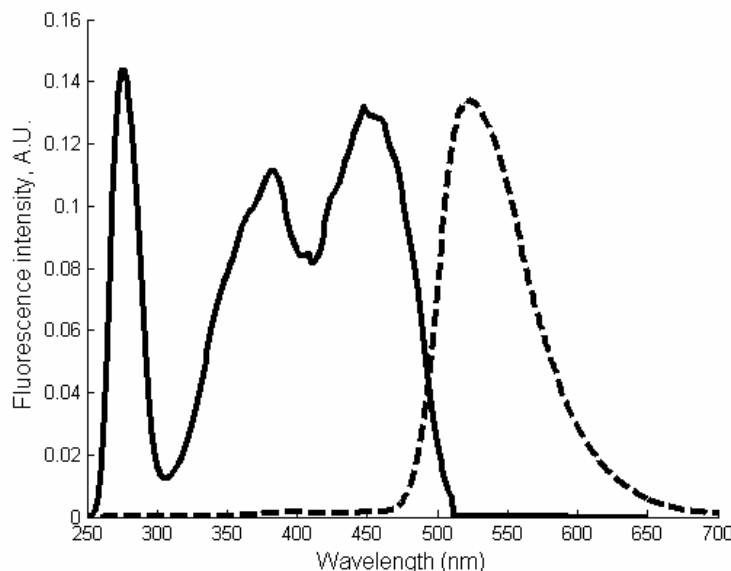


Figure 3. Excitation (full line) and emission profile (dotted line) of 10^{-5} M riboflavin. The profiles are derived from a decomposition of the recorded fluorescence landscape.

Fluorescence measurements

Normally, only emission or excitation spectra (i.e. one excitation or emission wavelength) are recorded when investigating the fluorescence of a sample. However, it can be beneficial and informative to obtain the entire fluorescence landscape (also known as 2-D fluorescence spectroscopy) in order to find the exact excitation and emission maxima as well as the correct structure of the peaks. Furthermore, it facilitates more appropriate analysis of fluorescence data from complex samples with more fluorophores present.

The measurements described in this thesis are all fluorescence landscapes, based on so-called steady-state fluorescence measurements. Steady-state measurement is the most common fluorescence method, covering fluorescence intensity averaged over a constant time period. It is possible to

obtain even more detailed information on the fluorescence properties of a given sample. Time-resolved measurements can be performed, monitoring the fluorescence lifetime in the order of nanoseconds. The fluorescence decay curve of fluorophores can contain detailed information on their physical and chemical environment, such as the size, shape and flexibility of macromolecules. Instrumentation for time-resolved measurements are, however, typically complex and expensive.

Another extra dimension of fluorescence spectroscopy is fluorescence anisotropy. Anisotropy measurements are based on polarization of the light, and the orientation of transition moment of the fluorophores. Especially in combination with fluorescence lifetime measurements, fluorescence anisotropy is widely used to study the interactions of biological macromolecules⁸⁰.

Instrumentation

The basic set-up for an instrument for measuring steady-state fluorescence, a *spectrofluorometer*, is shown in Figure 4. The spectrofluorometer consists of:

- a light source
- a monochromator and/or filter(s) for selecting the excitation wavelengths
- a sample compartment
- a monochromator and/or filter(s) for selecting the emission wavelengths
- a detector which converts the emitted light to electric signal
- a unit for data acquisition and analysis

The sampling geometry can have substantial effect on the obtained fluorescence signal. The most common way to record the fluorescence is in right-angle geometry, where the excitation light travels into the sample from one side and the detector is positioned in the right angle of the centre of the sample. However this method only works for transparent media (e.g. aqueous solutions in a cuvette). For opaque material such as most food samples, front-face illumination can be performed. In this manner it is possible to measure more turbid or opaque samples, since the signal becomes more independent of the penetration of the light through the sample. However when front-face sampling is used, the amount of scattered light detected will increase due to the higher level of reflection from the surface topology of the sample and sample holder. To minimize these effects it is recommended not to place the sample surface oriented at an angle of 45°

to the incident beam, but rather to use a 30°/60° angle position to the light source and the detector, respectively⁸⁰.

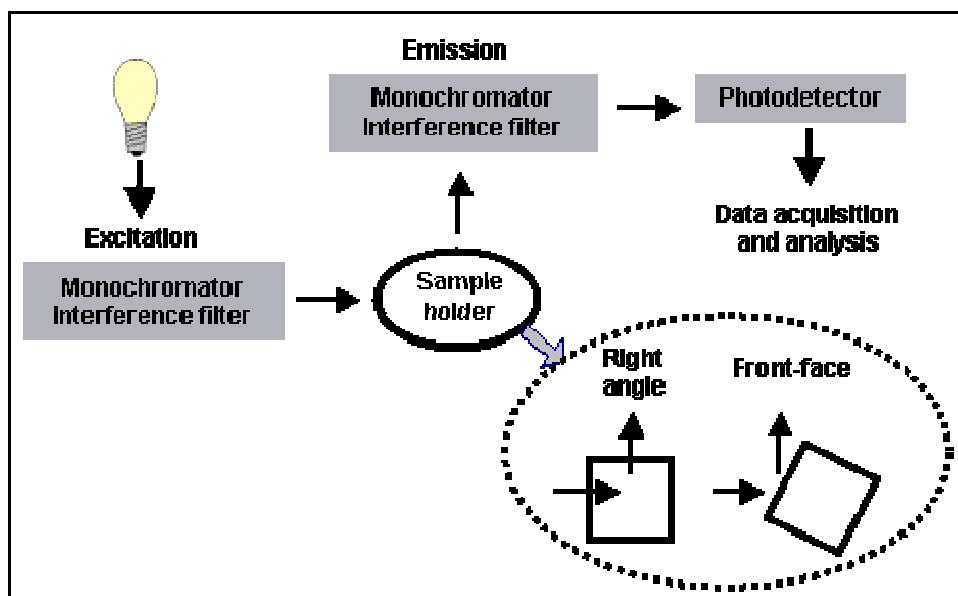


Figure 4. Basic set-up of a spectrofluorometer

Fluorophores

Although many molecules are capable of absorbing ultraviolet and visible light, only a few return to the stable ground state through emission of light. These are called fluorophores. Whether or not a molecule is fluorescent depends primarily on its molecular structure. Fluorescence is most often observed from highly conjugated organic molecules and aromatic compounds with rigid molecular skeletons. The less vibrational and rotational freedom, the greater is the possibility that the difference in energy between the excited singlet state and the ground electronic state is sufficiently large so that deactivation by luminescence will appear.

The aromatic amino acid tryptophan, depicted in Figure 5, is an example of a well-known fluorophore present in many foods. An aromatic ring with conjugated double bonds is evident in the molecular structure. This indole group is the most dominant fluorophore in protein, and since its emission is highly sensitive to its environment, it can be used to monitor changes in protein conformation, for example binding to substrate or denaturation.

Fluorophores can be divided into two major groups according to their occurrence: *intrinsic* and *extrinsic* fluorophores. Intrinsic or natural fluorophores occur naturally in the sample and exhibit intrinsic fluorescence also known as native fluorescence or autofluorescence. Extrinsic fluorescence comes from fluorophores added to the sample in order to label and monitor molecules of interest or their environment using fluorescence. Such techniques are widely used in biology and biotechnology and known as fluorescence labelling or fluorescence probing. Extrinsic fluorescence will not be further described in this thesis, which will only deal with the intrinsic fluorescence present in food products.

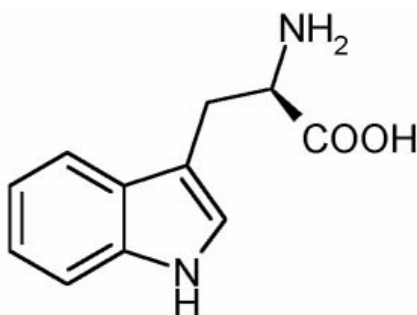


Figure 5. Chemical structure of tryptophan

Wolfbeis, 1985¹⁵⁹, made a review of organic natural products reported to be fluorescent. The list of fluorophores includes several amino acids, vitamins and cofactors, nucleic acid compounds, alkaloids, flavonoids, porphyrins, anthocyanidins, all of which can be present and of interest in analysis of food. A more detailed description of the fluorescent properties of some food-relevant fluorophores can be found in Appendix A which contains a list of the fluorescence landscapes of eleven compounds that frequently appear in food products.

Factors affecting fluorescence intensity

As mentioned above, the molecular structure is decisive for whether or not molecules exhibit fluorescence. However, several other factors and environmental conditions of the molecule affect the intensity and the

properties of the emitted fluorescence. The most important will be mentioned here, using the fluorescence of tryptophan as an example.

Quenching

Fluorescence quenching is a term which covers any process that leads to a decrease in fluorescence intensity of a sample⁸⁰. It is a deactivation of the excited molecule either by intra- or intermolecular interactions. Quenching can be divided into two main categories: Static and dynamic quenching. When the environmental influence (quencher) inhibits the excited state formation, the process is referred to as static quenching. Static quenching is caused by ground state complex formation, where the fluorophore forms non-fluorescent complexes with a quencher molecule.

Dynamic quenching or collisional quenching refers to the process when a quencher interferes with the behaviour of the excited state after its formation. The excited molecule will be deactivated by contact with other molecules or by intramolecular interactions (collision). A wide variety of substances can act as quenchers of fluorescence for different fluorophores. Oxygen is an example of a collisional quencher, which quenches almost all fluorophores. Higher temperature results in larger amount of collisional quenching due to the increased velocities of the sample molecules.

Another source of reducing fluorescence emission is resonance energy transfer, which can be considered as a kind of dynamic quenching. Resonance energy transfer occurs when the emission spectrum of a fluorophore overlaps with the absorption spectrum of an acceptor molecule. The energy transfer does not involve emission of light, but a dipole-dipole interaction between the donor and acceptor molecule, leading to a deactivation of the excited donor. The acceptor molecule – now excited – may also be fluorescent and therefore return to its ground state with or without luminescence.

Concentration and inner filter effect

The concentration of a given fluorophore is decisive for the fluorescence intensity. The fluorophore has to be within a certain concentration range to avoid phenomena known as concentration quenching and inner filter effects.

A formula for the fluorescence intensity of a molecule can be derived from Lambert-Beers law for absorption of light ($A = \varepsilon \cdot c \cdot l$), and the quantum

yield of fluorescence, ϕ_f (fluorescence efficiency) of the given molecule. Combining the two expressions, the following equation can be derived:

$$I_f = \phi_f \cdot I_0 \cdot (1 - 10^{-\varepsilon \cdot c \cdot l}) \quad \text{Eq. 1}$$

where I_f is the fluorescence intensity, I_0 the intensity of the incident light, ε the molar absorptivity, c the molar concentration of the fluorophore, and l the optical depth of the sample. For low absorbance levels the equation can be approximated to the following (for A below 0.02 according to Scharma & Schulman, 1999¹¹³ and below 0.05 according to Lakowicz, 1999⁸⁰):

$$I_f = 2.3 \cdot \phi_f \cdot I_0 \cdot \varepsilon \cdot c \cdot l \quad \text{Eq. 2}$$

Thus, under ideal conditions at low absorbance levels the fluorescence intensity is proportional to the concentration of a given fluorophore.

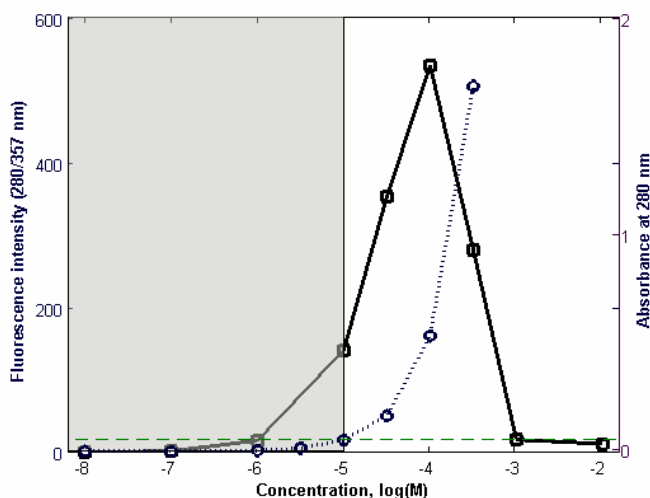


Figure 6. Fluorescence intensity (solid line, \square) and corresponding absorbance (dotted line, \circ) for tryptophan solutions as a function of concentration, logarithmic scale. Fluorescence recorded for excitation 280 nm, emission 357 nm. The horizontal dashed line is for $A=0.05$ and the grey area indicates the concentration levels where the measured absorbance is below this value.

Figure 6 shows a practical comparison of absorbance values and fluorescence intensities based on measurements of a concentration series of tryptophan solutions. The concentration range with sufficiently low absorbance is toned grey, indicating that the concentration of tryptophan needs to be below 10^{-5} M under the given measuring conditions in order to fulfil the requirements for Eq.2. For front-face illumination, the intensity is expected to become more independent of the absorbance level of the samples. For high-absorbing samples like food products (as opposed to transparent liquids), all incident light will be absorbed near the surface of the sample, which means that the optical depth, l , becomes very small.

Thus, the linear relationship between concentration and fluorescence intensities only holds for a very narrow range of concentrations, as indicated in Figure 6. According to the fluorescence graph, the practical detection limit for fluorescence under the given measuring conditions seems to be around 10^{-7} M (corresponding to 20 ppb), where practically no emission is detected. The measured fluorescence intensity is increasing with higher concentration - albeit not linearly correlated over the whole range - up till around 10^{-4} M, where the intensity starts to decline. The decline is due to so-called inner filter effect. Inner filter effects are defined as apparent decreases in emission quantum yield and/or distortion of bandshapes as a result of re-absorption of the emitted radiation, or by absorption of the incident radiation by other species than the fluorophore⁹¹ - also known as primary (absorption of incident light) and secondary (re-absorption) inner filter effects⁷⁷. A decrease in apparent quantum yield can be observed in Figure 6 for the higher concentrations of tryptophan, suggesting that a re-absorption is taking place, and that the conditions for the linearity according to Eq. 2 are not present.

In Figure 7, a considerable distortion of the peak shape is also evident for concentration at 10^{-3} M. The emission profiles seem to be similar, but the excitation profile is completely changed for the high concentrations because of the inner filter effect. Thus, the fluorophore has to be in a specific (low) concentration range - typically below 10^{-4} M¹¹³ - in order to be proportional to the concentration and to express its specific spectral properties. From a practical point of view there exist two apparent approaches in order to minimize inner filter effects: dilute the sample to obtain an appropriate concentration level of the fluorophore or use front-face illumination geometry to minimize the effective optical depth.

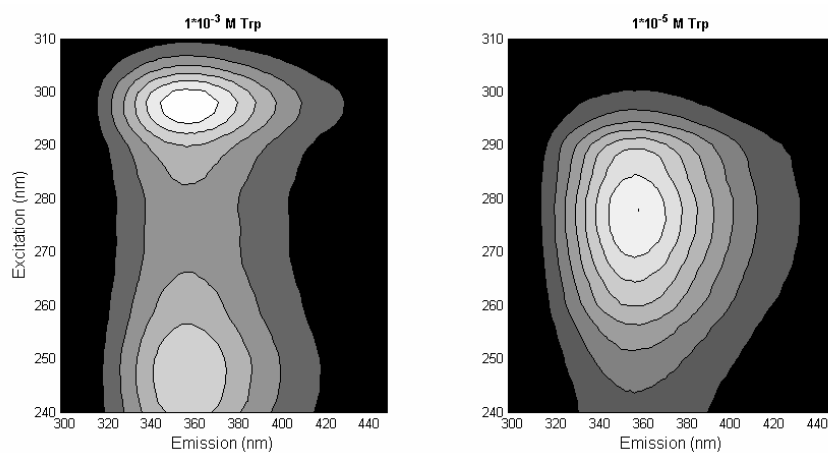


Figure 7. Fluorescence landscapes of tryptophan in water in different concentrations. Left: 10^{-3} M tryptophan. Right: 10^{-5} M tryptophan. Normalized contour plots, white indicate maximum fluorescence intensity.

Solvent effect

The polarity of the solvent or local environment of a fluorophore has a large effect on emission spectra of especially polar fluorophores. In more polar solvents/environments, the fluorophore in excited state will relax to a lower energy state of S_1 . This means that the emission of polar fluorophores will be shifted towards longer wavelengths (lower energy) in more polar solvents, as seen in Figure 8, showing the fluorescence of tryptophan diluted in different solvents. A shift in emission according to polarity of the solvent is evident. Hence, the highest emission wavelengths are observed for water and the lowest for ethanol, but still the same excitation profile is present in the two samples. For more apolar solvents like hexane even larger shifts in emission compared to water can be observed.

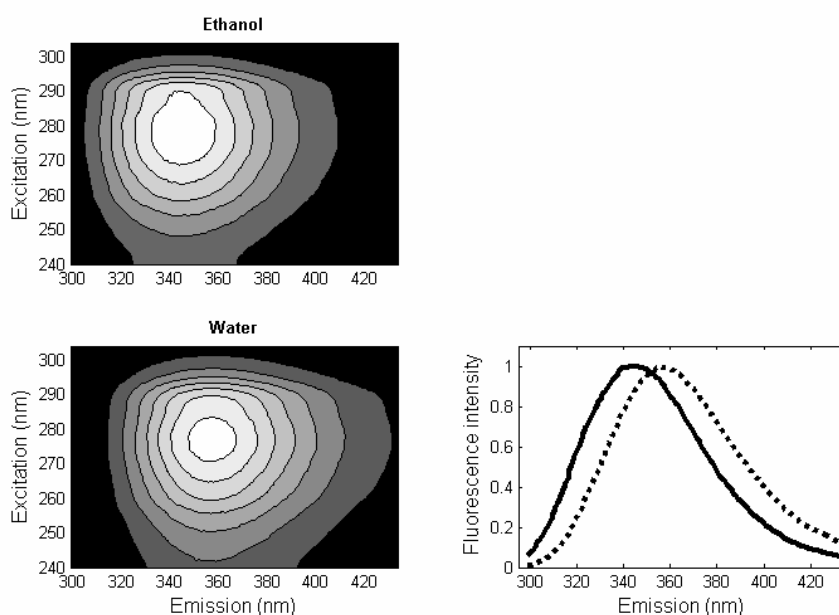


Figure 8. Fluorescence landscape of 10^{-5} M tryptophan in different solvents: Ethanol and water. Left: Contour plots normalized according to maximum intensity (white). Right: Emission spectra of tryptophan in ethanol (full line) and water (dotted line) upon excitation of 278 nm.

Macromolecules

The structure of macromolecules and the location in macromolecules can have a large effect on the fluorescence emission and quantum yield of a fluorophore. Especially protein fluorescence, in the form of the fluorescence from the aromatic amino acids, has been investigated thoroughly in this respect. The fluorescence properties of tryptophan residues can vary due to difference in the three-dimensional structure of the protein.

An example of this can be seen in Figure 9, showing the fluorescence of α -Lactalbumin, β -Lactoglobulin and casein. The excitation profiles of the three proteins look very similar, but the fluorescence emission is expressed at somewhat lower wavelengths for the whey proteins than for the casein. Especially α -Lactalbumin has a short Stoke's shift with a maximum intensity observed for emission at 329 nm, which is close to that of tryptophan in non-polar solvents, indicating that the tryptophan residues are buried in the protein. For casein, the maximum intensity is around 350 nm, and more

similar to the emission profile obtained from tryptophan diluted in water, indicating that the tryptophan residues in casein are situated in more polar environment, i.e. positioned near hydrogen-bonding groups and/or exposed to water.

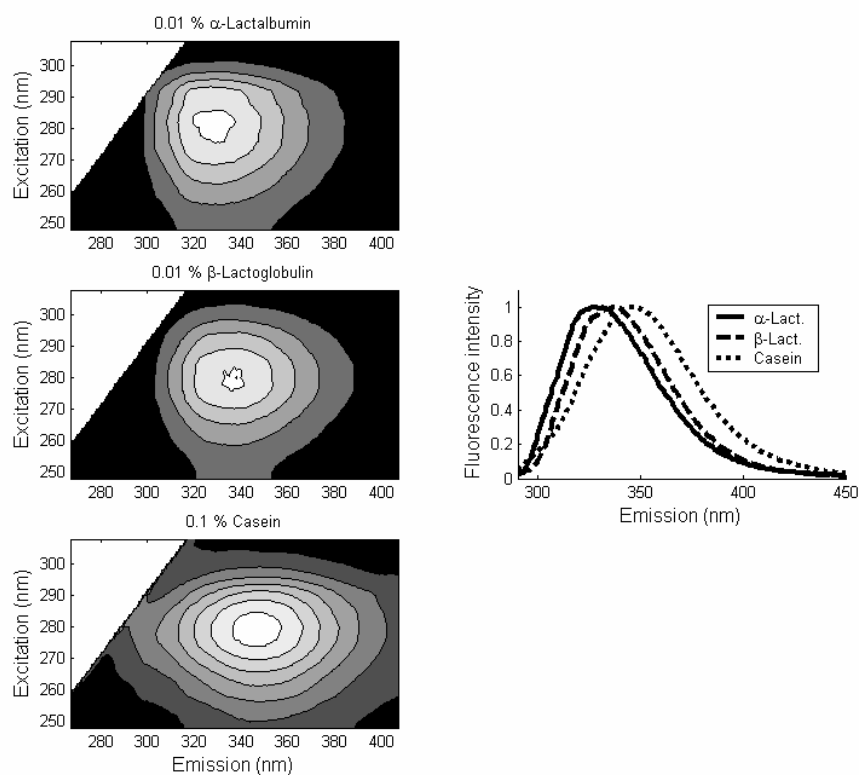


Figure 9. Fluorescence landscapes of three proteins diluted in water: α -Lactalbumin ($2.8 \cdot 10^{-5}$ M tryptophan), β -Lactoglobulin ($1.1 \cdot 10^{-5}$ M tryptophan) and casein ($6.7 \cdot 10^{-5}$ M tryptophan). Left: contour plots normalized according to maximum intensity (white). Right: emission spectra upon excitation of 282 nm.

pH

The pH value of the sample affects the fluorescence of a fluorophore, since protonation and dissociation can alter the nature and the rates of the non-radiative processes competing with fluorescence, and thereby change the quantum yield of the fluorophore. Tryptophan fluorescence as a function of

pH is showed in Figure 10. The maximum fluorescence signal is increasing with higher pH, because of dissociation of tryptophan.

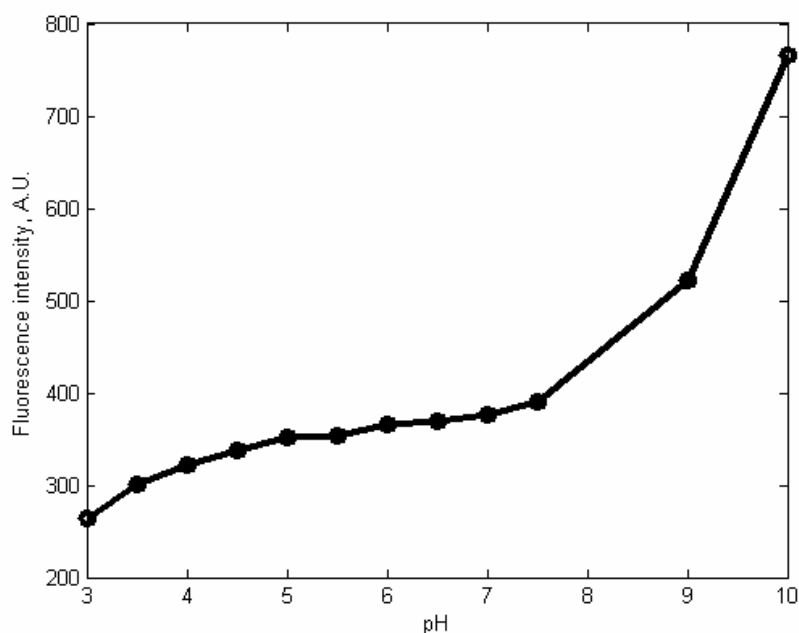


Figure 10. Maximum fluorescence of $5 \cdot 10^{-5}$ M tryptophan diluted in citric acid - Na_2HPO_4 buffer at different pH values. Fluorescence recorded for excitation 280 nm, emission 357 nm.

Scatter

When measuring fluorescence, scattering of the incident light can affect the obtained fluorescence signal. As mentioned in the previous section, the absorbance of the sample measured, plays an important role in fluorescence measurements. Especially for turbid solutions and solid opaque samples (like most foods), the amount of scattered and reflected light affect the measurements considerably, both with respect to the sampling (i.e. the optical depth of the sampling), and on the obtained (fluorescence) signal. Scattered light can be divided into Rayleigh scatter and Raman scatter, according to its nature.

Rayleigh scatter refers to the scattering of light by particles and molecules smaller than the wavelength of the light. Rayleigh is so-called elastic scatter, meaning that no energy loss is involved, so that the wavelength of the

scattered light is the same as the incident light. The Rayleigh scatter can be observed as a diagonal line in fluorescence landscapes for excitation wavelengths equalling the emission wavelengths, as seen in Figure 11. The signal from fluorophores with little Stoke's shift will be situated close to the scattering line, and therefore be most affected by Rayleigh scatter. Due to the construction of grating monochromators used for excitation in most spectrofluorometers, also some light at the double wavelength of the chosen excitation will pass through to the sample. For this reason an extra band of Rayleigh scatter, so-called 2nd order Rayleigh will typically appear in fluorescence measurement for emission wavelengths at twice the given excitation wavelength (Figure 11).

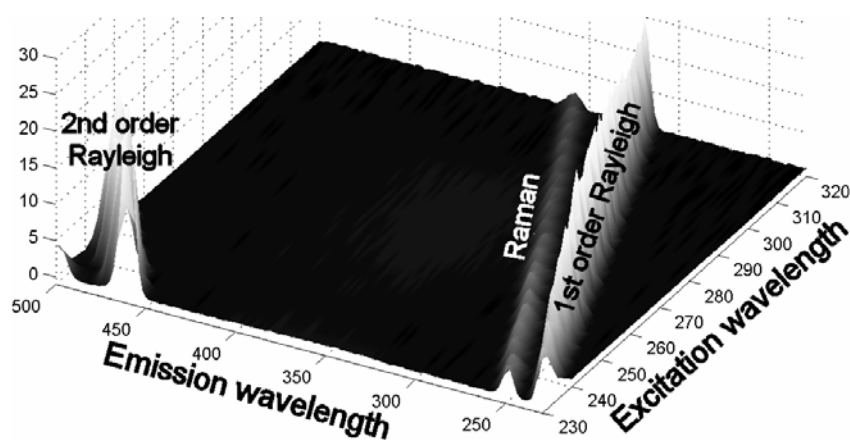


Figure 11. Excitation-emission matrix, highlighting Rayleigh and Raman scatter. Fluorescence landscape of pure water. From Rinnan, 2004¹⁰⁴.

Raman scatter is inelastic scatter, due to absorption and re-emission of light coupled with vibrational states. A constant energy loss will appear for Raman scatter, meaning that the scattered light will have a higher wavelength than the excitation light, with a constant difference in wavenumbers. In Figure 11 the Raman scattering can be seen as a diagonal line with a systematic, increasing deviation from the Rayleigh scatter line, since the axis is shown as wavelengths, which is not proportional to the energy of the light. In liquid samples, the solvent is decisive for the amount

and nature of Raman scatter, while for solid samples it will typically be an expression of the bulk substances.

In the data analytical approach used in this thesis, both Rayleigh and Raman scatter are non-desirable phenomena, since only the fluorescence intensity is of interest. Thus, the scatter effects should preferably be eliminated. The Rayleigh scatter can be disregarded by only measuring and considering fluorescence signal between 1st and 2nd order Rayleigh scatter. Raman scatter can in most cases be neglected because of its sparse contribution, which will be the general approach throughout this thesis. Otherwise, corrections of the fluorescence signal can be performed, either by subtracting the pure solvent/background scatter contribution or by specifically address the Raman and Rayleigh scatter in the modelling of the fluorescence data^{22,68}.

2. Chemometrics

Introduction

In this chapter the application of chemometrics to fluorescence spectroscopy – with emphasis on multi-way analysis of fluorescence landscapes – will be “illuminated”, subsequent to a short introduction to the concepts of chemometrics, multivariate and multi-way data analysis.

What’s chemometrics?

Chemometrics has been defined in broad terms as *the science of relating measurements made on a chemical system or process to the state of the system via application of mathematical or statistical methods* according to the International Chemometrics Society, 2002. However, the definition of the word *chemometrics* has been a subject of discussion and no exact consensus is available, despite of the fact that two international scientific journals and numerous of international and national scientific societies are dedicated to chemometrics and use the word in their titles. It is known that Svante Wold invented the word *chemometrics* in 1972 to describe the discipline of extracting chemically relevant information from chemical experiments¹⁵⁶. He tried later to re-define the word as *how to get chemically relevant information out of measured chemical data, how to represent and display this information, and how to get such information into the data*¹⁵⁷. A more precise definition can be found in a textbook by Massart et al., 1997⁸⁹, stating that *chemometrics is the chemical discipline that uses mathematics, statistics and formal logic (a) to design or select optimal experimental procedures; (b) to provide maximum relevant chemical information by analysing chemical data; and (c) to obtain knowledge about chemical systems*. This definition is very close to the formulation used by Svante Wold and Bruce Kowalski when founding the first Chemometrics Society in 1974⁸⁹.

My understanding and the use of chemometrics in this thesis also explicitly implies the use of multivariate data analysis and the use of 2D data technology in which several related samples are analysed simultaneously. A

multivariate approach when handling and exploring complex chemical data and designing experiments is certainly part of the foundation of chemometrics, but strangely enough not directly part of any formal definition.

Multivariate Data Analysis

Multivariate data analysis as opposed to using only one or a few variables in the data analysis is based on the fact that complex problems - by nature - need multiple variables to be described. Thus, by using and combining more variables, more information about the chemical system can be retrieved.

Concerning spectroscopy, instead of only recording one or a few peaks of interest, whole spectra, landscapes etc. are recorded and utilized in the evaluation of the chemical system. Such spectroscopic data is likely to consist of hundreds of variable, which are generally highly correlated, due to the fact that e.g. the absorbances for neighbouring wavelengths are typically closely related. Classical statistics cannot efficiently deal with such data whereas chemometric multivariate data analytical tools deal with the collinear data by extracting linear independent latent variables from the original variables. The two basic chemometric tools are Principal Component Analysis (PCA) and Partial Least Squares (PLS) regression. PCA and PLS are bilinear models based on a linear decomposition of the original data into a new set of *principal components* or latent variables. The techniques have proven extraordinarily robust and are able to improve the possibilities for outlier detection and to handle background effects and possible interferences in analytical chemistry¹⁹.

Bilinear models

PCA

The basic and fundamental chemometric tool for multivariate and exploratory data analysis, PCA, was developed in the field of psychometrics in the early 20th century^{61,100}, and applied in the field of chemometrics many years later, as indicated in the previous section.

The general principles of PCA can be summed up in Eq. 3. A data matrix, X , representing a number of samples and variables is decomposed into a score matrix (T) and a loading matrix (P) expressing the main variation in data and leaving the unsystematic contribution in the residual, E .

$$X = T \cdot P^T + E \quad \text{Eq. 3}$$

where superscript T means transposed and X is properly centred and scaled. In this way, the multidimensional data in X is resolved into a set of orthogonal components, whose linear combinations approximate the original data in a least squares sense. The products of each of the score and loading vectors are called the principal components (PC's). The score values give the position of the samples according to each of the extracted principal components. The loading vectors can be considered as the new variable space, the direction of each of the principal components according to the original variables. For spectral data, score values ideally represent the concentration of a given chemical species in the sample, while the loading vector represents the spectral profile of the species.

By extracting only the major variation into a limited set of principal components the dimension of the original data matrix is likely to be decreased considerably, due to the handling of the extensive collinearity and noise filtering. The PCA models still represents the high-dimensional original data, however, in a compressed format. Thus, the objective of the linear decompositions in multivariate data analysis is (a) to keep all the information in the data analysis by recording and analysing multiple variables and (b) afterwards to decrease the effective dimensionality of the data in order to be able to evaluate the results and focus on the relevant information. You give and you take.

PLS

Partial Least Squares regression, as first proposed by Wold, Martens and Wold in the beginning of the 1980's¹⁵⁸, makes up the second major fundamental multivariate tool in chemometrics. PLS regression models are based on a similar decomposition of the X matrix as known from PCA. However, PLS models are developed for correlating two data sets, X and y, as seen in Eq. 4.

$$y = X \cdot b + e \quad \text{Eq. 4}$$

X contains the measured multiple variables properly centred and scaled, b contains the regression coefficients determined in the calibration routine, while y represent one or a few variables or quality parameters, desired to be

predicted from X . PLS is a two-block regression method where the decomposition of X are performed under the consideration of y in a simultaneous analysis of the two data sets. The method is typically used in spectroscopy to correlate spectra with a related physical or chemical parameter such as the concentration of a given chemical species.

Applications of PCA and PLS to fluorescence spectroscopy

The application of multivariate data analysis in the form of bilinear models in the evaluation of fluorescence spectroscopy was first proposed in 1982⁶⁵ in a study describing the botanical constituents of wheat in wheat milling fractions. PLS regression was successfully used to correlate emission spectra from intrinsic fluorescence of wheat milling fractions to the concentration of each of the botanical constituents pericarp, aleuron and endosperm in the flour; probably based on the fluorescence signal from ferulic acid, tryptophan and riboflavin. Only a few studies in the cereal science^{64,76} followed up on this multivariate approach in the evaluation of intrinsic fluorescence in the following years. After this, there seems to be a time gap of around ten years in the history of studies reported on applications of bilinear chemometric models to autofluorescence, until 1995 where Nørgaard applied PCA and PLS regression models to classify and predict quality and process parameters of sugar juice, based on their fluorescence emission spectra⁹⁸. After this, numerous examples of chemometrics applied to fluorescence spectroscopy has been published, probably due to the propagated use of chemometrics and the tremendous increase in computer power and there from derived reduction of calculation time.

Within food science, fluorescence spectroscopy evaluated with chemometrics, has been applied in dairy research in a few studies to monitor structural changes in milk proteins and their environment during milk heating³⁹ milk coagulation⁵⁶ and cheese manufacture^{36,90}. Changes in vitamin A in dairy products have been monitored in several fluorescence studies^{38,57,74}, and front-face fluorescence spectroscopy has been used for measuring light-induced oxidation in various dairy products¹⁴⁹, as well as proposed as a new method for rapid quantification of riboflavin (Paper IV)¹⁴. Recently fluorescence spectroscopy was also introduced in authenticity analysis of cheese⁷².

In meat science, autofluorescence of connective tissue and protein has been investigated and utilized in several multivariate studies^{118,151,152}, in order to

correlate the recorded fluorescence “fingerprints” to quality parameters such as toughness¹³⁴, water holding capacity²⁴ tensile properties⁴³ and tenderness⁴⁷. Also poultry^{150,153}, fish^{4,37} and the texture of meat emulsions² has been investigated, based on their intrinsic fluorescence properties evaluated with chemometrics.

Exploratory studies investigating the deterioration of frying oil⁴⁵, the characterization of edible oils¹¹⁶ and apple juice¹¹¹ and the oxidative stability of various snack foods and oat meal products (Paper III)⁶³ has been reported involving a multivariate analysis of obtained autofluorescence, and the technique has recently been suggested for classification of wheat cultivars¹⁰². In biotechnology, several bioprocesses have been monitored using 2D-fluorescence spectroscopy, demonstrating the potential of autofluorescence and chemometrics for on-line analysis of fermentations^{16,94,117,120}.

An example of the application of PCA to a multivariate fluorescence signal from a food product, is shown in Figure 12 in the form of a score plot based on unfolded fluorescence emission spectra of yogurt samples throughout a storage experiment (PAPER V)¹⁴. The distribution of the yogurt samples can be observed in the score plot, according to the two first principal components, representing the major trends in the multivariate fluorescence signal. The experimental plan is evident in the distribution with a general decrease in both the first and second principal components throughout the storage. The decrease in the first PC is very dependent on the light exposure; as indicated by samples stored dark are situated in the opposite direction of the samples stored in the packaging with the highest light transmission. The corresponding loading plot (not shown) can reveal the spectral profiles responsible for the distribution of samples in the score plot. In this case, changes in riboflavin fluorescence are largely determining for the first PC, which makes good sense, since riboflavin is light sensitive and considered to be an early marker of oxidation, which is likely to happen during storage, when the sample is exposed to light.

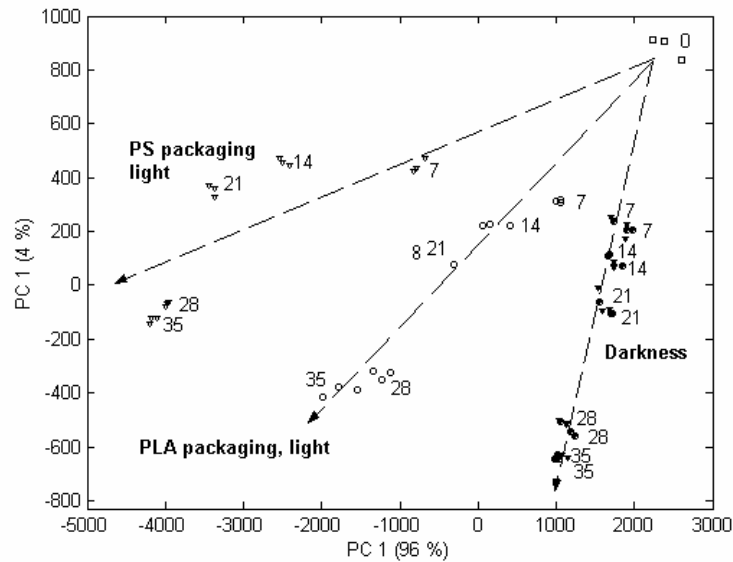


Figure 12. Score plot of principal component 1 and 2 from a PCA on unfolded fluorescence emission spectra of yogurt samples packaged in two different materials, (○) or (∇) and stored at 4°C under continuous light exposure (open symbol) or in darkness (closed symbol). Day 0 is indicated with (□). Samples are numbered according to days of storage, and arrows indicate increasing storage time. Values in brackets note the degree of variation explained by each PC. Plot taken from Paper IV¹⁴.

Multi-way analysis

The described bilinear models are used in analysis of data matrices in 2 dimensions, usually containing samples x variables. Multi-way data analysis refers to multivariate data analysis performed of data arrays in higher dimensions than two. In the following description of multi-way data analysis, focus will specifically be on the application of Parallel Factor Analysis (PARAFAC) on fluorescence data in three dimensions, *three-way arrays*, containing fluorescence intensity as a function of samples, excitation wavelength and emission wavelength.

PARAFAC

PARAFAC can be considered as an extension of PCA to higher order data; it is a decomposition of the original data matrix with multiple variables to a set

of object scores and variable loadings, but with loadings in more than one direction. PARAFAC^{26,55} was like PCA developed in the field of psychometrics, and much later adapted in the field of chemometrics^{49,105,106,119}. However, other and similar factor analysis methods were developed, introduced and used in the evaluation of three-way chemical data already from the late seventies^{58,87,108}.

The principle behind the PARAFAC decomposition is to minimize the sum of squares of the residual, e_{ijk} , as indicated in Eq. 5 for a three-way PARAFAC model.

$$x_{ijk} = \sum_{f=1}^F a_{if} b_{jf} c_{kf} + e_{ijk} \quad \text{Eq. 5}$$

The element x_{ijk} represents the data for sample, i , in variable j and k of the two different variable dimensions. The three way data array are thus decomposed into a set of sample scores a_{if} , loadings in the first variable directions, b_{jf} and loadings in the second variable direction, c_{kf} . The rank of the PARAFAC model is given by the number of factors, F needed to describe the variation in the data array. A graphical presentation of the decomposition can be seen in Figure 13, where the data cube \underline{X} is decomposed into scores and loadings, a , b and c , using two factors or PARAFAC components, leaving the unmodeled part of \underline{X} in the residual cube, \underline{E} , which ideally only contains unsystematic noise.

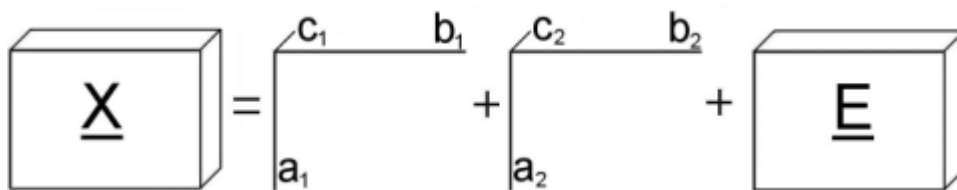


Figure 13. Principles of a PARAFAC decomposition of a three-way data array, using two factors.

The shown PARAFAC model is a trilinear decomposition that requires trilinearity of the data. This means that each phenomenon in data which is to be modelled, can be explained by the product of a score value and a set of

loading vectors, cf. Eq. 5, implying that the structure in the two variable directions are independent.

Several algorithms has been suggested for decomposition of trilinear data, as recently compared and reviewed by Tomasi and Bro¹⁴³. Rank annihilation methods^{6,58,59,108} and direct trilinear decomposition techniques^{86,107} has been used in trilinear decompositions of chemical data, similar to the one shown in Figure 13, however not fitting a least-squares solution as a PARAFAC model based on an alternating least squares algorithm, used in the present work.

In contrast to PCA, PARAFAC models compute all the factors in the model simultaneously and gives unique solutions to the decomposition, which makes the technique very useful for curve-resolution²⁰. Furthermore, analysis with three-way arrays can increase the selectivity of calibration models compared to bilinear models - a phenomenon known as the second order advantage¹⁷. The unique trilinear decomposition makes it possible to use and extrapolate calibration models on new samples containing new interferences. This is not the case in bilinear calibration models for which it is important to span all possible future variations and include them in the model. Ideally, this means that a calibration model based on PARAFAC performed on model solutions can be used directly for prediction in real-life applications, which was demonstrated by Moberg et al.⁹² studying chlorophylls and pheopigments in seawater using 2D-fluorescence spectroscopy.

In the development of PARAFAC models, determination of the rank and validation of the result is a crucial point; however this subject will not be further studied here. Thorough explanations and practical aspects of PARAFAC modelling can be found in tutorials in the literature^{3,20}.

PARAFAC and Fluorescence spectroscopy

The fluorescence intensity of a given fluorophore can be expressed as a function of the concentration of the fluorophore and the specific excitation and emission spectral profiles of the compound. Under ideal conditions, as discussed in the introduction to fluorescence spectroscopy, the intensity will be linearly dependent of the concentration and the excitation and emission spectra will be independent of one another. Assuming that the overall

fluorescence of a mixture sample equals the sum of the signal from the inherent fluorophores, this implies that fluorescence landscapes can be considered as trilinear data⁸³. The fluorescence signal can then be expressed as in the PARAFAC model in Eq. 5, where the score values, a , represent the concentration for each of the components (fluorophores) and the b and c loadings represents the excitation and emission profiles of each of the fluorophores present in the landscapes. Thus, the PARAFAC model can be used for a unique decomposition of the fluorescence data from a complex sample into a set of PARAFAC components according to the number of fluorophores present in the samples. This can facilitate the analysis of fluorescence measurements of complex biological samples, also in more exploratory situations, when the contained fluorescence phenomena *a priori* are unknown. In the data analysis, the relative concentration of each of the present fluorophores in the mixture can be determined, and the excitation and emission loadings can be used for identification of the fluorophores.

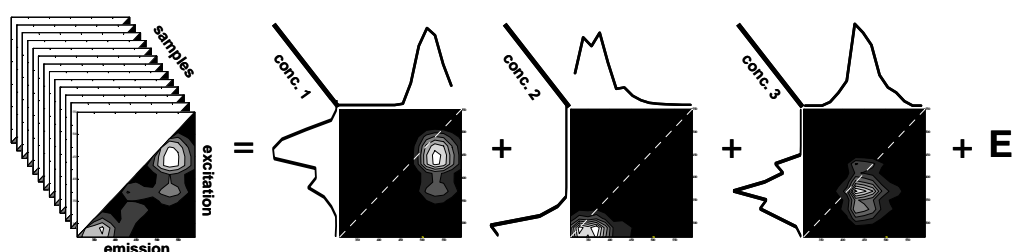


Figure 14. PARAFAC decomposition of fluorescence landscapes from yogurt samples into three factors. Curves in the vertical direction depict the loading vector for excitation for each of the factors, and the curves in the horizontal direction show the emission loading profiles. The three contour plots express the product of the excitation and emission loadings; fluorescence is only measured below the dotted line. Data taken from Paper II²⁸.

An example of PARAFAC decomposition of fluorescence data is shown in Figure 14, based on a series of fluorescence landscapes of yogurt samples measured throughout a storage experiment (PAPER II)²⁸. The obtained fluorescence signal is decomposed into three factors or PARAFAC components that describe each of the fluorescence phenomena present in the yogurt samples. Scrutiny of the excitation and emission spectra of each of the resolved components can then be used for an identification of the

present fluorophores which are suggested to be riboflavin, tryptophan and lumichrom in this case. The contribution of each of the constituents in the samples is indicated with the score values of the three components, that ideally gives the relative concentration of the three given compounds. However, working with fluorescence of intact food samples, the conditions might not be ideal to obtain perfectly trilinear data with respect to concentration levels and possible quenching, as indicated by the fact that the obtained and resolved fluorescence signal from riboflavin in this example only seems to have two excitation peaks (around 370 and 450 nm). In pure solutions, strong absorption will also appear at around 270 nm (see Appendix A), which is not evident in the yogurt study probably due to quenching, assigned to competition with the strong absorption of this light by tryptophan (with excitation maximum around 285 nm).

Applications of PARAFAC to fluorescence spectroscopy

The advantages of recording and analysing fluorescence landscapes in the investigation of a fluorescent sample containing multiple fluorescent components was first explored by a research group at University of Washington in the end of the 1970's. In a series of papers, Warner et al.^{145,146,146-148} introduced the principles of utilizing the experimental "*Emission-Excitation Matrix*" in a quantitative analysis of a multicomponent sample for determining the number and spectra of the emitting components in the sample. Ho et al.⁵⁸⁻⁶⁰ and others from the same research group^{6,25,70} proceeded this work and developed a rank annihilation factor analysis of fluorometric data in order to obtain a decomposition similar to Eq. 5. In these first studies, the multi-way approach was only applied and explored on simulated fluorescence data and fluorescence measurements on model solutions. Later, factor analyses were applied on biological samples to resolve the fluorescent components in spinach chloroplasts and green algae⁸⁷ and plant pigment-complexes¹⁰⁵.

In the last decade, several applications of PARAFAC to fluorescence landscapes have been reported. In environmental science, PARAFAC and fluorescence has used for determination of aromatic hydrocarbons^{18,69,112} and pesticides⁶⁷ in water, and for quantification of dissolved organic matter in water and soil^{27,122}.

Within food research, applications of multi-way data analysis of intrinsic fluorescence obtained from food products can be found in analysis of sugar,

meat, oil and dairy products. In analysis of sugar and sugar solutions^{9,10,12,21}, information on sugar quality at a molecular level, ascribed to the colour impurities in sugar, has been thoroughly investigated through decomposition of fluorescence landscapes. Fluorescence spectroscopy and PARAFAC has been used in analysis of olive oil⁵¹ and suggested as a potential screening method for dioxin contamination in fish oil¹⁰¹, however, based on an indirect correlation. Furthermore the technique has been demonstrated to hold relevant information when monitoring chemical changes of Parma ham during maturation⁹³ and the oxidative stability of dairy products during storage (Paper II²⁸ + Paper V³¹). In biotechnology, PARAFAC has been applied to fluorescence data from yeast fermentation as a tool to monitor the bioprocess on-line⁵².

3. Literature Food Fluorescence

In this chapter examples of autofluorescence applied in the analysis of intact food will be reviewed and discussed. The review of the studies of food fluorescence found in the literature will be divided into subgroups, according to food products. Thus, fluorescence from meat, fish, dairy products, edible oils, cereals, beer, sugar, fruit and biotechnology cases will be presented separately. The categories are chosen to compare studies of similar products with similar fluorescence properties, but also based on the amount of research in each of the fields.

In most of the studies, the obtained fluorescence signal was assigned to specific fluorophores, in many cases based on single excitation or emission spectra. The suggested assignments will be mentioned in this review, omitting a thorough discussion on the origin of the fluorescence, which in some cases perhaps arises from more fluorescent compounds or could/should be assigned differently. An overview of the literature survey and the assignment is given in Table 1, which lists all the studies found on autofluorescence of intact food. Only first author and year of publication appear in the overview and some of the citations cover more than one study.

Meat

Studies on applications of autofluorescence in analysis of meat have mainly been assigned to measurements of the fluorescence from collagen in connective and adipose tissues, but also protein fluorescence and suggestions for some fluorescent oxidation compounds has been described.

Table 1. Overview of literature survey on autofluorescence studies of intact food. References (first author and year of publication) are listed according to food product group and assigned fluorophores.

Meat	Fish	Dairy Products	Edible oils	Cereals	Beer	Sugar	Fruit	Biotech
<p>Amino acids Wold, 1999 Møller, 2003 Allais, 2003, 2004</p> <p>Collagen Jensen, 1986 Swatland, 1987-2003 Wold, 1999 Bronlum, 2000 Egeland, 2002, 2005</p> <p>NADH Jensen, 1986 Bronlum, 2000</p> <p>Oxidation products Wold, 2000, 2002 Møller, 2003</p>	<p>Amino acids Dufour, 2003</p> <p>Collagen Jensen, 1986 Andersen, 2003</p> <p>NADH Jensen, 1986 Dufour, 2003</p> <p>Chlorophyll Pedersen, 2002</p>	<p>Amino acids Dufour, 1997, 2001 Birlouez-Aragon, 1998 Herbert, 1999, 2000 Lopez, 2001 Mazrolles, 2001 Lecle, 2001 Christensen, 2003, 2005 Karoui, 2003-2004 Leriche, 2004 Kulmyrzaev, 2005 Garmelle Purna, 2005</p> <p>Vitamin A Dufour, 1997, 2000 Herbert, 2000 Christensen, 2003 Karoui, 2003-2004</p> <p>Riboflavin Wold, 2002 Christensen, 2003, 2005 Mortensen, 2003</p> <p>NADH Kulmyrzaev, 2005</p> <p>Maillard products Birlouez-Aragon, 1998 Léclere, 2001</p> <p>Oxidation products Christensen, 2003, 2005</p> <p>Chlorophyll Wold, 2005</p>	<p>Chlorophyll Engelsen, 1997 Kyriakidis, 2000 Pedersen, 2002 Diaz, 2003 Guimet, 2004 Sikorska, 2004, 2005 Zandomeneghi, 2005</p> <p>Tocopherol Kyriakidis, 2000 Guimet, 2004 Sikorska, 2004, 2005 Zandomeneghi, 2005</p> <p>Polyphenols Sikorska, 2004, 2005 Zandomeneghi, 2005</p> <p>Oxidation products Engelsen, 1997 Sikorska, 2004, 2005 Guimet, 2004</p> <p>Riboflavin Zandomeneghi, 2005</p>	<p>Amino acids Jensen, 1982 Zandomeneghi, 1999 Jensen, 2004</p> <p>Ferulic acid Jensen, 1982 Symons, 1991-1996</p> <p>Riboflavin Zandomeneghi, 2003 Jensen, 2004</p> <p>Oxidation products Jensen, 2004</p>	<p>Amino acids Apperson, 2002 Sikorska, 2004 Christensen, 2005</p> <p>Iso-alpha acids Taktar, 1995 Tomlinson, 1995 Apperson, 2002 Sikorska, 2004 Christensen, 2005</p> <p>Polyphenols Apperson, 2002 Christensen, 2005</p> <p>Riboflavin, NADH, pyridoxine Sikorska, 2004</p>	<p>Amino acids Nørgaard, 1995 Munk, 1998 Bro, 1999 Baunggaard, 2000-2001</p> <p>Polyphenols Baunggaard, 2000-2001</p> <p>Maillard products Baunggaard, 2000-2001</p>	<p>Chlorophyll Franck, 1969 Schreiber, 1975 Yamada, 1996 Song, 1997 Cohen, 1998 Moshou, 2003 Codrea, 2004</p>	<p>Tryptophan Lindemann, 1998 Marose, 1998 Skibsted, 2001 Harbeck, 2001 Haack, 2004 Rhee, 2005</p> <p>NADH Lindemann, 1998 Marose, 1998 Skibsted, 2001 Lee, 2002 Boehl, 2003 Mørel, 2004 Haack, 2004 Rhee, 2005</p> <p>Riboflavin Lindemann, 1998 Marose, 1998 Boehl, 2003 Haack, 2004 Rhee, 2005</p> <p>Pyridoxine Marose, 1998 Mørel, 2004 Rhee, 2005</p> <p>Alkaloids Boehl, 2003</p>

Autofluorescence for analysis of meat was first proposed in 1986 in a patent⁶⁶, suggesting a method for quality control of meat and fish products, based on their intrinsic fluorescence characteristics. The method was based on excitation at 340 nm and the fact that bone, cartilage, connective tissues and meat possess different fluorescent properties. Thus, hardly any fluorescence signal was obtained for pure meat at this excitation, whereas the non-desired substances (fat, bone, cartilage and connective tissue) all yielded considerable fluorescence emission. The emission spectra for these compounds look different in structure but they all have a peak with maximum at 390 nm and a shoulder peak with emission at 455 nm (bone, cartilage, and connective tissue) or 475 nm (fat), which can probably be assigned to different types of collagen and NADH.

H.J. Swatland must also be considered a pioneer in the field with a series of articles on different aspects of the autofluorescence of meat since 1987¹²⁴. His work has been focused on measuring collagen and elastin fluorescence from the connective tissues in meat with excitation at 365 nm. The obtained autofluorescence signal of various meat has been correlated to several quality parameters related to sensory properties such as gristle content in beef¹²⁵, skin content and processing characteristics of poultry meat slurry¹³² and turkey meat^{128,133} as well as palatability¹³⁶, chewiness¹³⁵ and toughness¹³⁴ of beef. All these correlations can be considered as indirect analyses, caused by the fact that the quality parameters are suggested to be related to the amount and distribution of connective and adipose tissue in the meat. Swatland has also investigated technical aspects of the fluorescence measurements and instrumentation (back-scatter, reflectance, direction of light), leading to the development of on-line meat probes based on fibre optics^{126,127,129,130} with simultaneous measurements of reflectance¹³¹. All these studies were carried out with a univariate data analytical approach; univariate regression models were calculated between the desired quality parameters and single selected wavelengths or extracted fluorescence peak features. However, in a few papers, multiple linear regression of a few parameters was applied using a stepwise selection procedure^{134,135}, pointing towards a more multivariate approach.

Egelandsdal, Wold and co-workers picked up the thread and applied PCA and PLS in evaluation of autofluorescence emission spectra of meat, obtained from selected excitation wavelengths in the UV region between 300 and 400 nm. Thus, fluorescence emission spectra assigned to various types

of collagen in meat products has been found to correlate with tensile properties⁴³, tenderness⁴⁴, water holding capacity²⁴, and suggested for quantification of connective tissue and collagen^{42,152}. Fluorescence emission spectra assigned to fluorescent oxidation products has been found to correlate with lipid oxidation¹⁵³ and rancidity¹⁵⁴ of meat. Furthermore, tryptophan fluorescence (excitation 290 nm) has been correlated to the texture of meat emulsions and sausages^{1,2}. An extra dimension of the autofluorescence analyses can be obtained by recording fluorescence images of the samples, which obviously increase the sampling area, which is desirable when working with intact heterogeneous biological samples. Autofluorescence images, reflecting the collagen fluorescence have been proposed for quantification of intramuscular fat content in beef¹⁵¹, and for mapping of the lipid oxidation in chicken meat¹⁵⁰.

Multi-way studies

All the described multivariate fluorescence studies were using bilinear models to evaluate single emission spectra. The only multi-way study of autofluorescence of meat reported so far was on dry-cured Parma ham, which was monitored throughout processing and ageing⁹³. A PARAFAC decomposition of the recorded fluorescence landscapes revealed five apparent fluorophores, of which tryptophan was assigned to be the dominating one. The remaining four components were more difficult to assign; one was suggested to arise from the salting and two others were related to oxidation. The second PARAFAC component with excitation/emission maxima at 370/470 nm accounted for the largest fluorescence contribution next to tryptophan, and could perhaps be assigned to collagen or NADH in accordance with previous meat studies.

Fish

In 1985 fluorescence was proposed as a method for detecting bones in fish fillets⁶². Autofluorescence of fish was later reported in the form of collagen fluorescence found in cod and salmon upon excitation at 332 nm⁴. Fluorescence images from this study revealed a noticeable inner filter effect in the salmon flesh probably caused by strong absorption of the emitted fluorescence light by red pigments as astaxanthin. Front-face fluorescence has also been suggested for assessment of the freshness of fish³⁷. Normalized fluorescence emission spectra with excitation of 260 nm (assigned to aromatic amino acids) and 336 nm (NADH) was evaluated by PCA, and

suggested to be used for discrimination between different storage times for whiting and mackerel fillets. PARAFAC was applied on fluorescence landscapes of fish oil¹⁰¹. The decomposition yielded four fluorophores present in the oil samples, of which one was assigned to chlorophyll. The obtained complex fluorescence fingerprint was shown to correlate (indirectly) to dioxin content in the fish oil, and suggested as a screening method for dioxin contamination.

Dairy products

Fluorescence studies of dairy products found in literature are dominated by fluorescence assigned to tryptophan, vitamin A and riboflavin, but also fluorescent oxidation and process derived products have been described. In addition, naturally occurring chlorophyllic compounds were recently analysed in dairy products using fluorescence emission spectra from 400 to 750 nm obtained from illumination with excitation light of 380 nm¹⁵⁵. Emission peaks between 600 and 700 nm were observed in agreement with the findings for chlorophyll A and hematoporphyrin found in Appendix A.

Normalized tryptophan emission spectra

In several studies emission spectra of tryptophan normalized according to peak area have been investigated as an indicator of the protein structure in dairy products. Minor shifts in the emission profile evaluated with multivariate data analysis can apparently be connected to different location and environment of the tryptophan residues in the protein. Thus, front-face fluorescence emission spectra upon excitation at 290 nm of soft cheese were correlated to sensory profiles of texture and used for discrimination of the cheese type³⁶. A similar approach was applied to study molecular interactions during milk coagulation^{56,85}, cheese ripening⁹⁰ and it was also suggested as a rapid method for estimation or screening of process cheese functionality⁴⁸ and geographic origin of Emmental chesses⁷².

Vitamin A

Vitamin A fluorescence has been measured in studies of dairy products by recording excitation spectra with emission at 410 nm, which seems rather low compared with the fluorescence profile of vitamin A shown in Appendix A with emission maximum at 480 nm. Nevertheless, the assignment is not documented, nor questioned in the articles, where the vitamin A fluorescence has been related to phase transition of triglycerides

in cheese³⁸. A combination of the proposed vitamin A fluorescence and fluorescence assigned to tryptophan has also been applied in several studies of cheese. The common fluorescence signal was found to correlate with the identity and structure of soft cheese⁵⁷, the rheological characteristics of various cheese^{71,75} and classification of Emmental cheese according to origin⁷³.

Heat treatment of milk

Rapid fluorometric methods have been suggested for estimation of the heat treatment of milk, based on the intrinsic fluorescence of milk. A combination of fluorescence assigned to tryptophan (emission spectra, excitation 295 nm) and vitamin A (excitation spectra, emission 410 nm) was applied in a front-face fluorescence study of milk³⁹. Classifications based on PCA of the fluorescence spectra clearly separated the milk samples according to heating and homogenisation. Another study used the relation between the excitation/emission peaks at 290/340 nm and 350/440 nm, assigned to fluorescence from tryptophan and advanced Maillard products, for a classification according to heat treatment, based on fluorescence measurements of water soluble milk fractions¹⁵. The same method was demonstrated to correlate with lysine degradation in milk during heating, however with an adjustment of the peak selection to 330/420 nm for the proposed fluorescent Maillard products⁸¹. Front-face fluorescence emission has also been monitored of intact milk samples upon excitation of 250 and 360 nm, which in this study was assigned to fluorescence of aromatic amino acids and NADH/FADH respectively⁷⁸. The suggested NADH/FADH fluorescence was shown correlating with heat treatment indicators using principal component regression models.

Riboflavin

Riboflavin is considered to be a marker of photo-oxidation in dairy products and autofluorescence assigned to riboflavin have been used to describe light-induced changes in dairy products. Thus, front-face fluorescence emission spectra were obtained from Jarlsberg cheese, sour cream and cream cheese upon illumination with light of 380 nm¹⁴⁹. The fluorescence spectra revealed a significant reduction in fluorescence intensity at 525 nm and a corresponding increase around 415-490 nm upon expected oxidation of the samples. The result was ascribed to photo degradation of riboflavin, leading to a fluorescent product. Oxidation of Havarti cheese was also monitored based on fluorescence excitation/emission peaks at 370/530 nm and 430/530

nm, ascribed to riboflavin⁹⁵. Paper IV¹⁴ applying autofluorescence in analysis of yogurt, confirmed the previous findings by relating storage conditions to the fluorescence signal obtained for emission around 530 nm. Furthermore, a high correlation to riboflavin content ($R^2 = 0.98$) was found, verifying the dependency.

Multi-way studies

The only reported multi-way studies of autofluorescence landscapes of dairy products are so far described in Paper V³¹ and Paper II²⁸, where PARAFAC was applied in the evaluation of fluorescence landscapes of processed cheese and yogurt, respectively, throughout storage experiments. The study of cheeses was restricted to handle the UV fluorescence part of the fluorescence landscapes with excitation wavelengths from 240-360 nm and emission of 275-475 nm. The dominating contribution from tryptophan was determining for the experimental conditions, leaving hardly any signal from e.g. riboflavin, which is why only UV excitation light was used. The fluorescence landscapes of the cheese samples were decomposed to four different PARAFAC components assigned from tryptophan, vitamin A and some kind of oxidation product. Two of the resolved PARAFAC components yielded slightly different excitation profiles, but could both resemble the fluorescence properties of tryptophan with very similar emission loadings with maximum at 347 and 339 nm. Both components were assigned to tryptophan, representing two different populations of tryptophan residues, even though the observed shift in excitation maxima should not be affected by different local environment according to the fluorescence theory described in the first chapter, but only the emission profile. However, inner filter effects, which can alter the excitation profile as previously described and the poor resolution of the excitation wavelength in the study can perhaps justify the assumption. An alternative explanation could be that tyrosine residues were actually responsible for the absorption in the PARAFAC component with the lowest excitation maximum, and subsequently the energy was transferred to tryptophan by resonance energy transfer⁸⁰. In that case, the second PARAFAC component should correctly have been assigned to tyrosine.

Edible Oils

Several studies characterising edible oils using autofluorescence has been presented in the last decade. In 1996, frying oil deterioration was followed

with fluorescence emission spectra from 5 selected excitation wavelengths from 395 to 530 nm, as evaluated with multivariate data analysis and found correlating with quality parameters describing the deterioration⁴⁵. In another study, fluorescence emission spectra from common vegetable oils were obtained upon illumination by 360 nm. The fluorescence signal was partly assigned to tocopherol and chlorophyllic compounds⁷⁹, even though that the proposed tocopherol fluorescence emission at 525 nm certainly not match the fluorescence properties of pure α -tocopherol as shown in Appendix A.

In olive oil, autofluorescence has been suggested for determination of chlorophylls and pheophytins³⁵. PLS regression models were applied on single excitation, emission and synchronous spectra, which all were highly correlated to the content of the different pigments ($R^2 > 0.99$). Excitation spectra obtained for emission at 662 nm were found to be the optimal data to use, which makes sense when comparing to the fluorescence landscape of chlorophyll A in Appendix A. A further exploration of the autofluorescence of olive oils proved that the obtained fluorescence signal most likely could be assigned to tocopherol, polyphenols, riboflavin and chlorophyllic compounds. This was found in a study, where also front-face and right angle sampling geometry was compared¹⁶².

Recently a few studies have been published, characterising complete autofluorescence landscapes with excitation wavelengths of 250-450 nm and emission recorded up to 700 nm of a wide range of edible oils. Fluorescence from various diluted and undiluted oils was investigated, and the obtained signal was assigned to tocopherol and pigments of the chlorophyll group¹¹⁶. Furthermore, some fluorescence was suggested to originate from polyphenols, and fluorescence appearing with excitation around 350 nm and emission between 400 and 500 nm was shown to arise from thermal oxidation. Inner filter effects were clearly evident in the undiluted oils, as seen by the fact that the tocopherol hardly was detectable in the neat oils, as opposed to the diluted oils, whereas the polyphenolic and thermal induced compounds were considerably diminished upon dilution. Similar fluorescence landscapes were also used for classification of edible oils¹¹⁵.

Multi-way studies

Guimet et al., 2004⁵¹ took one step further and applied PARAFAC in the evaluation of the recorded complete fluorescence landscapes of olive oils. The decomposition of the olive oil fluorescence revealed four different

fluorophores present, of which the far dominating one was assigned to chlorophyll. Two of the derived fluorophores were assumed to be oxidation products with excitation around 350 nm in agreement with previous findings and verified by the fact that they hardly appeared in the virgin olive oils, as opposed to the refined oils. The last PARAFAC component in the study with excitation/emission maximum round 350/525 nm was somehow assigned to tocopherol with reference to the earlier study of olive oils⁷⁹. However this is not in agreement with the fluorescence characteristics of pure tocopherol found in this thesis and in literature⁴⁰.

Cereals

Flour

From the early 1980's fluorescence spectroscopy in combination with PLS regression was used for prediction and classification of botanical tissue components of complex wheat flour samples⁶⁵. The classification was based on excitation at 275, 350 and 450 nm, yielding fluorescence emission maximum at 335, 420 and 520 nm, respectively. The fluorescence was assigned to aromatic amino acids (ex. 275 nm) and ferulic acid (ex. 350 nm). The fluorescence peak at 450/520 nm was not assigned in the study, but could perhaps origin from riboflavin (cf. Appendix A), as later verified in a study of wheat flour fluorescence, where a standard addition technique was used for validation of this assignment¹⁶³. The assigned ferulic acid fluorescence and the fluorescence peak presumably from riboflavin was later applied in several studies monitoring wheat flour refinement and milling efficiency using fluorescence imaging¹³⁷⁻¹⁴⁰. Zandomeneghi, 1999, investigated the intrinsic fluorescence of cereal flour more thoroughly and worked on optimising the conditions for recording front-face fluorescence from intact samples¹⁶¹. He found three major fluorescence peaks present in the flour samples, similar to the ones previously described; one was assigned to amino acids and later another one to riboflavin¹⁶³. The signal previously assigned to ferulic acid was not assigned in this study, but vaguely suggested to origin from vitamin E or B6. In paper III, fluorescence landscapes of oatmeal samples were obtained in order to monitor oxidative changes. The obtained fluorescence signal was comparable to the findings in flour samples and assigned to tryptophan, riboflavin and an oxidation product.

Beer

In 1995 a patent suggested to use autofluorescence as a novel and rapid method for monitoring of bitterness in beer¹⁴¹, as pursued in Paper I²⁹. Bitterness in beer is determined from the amount of the iso-alpha acids, which originate from hops. Thus, fluorescence was suggested for quantification of these presumable fluorescent bitter acids, which normally appear in concentrations around 10-40 ppm in beer. An alternative approach towards bitterness determination in beer was proposed by Tomlinson et al., 1995¹⁴⁴, using europium-induced delayed fluorescence to detect the amount of iso-alpha acids in beer. This technique implies a sample preparation by addition of europium in order to amplify the fluorescence from the bitter acids and separate it from the background fluorescence through a delay, as described in Paper I²⁹. The sample preparation step obviously makes the approach somewhat more cumbersome compared to measuring autofluorescence of intact beer. However, the method is still considered to be much faster than the traditional bitterness determination of beer that involves an extraction step. The topic is of commercial interest since the traditional method today is carried out as a routine quality control analysis in all modern breweries.

A more thorough description of the intrinsic fluorescence in beer was reported by Apperson et al., 2002⁷, suggesting that the complex fluorescence characteristics of beer arise from amino acids, complex polyphenols and iso-alpha acids. The findings were to some extent was resembled in Paper I²⁹; however the fluorescence contribution from the bitter acids did not appear obvious upon visual inspection of the signal. In a recent study of fluorescence landscapes of beer¹¹⁴, classification of beers was performed based on their intrinsic fluorescence characteristics. The obtained fluorescence signal from the beer was suggested to originate from aromatic amino acids, NADH, riboflavin and vitamin B₆.

Fruit

Chlorophyll fluorescence has for several decades been considered as an intrinsic probe of the photosynthesis in plants^{46,109}. Thus, chlorophyll fluorescence has been suggested as a tool for evaluating the heat tolerance of tropical fruits¹⁶⁰, changes in apples during maturation, ripening and senescence¹²¹, the quality of apple juice during processing³³ as well as the

ripening of papaya fruit²³ among many others. The mentioned studies all evaluate the fluorescence measurements by calculating various fluorescence indices or ratios and comparing them univariately to the quality parameters. A few studies implied a multivariate approach when performing classification of apples using fluorescence imaging³² and predicting mealiness in apples with fluorescence kinetics⁹⁶.

Chlorophyll, giving rise to fluorescence found in plants can be considered to be of special interest due to the fact that the chlorophyll can be retrieved in food products during processing and in several steps throughout the food chain, as seen from the presence of chlorophyll found in fluorescence studies of dairy products¹⁵⁵ and fish oil¹⁰¹.

The autofluorescence of apple juice has also been explored, based on excitation at 265 and 315 nm. The obtained fluorescence emission spectra evaluated using PCA and PLS models, was used for classification according to variety and related to maturity of the apples¹¹¹.

Sugar

Several examples of application of fluorescence and chemometrics in analysis of sugar have been published within the last decade, and the area has somehow pioneered in the field of applying multi-way models to autofluorescence landscapes within food science. Fluorescence analyses of sugar and sugar solution are all based on measuring the impurities in the sugar, since sucrose itself does not possess fluorescence. The foundation for applying fluorescence in analysis of sugar was discovered many years ago, as the purity of sugar samples already in the 1940's was evaluated based on a visual inspection of the fluorescence arising upon illumination with ultraviolet light⁹⁸. This kind of quality control was further investigated and approached more scientifically in 1995 where fluorescence of crystalline beet sugar and beet sugar juices was recorded and evaluated with chemometrics^{98,99}. The fluorescence emission spectra upon excitation of 230, 240, 290 and 330 nm was concatenated and bilinear multivariate models applied. The fluorescence signal, presumably dominated by the aromatic amino acids, was used for classification of the sugars according to factory and prediction of quality and process parameters. The findings were later verified on sugar solutions⁹⁷ and sugar crystals¹¹.

Multi-way studies

More thorough investigations of the impurities in various sugar juices were carried out the following years, where multi-way chemometrics was applied in the evaluation of fluorescence landscapes of sugar. PARAFAC analyses revealed that four fluorophores was responsible for the fluorescence obtained of beet sugar solutions. Two of the components were assigned to tyrosine and tryptophan originating from the beet, based on their derived fluorescent properties^{21,97}. PARAFAC was also applied specifically on fluorescence landscapes of raw cane sugar¹³ and solid beet sugar¹⁰. Further investigation of the underlying fluorescence phenomena in various sugar and sugar juice samples were carried out by comparing the decomposed fluorescence components to chromatographic separation of sugar solution^{9,12}. The fluorescence was suggested to arise from colorant polymers formed in Maillard reactions during the sugar processing and a polyphenolic compound in addition to the more obvious assignments of tyrosine and tryptophan. The practical feasibility for on-line monitoring of sugar juice using fluorescence spectroscopy and chemometrics has also been demonstrated at a sugar refinery plant³⁰. However, to my knowledge, the technique has not yet been applied commercially in process control.

Biotechnology

The potential of using fluorescence landscapes (typically referred to as two-dimensional fluorescence within biotechnology) to monitor bioprocesses has been described in several studies, mainly based on the fluorescence from tryptophan, NADH and riboflavin. Thus, fluorescence measurements with excitation from 250 to 550 nm and emission in the range 300-600 nm was suggested for on-line monitoring of cultivations of yeast^{84,88}. High correlation to tyrosine and serine (indirectly) concentration was found in a fluorescence study of a chromatographic separation of molasses⁵⁴, and a bacterial denitrification process was monitored using NADH fluorescence⁸².

All the mentioned studies were evaluated by correlating single excitation-emission wavelength to changes in the biomass. Within this century, chemometrics has been more applied in the evaluation of 2D fluorescence in biotechnological studies. Various cultivations and fermentations have been followed with on-line fluorescence probes, and multivariate regression models to process variables like content of biomass, protein and the composition of exhaust gas has been performed successfully^{16,53,94,103,117}.

Multi-way studies

So far, only one study can be found that address the evaluation of fluorescence landscapes of a fermentation processes with a multi-way approach. Haack et al., 2004⁵² performed an on-line monitoring of a yeast cultivation and applied PARAFAC on the obtained fluorescence data with excitation range 270-550 nm and emission from 310 to 590 nm. The PARAFAC model decomposed the complex fluorescence matrix into three distinct fluorophores that was assigned to tryptophan, NADH and riboflavin. The assignment was verified by comparing the derived PARAFAC components with the fluorescence of the pure fluorophores, which increases the reliability of the assignment considerably and thus underlines the advantage of the multi-way approach.

4. Experimental Food Fluorescence

Fluorescence measurements of a broad variety of intact food products will make up an experimental benchmark for the applications of autofluorescence spectroscopy and chemometrics in the analysis of food as described in the previous chapter.

In this chapter, highlights of the results from the measurements of a series of food relevant fluorophores as well as a series of intact food samples will be presented. A detailed description of these two experiments can be found in Appendix A and B. The data from the experiments is also available on the internet under www.models.kvl.dk, where they serve as the start-up of a “fluorescence food library”. The intention is that such a work of reference can inspire and help scientists that want to start exploring the intrinsic fluorescence of food in the future.

At first, the fluorescence profiles of the measured fluorophores will be presented. Then, a few of the obtained fluorescence landscapes of the intact food samples will be presented, followed by a suggestion for a global PARAFAC model characterising the overall fluorescence phenomena and common fluorescence structures in the food products. The PARAFAC results will be discussed and compared with the fluorescence properties of the pure compounds measured.

Food fluorophores

Fluorescence landscapes of a series of fluorophores were measured in pure solutions. The criteria for selection of the fluorophores were to represent compounds frequently appearing in food, but also practical reasons such as availability and price was determining for the selection. This resulted in a list of eleven fluorophores, representing protein fluorescence, vitamin and cofactor fluorescence and fluorescence from pigments. The documentation

and experimental conditions can be found in Appendix A. The fluorescence properties of the fluorophores can be seen in Figure 15 in the form of contour plots of the fluorescence landscapes. The aromatic amino acids, phenylalanine, tyrosine and tryptophan all show fluorescence in the UV region with excitation maxima below 300 nm and are slightly overlapping, but demonstrated separable in mixtures, when using multi-way chemometrics²⁰.

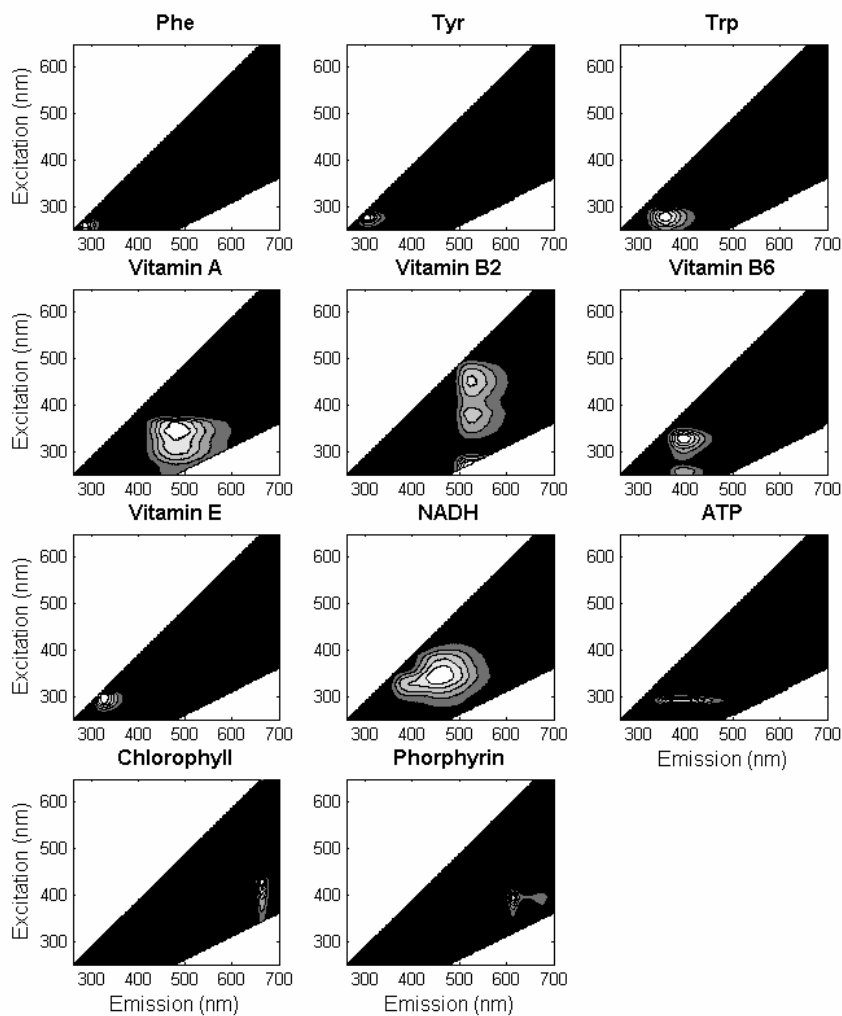


Figure 15. Fluorescence landscapes of the eleven measured food relevant fluorophores.

Protein fluorescence is normally dominated by tryptophan, because it has high quantum yield, and the fact that energy absorbed by phenylalanine and tyrosine residues can be transferred to tryptophan residues in the same protein⁸⁰.

Vitamin fluorescence is represented by water-soluble vitamin B2, B6 and fat-soluble vitamin A and E as well as the co-factors NADH and ATP. Chlorophyll A and hematoporphyrin are two examples of pigments possessing fluorescence. They both contain a porphine ring structure and belong to the class of chlorophylls. Chlorophyll is present in plants and porphyrins are involved in many biological and physiological processes in practically all living cells. Both compounds yield fluorescence in the visible wavelength range with emission above 600 nm, separating them spectrally from the other compounds measured here.

Fluorescence of intact food samples

When measuring autofluorescence of intact food samples, the ideal conditions for measuring trilinear spectroscopic data might not be fulfilled. The concentration levels are not always in the appropriate linear range and a broad variety of absorbing species and quenching phenomena can appear in the complex chemical systems of food. Nevertheless, this is the selected approach under investigation in this study. The complex fluorescence patterns from fluorescence landscapes of food samples can be considered with two parallel approaches; as an *ideal additive fluorescence system* or as a *spectral fingerprint*.

1. Ideal fluorescence system. The fluorescence from food systems can be considered as an ideal trilinear data system. The complexity is ignored, and trilinear resolution techniques applied. An example of a food product yielding more or less ideal autofluorescence, with respect to trilinearity, quenching etc., is solutions of refined sugar, which is described thoroughly using fluorescence spectroscopy⁸. The sucrose itself does not fluoresce and sugar products normally contain less than 0.1 ‰ impurities (i.e. not sucrose). Hence, sugar can be considered as a dilution of the impurities in low concentrations, appropriate for fluorescence measurements as is.
2. Spectral fingerprint. The complex fluorescence pattern can also be approached more pragmatically and considered as a chemical fingerprint characterising the sample based on its intrinsic

fluorescence characteristics as well as on its absorbing and quenching abilities, as formulated by Munck, 1998⁹⁷. In this way, also classifications^{73,98} and indirect correlations to quality parameters¹⁰¹ can be considered.

A combination of the two described approaches will be used in this work. In the data analysis, the fluorescence data will be handled as if they are trilinear data and PARAFAC decomposition will be applied, even though the conditions might at all not be strictly fulfilled. However, this way of data analysis generate very detailed information about the intrinsic fluorescence in the food sample, yet comprising all the factors affecting the shape and reducing the intensity of the fluorescence signal. Hence, in the interpretation of the results, this diversity should be kept in mind, even if the decomposition is applied in order to simplify the obtained fluorescence patterns and focus on the main common structures in data. The approach can also be considered to be truly exploratory⁹⁷, since no pretreatment are applied and the intact food systems is monitored without any prior hypotheses. This work can be considered as a mapping of the steady-state autofluorescence of intact food systems with an exploratory multi-way approach.

Fluorescence landscapes of food products

Fluorescence landscapes of a variety of intact food samples – liquid as well as solid - were measured using a front-face 60° sampling geometry. The food samples were chosen to represent a wide range of food products, including raw vegetables and meat as well as dairy products, juices, beers, wines and a variety of more or less processed products. The experimental conditions and the comprehensive list of samples can be found in Appendix B.

An example of the obtained fluorescence landscapes is seen in Figure 16 showing the fluorescence of a porcine meat sample. It is evident that the overriding fluorescence signal from the meat arises for excitation wavelengths just below 300 nm and emissions between 300 and 350 nm, which can be ascribed to tryptophan. Some vague indications of further signal peaks at higher wavelengths can be discerned, however not really visible in the presented scale. Apparently no fluorescence signal is obtained from collagen in connective and adipose tissue in the meat, as thoroughly described by Swatland^{124,129,131}, Egeland⁴³ and Wold¹⁵² using excitation wavelengths of 365 and 335 nm. The missing contribution is probably due to

low signal relative to the tryptophan fluorescence and the fact that a pure and lean meat slice was sampled.

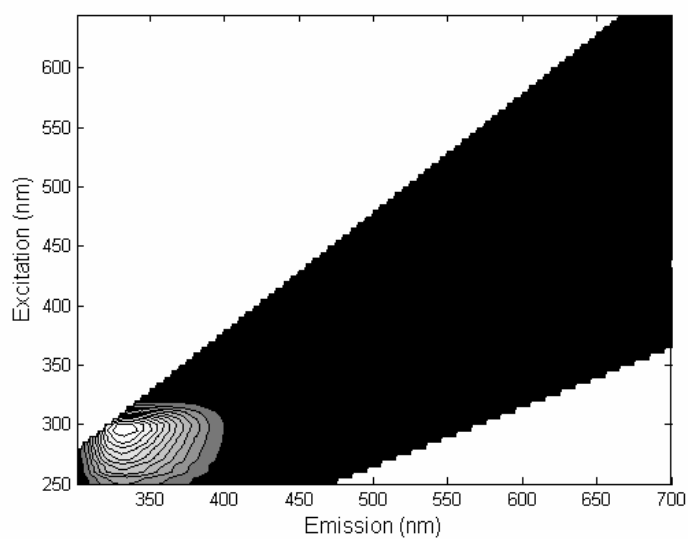


Figure 16. Fluorescence landscape of a porcine meat sample. White indicates the maximum fluorescence intensity in arbitrary units.

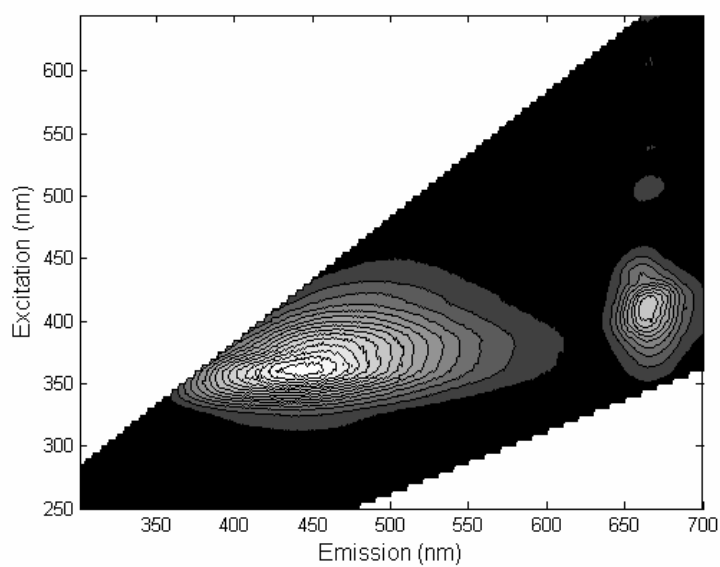


Figure 17. Fluorescence landscape of a rape seed oil sample. White indicates the maximum fluorescence intensity in arbitrary units.

Figure 17 contains another example of a fluorescence landscape of an intact food product, namely rape seed oil. A broad peak or perhaps a combination of more peaks with excitation maximum around 360 nm and emission maximum around 450 nm can be observed. This peak corresponds fairly well to findings in literature for autofluorescence of frying oil (rape seed + palm oil)⁴⁵ olive oils⁵¹ and refined soybean, sunflower and rapeseed oil by Sikorska et al., 2004¹¹⁶, who suggested that fluorescence could arise from polyphenols or as a result of a thermal oxidation. In the latter study, also fluorescence from vitamin E was found present in oils with excitation just below 300 nm and emission 320 nm, especially in diluted oil samples. Apparently no vitamin E fluorescence is measured in the rape seed oil in the present study, probably due concentration quenching combined with a high degree of refinement (which imply an extensive heat treatment) of the oil, which can deteriorate the vitamin¹¹⁶. Furthermore, one major peak and some more vague ones appear in the fluorescence landscape with emission just above 650 nm, also in agreement with previous findings, resembling the fluorescence properties of chlorophyllic compounds (compared with the fluorescence landscapes of chlorophyll A and hematoporphyrin in Appendix A).

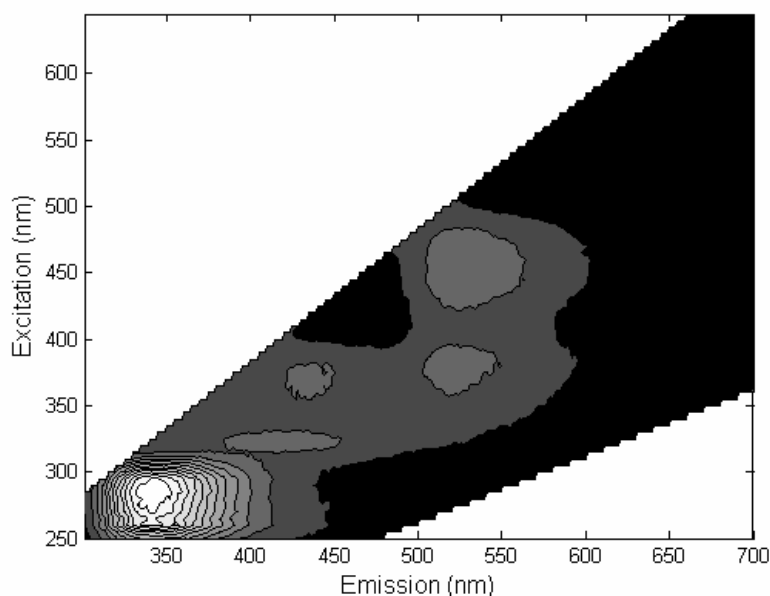


Figure 18. Fluorescence landscape of a milk sample (1.5 % fat). White indicates the maximum fluorescence intensity in arbitrary units.

Finally, as an example of fluorescence from dairy products, the fluorescence properties of a milk sample are depicted in Figure 18. Here, several fluorescence peaks (five major peaks) are observed and assignments can be made. As with the meat sample the main contribution yielding the highest fluorescence intensity arises from protein fluorescence, dominated by tryptophan. The two peaks with fluorescence emission around 520 nm can be ascribed to riboflavin, as reported by Wold¹⁴⁹ and also observed for yogurt in Paper II and IV. The peak with excitation between 300 and 350 nm and emission between 400 and 450 nm has previously been assigned to vitamin A³⁹. The remaining fluorescence peak with excitation/emission maxima around 360/440 nm corresponds very well to the fluorescence properties of a riboflavin oxidation product suggested in Paper IV in yogurt. However it is also possible that the signal arise from a fluorescent advanced Maillard product, which has been suggested to appear in milk after heat treatment¹⁵.

The full list of fluorescence landscapes of all the food samples can be found in Appendix B.

Global PARAFAC of all food products

A PARAFAC model comparing all the fluorescence landscapes was developed in order to get an overview of the fluorescent substances in the food products and to explore the common structures in the data. Obviously the food samples makes up a very heterogeneous sample set, which is perhaps not optimal for a joint decomposition model. However, the PARAFAC “exercise” was performed - with the aim to take the method to the limit and demonstrate its feasibility to map the measurable fluorescence phenomena present in intact food samples.

A PARAFAC model developed with non-negativity constraints and with eight factors was considered optimal and presented here. Modelling details on the developed PARAFAC model can be found in Appendix B.

PARAFAC loadings

The resulting PARAFAC model with eight factors are shown in Figure 19, where the derived excitation and emission loadings for all eight components are depicted in the form of reconstructed fluorescence landscapes, made from multiplication of each of the normalized excitation and emission loadings.

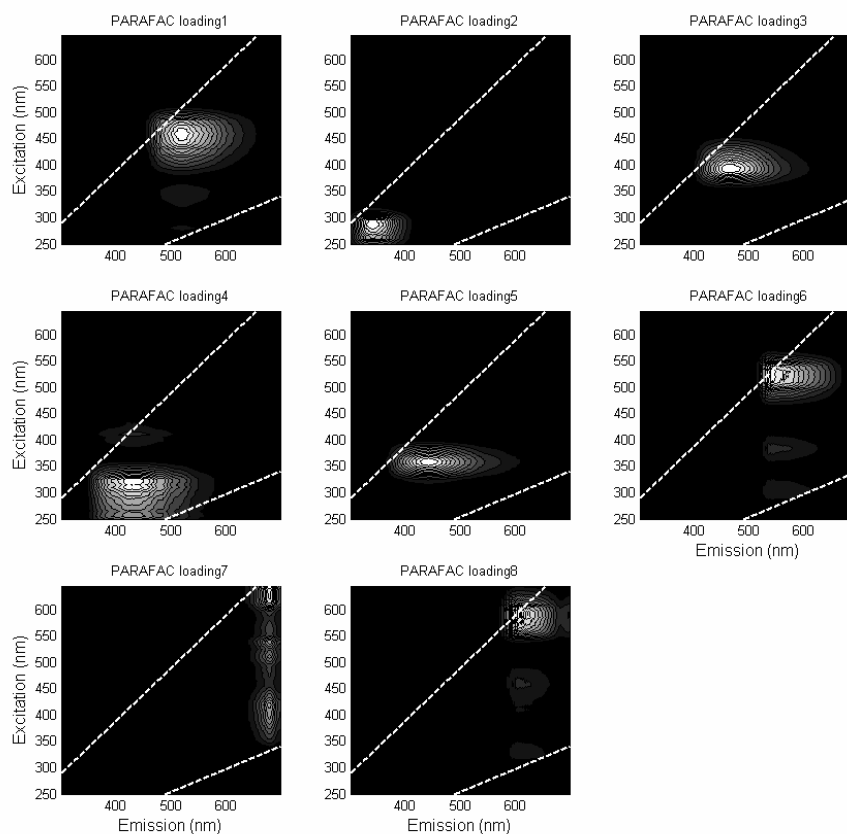


Figure 19. PARAFAC component 1 to 8 of a model on 26 fluorescence landscapes of intact food samples with 8 PARAFAC factors. The shown "fluorescence loadings" is the product of each of the excitation and emission loadings. The white dotted lines indicate the area in which fluorescence is measured.

Inspection of the fluorescence peaks in the loadings indicates that the first component can be ascribed to riboflavin and the second component to tryptophan fluorescence. In Figure 20, the derived excitation and emission profiles of these two first PARAFAC components are shown together with the profiles of the two pure compounds. It is evident that the suggested tryptophan component matches the fluorescence profile of the pure compound fairly well, whereas the suggested riboflavin component differs

considerably from the ideal fluorescent properties of riboflavin. The emission profile of the PARAFAC riboflavin component is somewhat broader, which partly can be ascribed to the fact that the emission slit width was 5 nm larger for the measurements of the food samples. The structure of the derived PARAFAC excitation loading looks quite different from that of riboflavin, but the three same peaks seems to be appear at approximately the same wavelength; however in very different proportions. The small shifts in the wavelength and the alterations in structure can be explained by all the absorbing, quenching, reflecting and scattering phenomena present in the intact food samples, which make the resulting fluorescence signal a chemical fingerprint rather than an ideal mixture of fluorophores, as discussed earlier. An additional complication is that the sampling geometry was different for the food samples and the pure fluorophores.

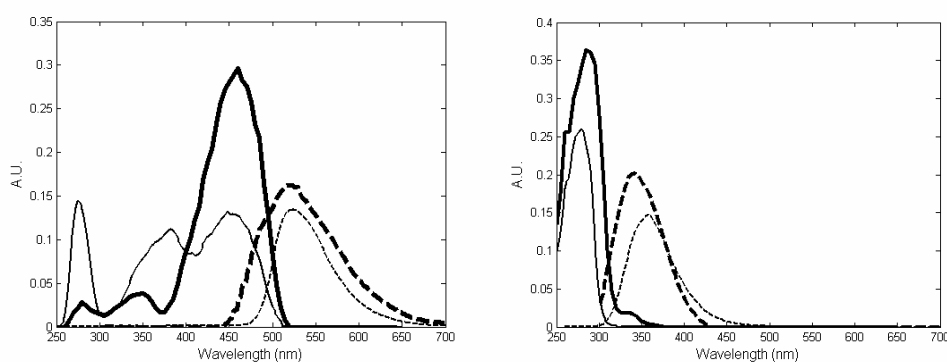


Figure 20. Excitation (full line) and emission loadings (dashed line) for the first (left) and second (right) PARAFAC component (thick line) and the spectral profile for a pure solutions (thin line) of riboflavin (left) and tryptophan (right). PARAFAC model was computed with 8 factors from fluorescence landscapes of 26 food samples.

The remaining six PARAFAC components are more challenging to identify. Component four and five could with some good intensions be associated with the fluorescence of vitamin A, vitamin B6 or NADH, when compared to their fluorescence landscapes in Figure 15. Component seven can unambiguously be ascribed to fluorescence from a chlorophyllic compound. The derived PARAFAC component is quite similar to the fluorescence properties of chlorophyll A, as shown in Figure 15. PARAFAC component

eight also describes fluorescent compounds with emission above 600 nm which could indicate that also a compound with a porphine ring is responsible for this contribution to the fluorescence signal.

PARAFAC scores and loadings

Inspection of the score values from the food sample provides a more complete evaluation of the PARAFAC model. Figure 21 shows the score values of nine selected food samples (The complete list can be found in Appendix B). The first PARAFAC component suggested to be riboflavin are as expected present in milk, indicated by the fact that the milk sample has a high score value for this PARAFAC component, supporting knowledge that this fluorophore contributes considerably to the fluorescence of milk. From Figure 21 it is evident that riboflavin apparently also gives rise to fluorescence signal in the beer and oatmeal samples as well as a minor contribution in the green olive. This make common sense since riboflavin is known to appear in cereals and riboflavin fluorescence has previously been investigated in wheat¹⁶³ and beer^{41,114}.

Tryptophan fluorescence in the form of the second PARAFAC component dominates as expected the animal food products. The milk, cheese, meat and to a lesser extent the butter sample has high score values for this component, which also contributes to the fluorescence obtained from oatmeal, in agreement with the findings in Paper III. The oatmeal sample has high scores values for most of the derived components, not because it yielded a high fluorescence intensity, since all the fluorescence landscapes were normalized to their maximum fluorescence intensity prior to the PARAFAC modelling. On the other hand, the oatmeal yielded a very low and broad fluorescence signal (cf. Appendix B) probably due to a considerable amount of reflected light from the surface of the oatmeal grains.

No tryptophan fluorescence is apparently measured in the beer sample, which is surprising compared to the findings in Paper I, where tryptophan is responsible for the major autofluorescence signal from diluted beers. This turns out to be another example of fluorescence concentration quenching, which confirms the findings by Apperson et al., 2002⁷, where the tryptophan fluorescence only appear upon dilution of the beer sample.

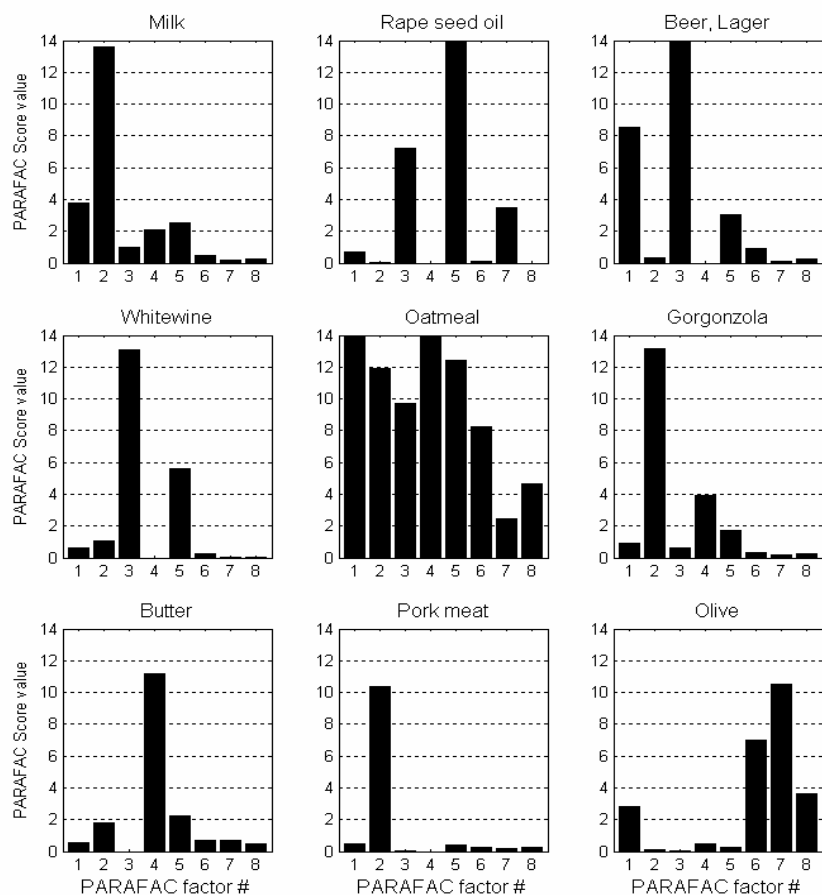


Figure 21. Score values for 9 selected food samples from a PARAFAC model with 8 factors made on the fluorescence landscapes of 26 food samples. Each plot represents a food sample with 8 bars giving the scores value (relative concentration) of each of the 8 PARAFAC components.

The third PARAFAC component is only present in plant derived products: rape seed oil, beer, white wine and oatmeal and could be assigned to polyphenolic compounds, as previously suggested^{7,116}.

Vitamin A is assigned as the fourth PARAFAC component. As mentioned above the fluorescence profile resemble to some extent that of vitamin A,

and the fact that this component primarily appears in all the dairy products, as described in the literature^{38,57,71} supports the hypothesis.

The fifth PARAFAC component is as component three present in all plant derived processed products, but also present in the dairy products. The fluorescence profile of this component resembles the fluorophore present in refined oils and the oxidation production derived upon thermal treatment¹¹⁶, suggesting that this compound arise from the refinement process, most likely the heat treatment. Therefore, assignment of this PARAFAC component is a product associated with a thermal process leading to oxidation or Maillard products, as suggested for milk¹⁵. Having the experimental conditions and the heterogeneity of the sample set in mind, it is also a possibility that the common fluorescence structure in this PARAFAC component arise from a coincidence of two or more fluorescent substances with more or less identical fluorescent profiles, as indicated by the fact that the fluorescence properties of this component also resembles the peak assigned to the riboflavin oxidation product in Paper II.

Table 2. List of properties of PARAFAC components from a model with eighth factors based on fluorescence landscapes of all 26 intact food samples.

PARAFAC component	EX λ_{\max}	EM λ_{\max}	Suggestions for fluorophore
1	460	523	Riboflavin
2	285	341	Tryptophan
3	395	469	Polyphenol
4	325	423	Vitamin A
5	360	443	Process derived product
6	530	541	Unknown, red
7	645	679	Chlorophyll1
8	585	605	Chlorophyll2

In Table 2, the wavelength maxima and suggested assignments is listed for all eight PARAFAC factors. No suggestions for PARFAC component six will be given. This component is apparently both absorbing and emitting light in the greenish wavelength area of the light between 500 and 550 nm, which indicate that the responsible fluorophore is red pigmented. This compound

is present in the olive sample and most of the plant food samples according to the scores values in Appendix B.

PARAFAC component seven and eight can be assigned to some chlorophyllic compound, supported by the fact that these fluorophores are expressed in the olive sample and the rape seed oil, where such compounds normally appear and exhibit considerable fluorescence^{50,116}.

Overview of PARAFAC result

To sum up the overall results of the calculated PARAFAC model, a PCA model on the eight PARAFAC score values of all the samples was performed. Ideally this can be considered as an overview of the calculated concentrations of eight different fluorophores. However in this context the absorbing, quenching and reflecting properties are very different for each of the samples and the fluorescence intensity can therefore not directly be translated to concentration, but rather as the relative measurable fluorescence contribution.

The PCA bi-plot of scores and loading for the first four principal components representing 89 % of the variation can be seen in Figure 22, illustrating the overall distribution of the samples and covariation of each of the PARAFAC components/ fluorescence phenomena. From the bi-plot it is evident that the animal food products are grouped separately along PC1, primarily based on their high amount of tryptophan fluorescence. The chocolate has high milk content and appear also in this group, but more surprisingly also potato and carrot are somewhat dominated by tryptophan fluorescence.

The wine, beer, juice and rape seed oil samples appear in another direction in the score plot, dominated by the suggested polyphenol component with low score in PC1 and high score in PC2. All these samples are derived from plants, and are characterized by a light brownish colour, which probably also affect the obtained fluorescence signal and thus which fluorophore will be expressed. The vitamin A PARAFAC component is drawing in the opposite direction in PC2, where the butter, but also the apple and tomato sample has a high contribution from this component, as expected.

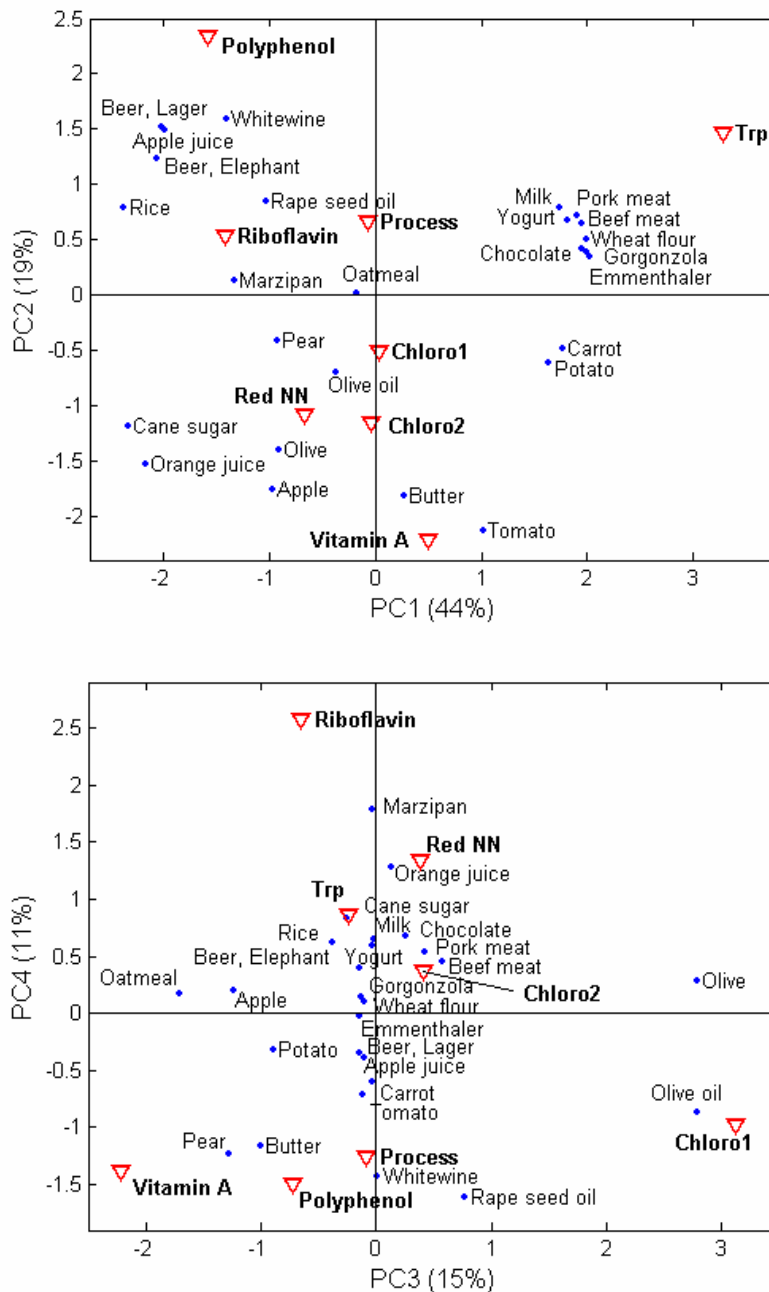


Figure 22. Bi-plot with scores (•) and loadings (v, bold text) of PC1 and PC2 (top) and PC3 and PC4 (bottom) from a PCA model of all PARAFAC scores from a 8 factor model of 26 fluorescence landscapes of intact food samples. Values in brackets indicate the degree of explained variation for each PC.

In PC3 the olive oil and olive sample is separated from the other samples based on their expected high fluorescence from the chlorophyll component. In PC4 the marzipan sample is extreme, apparently with high fluorescence signal from riboflavin. In the opposite direction the PARAFAC components assigned to vitamin A, polyphenol and the process-derived product seems to be somewhat co-varying, as seen for the pear, butter, white wine and rape seed oil sample.

The presented global food fluorescence study ends up in a rough map of the measurable fluorescence signal in food products and the distribution of food according to their autofluorescence properties, which is a product of their content of fluorophores and their absorbing, quenching and reflecting characteristics as well as their pH, hydrophilicity and composition as such. The papers included in the thesis are investigating yogurt, cheese, beer and various dry food products, which make out at least three corners of the food fluorescence map:

- The dairy products (cheese, yogurt) highly dominated by tryptophan fluorescence
- Plant derived liquid food products (beer), dominated by the suggested polyphenolic PARAFAC component
- The investigation of pork scratching, peanuts and oatmeal represent a rather heterogeneous class of products, which all yields a low and broad fluorescence signal, apparently with contribution from many compounds but also affected by a high amount of reflection.

Notes on the presented models

PARAFAC models based on the 26 fluorescence landscapes of intact food samples were calculated with one to thirteen factors and compared. Several criteria were considered in the attempt to determine the appropriate rank of the PARAFAC model, i.e. the number of different fluorophores appearing in the sample set. Core consistency, split-half analyses and a visual inspection of the residuals as well as loadings were considered^{3,20}, leading to the model with eight factors. However, the decision was not very obvious, probably due to the rather unusual composition of the extremely heterogeneous sample set. In fact one can fear that common structures are difficult to find in such data and that each sample contains a series of unique appearing

fluorophores, making the true rank enormous (> 26), which obviously renders this way of modelling irrelevant!

Nevertheless, the modelling exercise was carried through and the core consistency value obtained for the eight-factor model was only 19% but similar values have appeared in apparently sound models³. The split half experiments failed to give exactly equal results since the data set was very difficult to split in representative halves, but fairly similar fluorescent loadings were derived for different subsample sets, though. The crucial point ended up being the critical inspection and interpretation of the PARAFAC loadings, which showed that all eight factors were reasonable and made chemically sense, as discussed above. When expanding the model with more factors, the fluorescence profiles of the derived components were all more or less resembled, but some components appeared to be split into two neighbouring peaks, which indicate some robustness in the modelling. However, systematic residuals could be found in all the calculated models, and some of the systematics disappeared with the splitting of the peaks, which is probably an indication of the high true rank, because the same fluorophore may be expressed differently in two food samples due to differences in quenching, absorbing and reflecting properties. The pragmatic choice of eight components for the PARAFAC model should be considered as a tool for discussion of the inherent fluorescent phenomena, rather than a well-founded spectral curve resolution.

All landscapes were normalized/scaled according to maximum intensity before PARAFAC modelling. Thus, the resulting scores cannot be considered as a term for the fluorescence intensity measured, but rather as the structure of the fluorescence landscape.

The PARAFAC scores were processed with standard normal variate (SNV) scaling prior to the PCA modelling in order to focus on the distribution between the different fluorophores for each sample rather than the general level of the score values; having the scaling of the fluorescence landscapes before the PARAFAC model in mind.

5. Conclusions and Perspectives

The present study demonstrates that the intrinsic fluorescence from intact food systems contains valuable information on the composition and nutritional value of food products. A brief summary of the most common fluorescence characteristics were shown in the overview of food fluorescence. Despite the fact that inherent fluorescence in food materials is scarce compared to for example vibrational spectroscopy, fluorophores from the raw food materials as well as process-induced fluorescent substances have been detected and provide information about the quality of the food product including authenticity and influence of processing.

The presented study of food fluorescence and the literature review on autofluorescence of intact food indicate that fluorescence spectroscopy, as evaluated with chemometrics, holds several possibilities and advantages. The literature survey revealed an increasing amount of research in the field within the last decades. Hopefully, the increasing research activities can address the problems and challenges of fluorescence measurements and further explore the prospects and applications of the method. In this chapter, some perspectives on the use of autofluorescence will be discussed and related to the presented papers. Suggestions for future challenges, technical options and promising application areas will be presented.

Challenges

Fluorescence spectroscopy can be used for monitoring fluorescent molecules and their molecular environment in intact food. The sensitivity to matrix effects holds great promise as an effective probe to study intact food systems. However, the very same sensitivity presents a challenge of using fluorescence spectroscopy as a robust quantitative probe for intact food samples. To obtain robust quantitative analyses it is crucial to have a spectrofluorometer with high reproducibility, giving standardized

fluorescence results. The standardisation or calibration procedure of the instrument/signal needs to be more or less inherent in the instrument if fluorescence probes are to be used for rapid screening methods, possibly for on-line monitoring. In combination with the desire for recording fluorescence landscapes, i.e. several excitation and emission wavelengths for each measurement, the standardisation and configuration of future fluorescence sensors constitute a challenge for instrument producers. The main problem is that fluorescence signal is not recorded relative to incident light beam (I/I_0) as in absorbance spectroscopy wherefore the signal becomes sensitive to light source intensity and spectral characteristics as well as the stability and spectral characteristics of the reference sample.

Efforts towards standardisation with respect to matrix effects have already been made. Combination of fluorescence with reflectance measurements to deal with interfering scattering and absorbing effects has been proposed for fluorescence probes^{131,163}, which then can facilitate fluorescence measurements that in theory only depend on the concentration of the inherent fluorophores in the sample. In this way the fluorescence signal and the background effects can ideally be distinguished and quantified separately, which sounds captivating and promising.

Technical trends and options

It is shown that the two-dimensional nature of fluorescence improves the selectivity of the method. With the application of multi-way chemometrics this inherent data structure of the technique can be utilized in the development of fluorescence sensors and analyses. In Paper II and Paper IV multi-way analysis of fluorescence measurements of dairy products revealed detailed information about the oxidation throughout storage. Assignment of the inherent fluorophores and the understanding of the chemical/physical system were facilitated by the multi-way approach. The next step could be to explore the possibilities for including further dimensions in the fluorescence measurements, which could possibly improve the selectivity even more. Time-resolved fluorescence can make up the extra interesting dimension, as documented in a recent environmental study¹¹², in which PARAFAC was employed in the analysis of four-way fluorescence data and facilitated a separation of a series of polycyclic aromatic hydrocarbons in mixtures.

For liquid samples, several dilution levels of each sample could make out an alternative extra dimension to include in the evaluation of fluorescence data. Inner filter effects in the analyzed samples would actively be addressed in this manner, despite the fact that the linearity of the fluorescence signal in certain dilution regimes will be spoiled. Another extra dimension of fluorescence that could be interesting to explore is the use of polarized light i.e. fluorescence anisotropy. Measurements at different pH values would probably also facilitate a further separation of the fluorescence phenomena in biological samples; however it would obviously imply an invasive pretreatment of the sample. With fluorescence imaging, extra spatial dimensions of fluorescence measurements are supplied^{150,151}, which can be relevant for heterogeneous food samples in order to avoid subsampling. A similar approach is widely used in fluorescence microscopy.

The exploratory approach applied throughout this study has implied the recording of autofluorescence of intact food samples and the use of multivariate and multi-way data analysis. The approach is in contrast to the more traditional use of fluorescence spectroscopy where fluorescence probes are applied in very specific analyses and separation steps are included in the analysis prior to the fluorescence measurement. However, in Paper I addition of europium to beer was suggested in a destructive analysis in order to enhance and change the fluorescence characteristics from the bitter substances in beer and to separate the signal from the background fluorescence. Despite the separation, a multivariate regression models was applied in the evaluation of the europium-induced fluorescence spectra. Thus, the story is an example of a combination of the described approaches, which often with advantage can complement each other. Combination of simple sample preparations and subsequent measurement of fluorescence landscapes and a multivariate or multi-way data analytical approach can be the solution for some problems. Such analyses based on fluorescence spectroscopy can still be performed rapidly compared to more cumbersome separation techniques. The europium case can be considered as a reminder not to be dogmatic in the approach to fluorescence spectroscopy.

Prospective applications

The possibility to perform rapid non-destructive fluorescence analyses in combination with the high sensitivity and specificity makes fluorescence spectroscopy a potential choice as a screening method of food products, both

in food production and in regulatory affairs. Autofluorescence can in some cases compete with time-consuming analyses of trace elements based on high resolution chromatography and tedious extraction steps, as exemplified by the promising results in the development of an indirect dioxin screening method¹⁰¹. The potential for fluorescence spectroscopy in environmental science seems even higher. The infinitely large sampling space that is evident in most environmental problems makes the need for screening methods inevitable in this field. Combined with the fact that several environmentally non-desirable compounds exhibit fluorescence, fluorescence spectroscopy, as evaluated with chemometrics seems obvious for use in environmental studies.

Suggestions for rapid analyses of food products based on autofluorescence are given in Paper I and Paper IV. It was demonstrated that the fluorescence analyses holds the potential to replace traditional methods for determination of the content of compounds in ppm levels in complex food samples. In determination of bitterness in beer (Paper I) as well as riboflavin in yogurt (Paper IV), tedious extraction steps - which are subject to laboratory error - are avoided in the proposed methods. The traditional methods are carried out by measuring absorbance and fluorescence, respectively, at single wavelengths subsequent to the extraction step. Hence, the approach is simply to replace the chemical extraction with a kind of mathematical extraction, as performed by the multivariate data analysis of the complex fluorescence signal.

Food authenticity is a term which refers to whether food purchased by the consumer matches its description. Recently, the development of rapid methods for directly confirming the authenticity of food and food ingredients has become an important research area. Branded, high-quality and processed products with a geographic affiliation such as various kinds of wine, meat, cheese, honey, olive oil and fruit purées are in considerable demand and command premium prices. Therefore such products are vulnerable to economic adulteration. Because of the high sensitivity, fluorescence spectroscopy has the potential to reveal minor differences in food products that can be related to its authenticity, as demonstrated in a few recent studies on cheese^{72,73}. The combination of the content of the fluorophores in low concentration levels, their molecular environment and the interfering food matrix makes up a unique fluorescence fingerprint, which can be used in analysis of food authenticity.

In 2002, the Office of Pharmaceutical Science of the U.S Food and Drug Administration (FDA) launched the Process Analytical Technology (PAT) initiative³⁴. FDA's definition of PAT is: *A system for designing, analyzing, and controlling manufacturing through timely measurements (i.e., during processing) of critical quality and performance attributes of raw and in-process materials and processes with the goal of ensuring final product quality.* The PAT strategy calls for relevant tools for process control, and in this context spectroscopy and multivariate data analysis are obvious candidates because of the ability to perform analyses on-line at site and to handle complex chemical systems. Recently, the FDA published a guide for implementation of PAT in pharmaceutical production, and thereby encouraged the industry to develop and implement new tools for process monitoring as a way of quality control. Fluorescence spectroscopy can possibly play an important role in this development, since the technique has some promising possibilities in analysis or on-line monitoring of biotechnological processes and production, as described in the literature review in Chapter 3. The PAT initiative was introduced for production for drugs, but the analogy to food production is straightforward.

References

1. Allais, I.; Dufour, E.; Pierre, A.; Viaud, C.; Chevallereau, V.; Curt, C.; Perrot, N. Monitoring the texture of meat emulsions by front-face fluorescence spectroscopy. *Sciences des Aliments* **2003**, *23* (1), 128-131.
2. Allais, I.; Viaud, C.; Pierre, A.; Dufour, E. A rapid method based on front-face fluorescence spectroscopy for the monitoring of the texture of meat emulsions and frankfurters. *Meat Science* **2004**, *67* (2), 219-229.
3. Andersen, C. M.; Bro, R. Practical aspects of PARAFAC modeling of fluorescence excitation-emission data. *Journal of Chemometrics* **2003**, *17* (4), 200-215.
4. Andersen, C. M.; Wold, J. P. Fluorescence of muscle and connective tissue from cod and salmon. *Journal of Agricultural and Food Chemistry* **2003**, *51* (2), 470-476.
5. Andersson, C. A.; Bro, R. The N-way Toolbox for MATLAB. *Chemometric and Intelligent Laboratory Systems* **2000**, *52* (1), 1-4.
6. Appellof, C. J.; Davidson, E. R. 3-Dimensional Rank Annihilation for Multicomponent Determinations. *Analytica Chimica Acta* **1983**, *146* (FEB), 9-14.
7. Apperson, K.; Leiper, K. A.; McKeown, I. P.; Birch, D. J. S. Beer fluorescence and the isolation, characterisation and silica adsorption of haze-active beer proteins. *Journal of the Institute of Brewing* **2002**, *108* (2), 193-199.

8. Baunsgaard, D. Analysis of color impurities in sugar processing using fluorescence spectroscopy and chemometrics. PhD thesis, The Royal Veterinary and Agricultural University, Denmark, Aug 2000.
9. Baunsgaard, D.; Andersson, C. A.; Arndal, A.; Munck, L. Multi-way chemometrics for mathematical separation of fluorescent colorants and colour precursors from spectrofluorimetry of beet sugar and beet sugar thick juice as validated by HPLC analysis. *Food Chemistry* **2000**, *70* (1), 113-121.
10. Baunsgaard, D.; Munck, L.; Norgaard, L. Analysis of the effect of crystal size and color distribution on fluorescence measurements of solid sugar using chemometrics. *Applied Spectroscopy* **2000**, *54* (11), 1684-1689.
11. Baunsgaard, D.; Munck, L.; Norgaard, L. Evaluation of the quality of solid sugar samples by fluorescence spectroscopy and chemometrics. *Applied Spectroscopy* **2000**, *54* (3), 438-444.
12. Baunsgaard, D.; Norgaard, L.; Godshall, H. A. Specific screening for color precursors and colorants in beet and cane sugar liquors in relation to model colorants using spectrofluorometry evaluated by HPLC and multiway data analysis. *Journal of Agricultural and Food Chemistry* **2001**, *49* (4), 1687-1694.
13. Baunsgaard, D.; Norgaard, L.; Godshall, M. A. Fluorescence of raw cane sugars evaluated by chemometrics. *Journal of Agricultural and Food Chemistry* **2000**, *48* (10), 4955-4962.
14. Becker, E. M.; Christensen, J.; Frederiksen, C. S.; Haugaard, V. K. Front-face fluorescence spectroscopy and chemometrics in analysis of yogurt: Rapid analysis of riboflavin. *Journal of Dairy Science* **2003**, *86* (8), 2508-2515.
15. Birlouez-Aragon, I.; Nicolas, M.; Metais, A.; Marchond, N.; Grenier, J.; Calvo, D. A rapid fluorimetric method to estimate the heat treatment of liquid milk. *International Dairy Journal* **1998**, *8* (9), 771-777.

16. Boehl, D.; Solle, D.; Hitzmann, B.; Scheper, T. Chemometric modelling with two-dimensional fluorescence data for *Claviceps purpurea* bioprocess characterization. *Journal of Biotechnology* **2003**, *105* (1-2), 179-188.
17. Booksh, K. S.; Kowalski, B. R. Comments on the Data-Analysis (Datan) Algorithm and Rank Annihilation Factor-Analysis for the Analysis of Correlated Spectral Data. *Journal of Chemometrics* **1994**, *8* (4), 287-292.
18. Booksh, K. S.; Muroski, A. R.; Myrick, M. L. Single measurement excitation/emission matrix spectrofluorometer for determination of hydrocarbons in ocean water. 2. Calibration and quantitation of naphthalene and styrene. *Analytical Chemistry* **1996**, *68* (20), 3539-3544.
19. Bro, R. Multivariate calibration - What is in chemometrics for the analytical chemist? *Anal. Chim. Acta* **2003**, *500* (1-2), 185-194.
20. Bro, R. PARAFAC. Tutorial and applications. *Chemometrics and Intelligent Laboratory Systems* **1997**, *38* (2), 149-171.
21. Bro, R. Exploratory study of sugar production using fluorescence spectroscopy and multi-way analysis. *Chemometrics and Intelligent Laboratory Systems* **1999**, *46* (2), 133-147.
22. Bro, R.; Sidiropoulos, N. D.; Smilde, A. K. Maximum likelihood fitting using simple least squares algorithms. *Journal of Chemometrics* **2002**, *16* (8-10), 387-400.
23. Bron, I. U.; Ribeiro, R. V.; Azzolini, M.; Jacomino, A. P.; Machado, E. C. Chlorophyll fluorescence as a tool to evaluate the ripening of 'Golden' papaya fruit. *Postharvest Biology and Technology* **2004**, *33* (2), 163-173.
24. Brondum, J.; Munck, L.; Henckel, P.; Karlsson, A.; Tornberg, E.; Engelsen, S. B. Prediction of water-holding capacity and composition of porcine meat by comparative spectroscopy. *Meat Science* **2000**, *55* (2), 177-185.

25. Callis, J. B.; Johnson, D. W.; Christian, G. F.; Davidson, E. R. Multidimensional, Multicomponent Fluorescence Analysis with A Video Fluorometer. *Abstracts of Papers of the American Chemical Society* **1978**, 176 (SEP), 5.
26. Carroll, J. D.; Chang, J. Analysis of individual differences in multidimensional scaling via an N-way generalization of 'Eckart-Young' decomposition. *Psychometrika* **1970**, 35, 283-319.
27. Chen, W.; Westerhoff, P.; Leenheer, J. A.; Booksh, K. Fluorescence excitation - Emission matrix regional integration to quantify spectra for dissolved organic matter. *Environmental Science & Technology* **2003**, 37 (24), 5701-5710.
28. Christensen, J.; Becker, E. M.; Frederiksen, C. S. Fluorescence spectroscopy and PARAFAC in the analysis of yogurt. *Chemometrics and Intelligent Laboratory Systems* **2005**, 75 (2), 201-208.
29. Christensen, J.; Ladefoged, A. M.; Norgaard, L. Determination of bitterness in beer using fluorescence spectroscopy and chemometrics. *Journal of the Institute of Brewing* **2005**, 111 (1).
30. Christensen, J.; Norgaard, L.; Lindemann, C.; Bagherpour, K. On-line process control of sugar juice using fluorescence spectroscopy and chemometrics. LMC Conference Poster 2002.
31. Christensen, J.; Povlsen, V. T.; Sorensen, J. Application of fluorescence spectroscopy and chemometrics in the evaluation of processed cheese during storage. *Journal of Dairy Science* **2003**, 86 (4), 1101-1107.
32. Codrea, M. C.; Nevalainen, O. S.; Tyystjarvi, E.; Vandeven, M.; Valcke, R. Classifying apples by the means of fluorescence imaging. *International Journal of Pattern Recognition and Artificial Intelligence* **2004**, 18 (2), 157-174.

33. Cohen, E.; Birk, Y.; Mannheim, C. H.; Saguy, I. S. A rapid method to monitor quality of apple juice during thermal processing. *Food Science and Technology-Lebensmittel-Wissenschaft & Technologie* **1998**, *31* (7-8), 612-616.
34. Davis, J. R.; Wasynczuk, J. The four steps of PAT implementation. *Pharmaceutical Engineering* **2005**, (1-2), 10-22.
35. Diaz, T. G.; Meras, I. D.; Correa, C. A.; Roldan, B.; Caceres, M. I. R. Simultaneous fluorometric determination of chlorophylls a and b and pheophytins a and b in olive oil by partial least-squares calibration. *Journal of Agricultural and Food Chemistry* **2003**, *51* (24), 6934-6940.
36. Dufour, E.; Devaux, M. F.; Fortier, P.; Herbert, S. Delineation of the structure of soft cheeses at the molecular level by fluorescence spectroscopy - relationship with texture. *International Dairy Journal* **2001**, *11* (4-7), 465-473.
37. Dufour, E.; Frencia, J. P.; Kane, E. Development of a rapid method based on front-face fluorescence spectroscopy for the monitoring of fish freshness. *Food Research International* **2003**, *36* (5), 415-423.
38. Dufour, E.; Mazerolles, G.; Devaux, M. F.; Duboz, G.; Duployer, M. H.; Riou, M. N. Phase transition of triglycerides during semi-hard cheese ripening. *International Dairy Journal* **2000**, *10* (1-2), 81-93.
39. Dufour, E.; Riaublanc, A. Potentiality of spectroscopic methods for the characterisation of dairy products. I. Front-face fluorescence study of raw, heated and homogenised milks. *Lait* **1997**, *77* (6), 657-670.
40. Duggan, D. E.; Bowman, R. L.; Brodie, B. B.; Udenfriend, S. A Spectrophotofluorometric Study of Compounds of Biological Interest. *Archives of Biochemistry and Biophysics* **1957**, *68* (1), 1-14.
41. Duyvis, M. G.; Hilhorst, R.; Laane, C.; Evans, D. J.; Schmedding, D. J. M. Role of riboflavin in beer flavor instability: Determination of levels of riboflavin and its origin in beer by fluorometric apoprotein titration. *Journal of Agricultural and Food Chemistry* **2002**, *50* (6), 1548-1552.

42. Egelandsdal, B.; Dingstad, G.; Togersen, G.; Lundby, F.; Langsrud, O. Autofluorescence quantifies collagen in sausage batters with a large variation in myoglobin content. *Meat Science* **2005**, *69* (1), 35-46.
43. Egelandsdal, B.; Kvaal, K.; Isaksson, T. Autofluorescence spectra as related to tensile properties for perimysium from bovine masseter. *Journal of Food Science* **1996**, *61* (2), 342-347.
44. Egelandsdal, B.; Wold, J. P.; Sponnich, A.; Neegard, S.; Hildrum, K. I. On attempts to measure the tenderness of Longissimus Dorsi muscles using fluorescence emission spectra. *Meat Science* **2002**, *60* (2), 187-202.
45. Engelsen, S. B. Explorative spectrometric evaluations of frying oil deterioration. *Journal of the American Oil Chemists Society* **1997**, *74* (12), 1495-1508.
46. Franck, U. F.; Hoffmann, N.; Arenz, H.; Schreibe, U. Chlorophyll Fluorescence As A Signal of Primary Photosynthesis Reactions. *Berichte der Bunsen-Gesellschaft fur Physikalische Chemie* **1969**, *73* (8-9), 871-878.
47. Frencia, J. P.; Thomas, E.; Dufour, E. Measure of meat tenderness using front-face fluorescence spectroscopy. *Sciences des Aliments* **2003**, *23* (1), 142-145.
48. Garimelle Purna, S. K.; Prow, L. A.; Metzger, L. E. Utilization of Front-Face Fluorescence Spectroscopy for Analysis of Process Cheese Functionality. *Journal of Dairy Science* **2005**, *88* (2), 470-477.
49. Geladi, P. Analysis of multi-way (multi-mode) data. *Chemometric and Intelligent Laboratory Systems* **1989**, *7*, 11-30.
50. Guimet, F.; Boque, R.; Ferre, J. Cluster analysis applied to the exploratory analysis of commercial Spanish olive oils by means of excitation-emission fluorescence spectroscopy. *Journal of Agricultural and Food Chemistry* **2004**, *52* (22), 6673-6679.

51. Guimet, F.; Ferre, J.; Boque, R.; Rius, F. X. Application of unfold principal component analysis and parallel factor analysis to the exploratory analysis of olive oils by means of excitation-emission matrix fluorescence spectroscopy. *Analytica Chimica Acta* **2004**, *515* (1), 75-85.
52. Haack, M. B.; Eliasson, A.; Olsson, L. On-line cell mass monitoring of *Saccharomyces cerevisiae* cultivations by multi-wavelength fluorescence. *Journal of Biotechnology* **2004**, *114* (1-2), 199-208.
53. Hagedorn, A.; Legge, R. L.; Budman, H. Evaluation of spectrofluorometry as a tool for estimation in fed-batch fermentations. *Biotechnology and Bioengineering* **2003**, *83* (1), 104-111.
54. Harbeck, C.; Hitzmann, B.; Lindemann, C.; Sosnitza, P.; Faurie, R.; Scheper, T. Use of 2D fluorescence spectroscopy for on-line monitoring of sugar extraction from molasses. *Chemie Ingenieur Technik* **2001**, *73* (7), 861-864.
55. Harshman, R. A. Foundations of the PARAFAC procedure: Models and conditions for an 'explanatory' multi-modal factor analysis. *UCLA working papers in phonetics* **1970**, *16*, 1-84.
56. Herbert, S.; Riaublanc, A.; Bouchet, B.; Gallant, D. J.; Dufour, E. Fluorescence spectroscopy investigation of acid-or rennet-induced coagulation of milk. *Journal of Dairy Science* **1999**, *82* (10), 2056-2062.
57. Herbert, S.; Riou, N. M.; Devaux, M. F.; Riaublanc, A.; Bouchet, B.; Gallant, D. J.; Dufour, E. Monitoring the identity and the structure of soft cheeses by fluorescence spectroscopy. *Lait* **2000**, *80* (6), 621-634.
58. Ho, C. N.; Christian, G. D.; Davidson, E. R. Application of Method of Rank Annihilation to Quantitative-Analyses of Multicomponent Fluorescence Data from Video Fluorometer. *Analytical Chemistry* **1978**, *50* (8), 1108-1113.
59. Ho, C. N.; Christian, G. D.; Davidson, E. R. Application of the Method of Rank Annihilation to Fluorescent Multicomponent Mixtures of Polynuclear Aromatic-Hydrocarbons. *Analytical Chemistry* **1980**, *52* (7), 1071-1079.

60. Ho, C. N.; Christian, G. D.; Davidson, E. R. Simultaneous Multicomponent Rank Annihilation and Applications to Multicomponent Fluorescent Data Acquired by the Video Fluorometer. *Analytical Chemistry* **1981**, 53 (1), 92-98.
61. Hotelling, H. Analysis of a complex of statistical variables into principal components. *Journal Of Educational Psychology* **1933**, 24, 417-441.
62. Huss, H. H.; Sigsgaard, P.; Jensen, S. A. Fluorescence of Fish Bones. *Journal of Food Protection* **1985**, 48 (5), 393-396.
63. Jensen, P. N.; Christensen, J.; Engelsen, S. B. Oxidative changes in pork scratchings, peanuts, oatmeal and muesli viewed by fluorescence, near-infrared and infrared spectroscopy. *European Food Research and Technology* **2004**, 219 (3), 294-304.
64. Jensen, S. A.; Munck, L.; Kruger, J. E. A Rapid Fluorescence Method for Assessment of Pre-Harvest Sprouting of Cereal-Grains. *Journal of Cereal Science* **1984**, 2 (3), 187-201.
65. Jensen, S. A.; Munck, L.; Martens, H. The Botanical Constituents of Wheat and Wheat Milling Fractions .1. Quantification by Autofluorescence. *Cereal Chemistry* **1982**, 59 (6), 477-484.
66. Jensen, S. A.; Reenberg, S.; Munck, L. Method for quality control of products from fish, cattle, swine and poultry. US patent US4631413, Dec 23, 1986.
67. Jiji, R. D.; Andersson, G. G.; Booksh, K. S. Application of PARAFAC for calibration with excitation-emission matrix fluorescence spectra of three classes of environmental pollutants. *Journal of Chemometrics* **2000**, 14 (3), 171-185.
68. Jiji, R. D.; Booksh, K. S. Mitigation of Rayleigh and Raman spectral interferences in multiway calibration of excitation-emission matrix fluorescence spectra. *Analytical Chemistry* **2000**, 72 (4), 718-725.

69. Jiji, R. D.; Cooper, G. A.; Booksh, K. S. Excitation-emission matrix fluorescence based determination of carbamate pesticides and polycyclic aromatic hydrocarbons. *Analytica Chimica Acta* **1999**, 397 (1-3), 61-72.
70. Johnson, D. W.; Ho, C. N.; Callis, J. B.; Christian, G. D. Results of Multicomponent Fluorescence Studies Using Video Fluorometer. *Abstracts of Papers of the American Chemical Society* **1977**, 174 (SEP), 38.
71. Karoui, R.; Dufour, E. Dynamic testing rheology and fluorescence spectroscopy investigations of surface to centre differences in ripened soft cheeses. *International Dairy Journal* **2003**, 13 (12), 973-985.
72. Karoui, R.; Dufour, E.; Pillonel, L.; Picque, D.; Cattenoz, T.; Bosset, J. O. Determining the geographic origin of Emmental cheeses produced during winter and summer using a technique based on the concatenation of MIR and fluorescence spectroscopic data. *European Food Research and Technology* **2004**, 219 (2), 184-189.
73. Karoui, R.; Dufour, E.; Pillonel, L.; Picque, D.; Cattenoz, T.; Bosset, J. O. Fluorescence and infrared spectroscopies: a tool for the determination of the geographic origin of Emmental cheeses manufactured during summer. *Lait* **2004**, 84 (4), 359-374.
74. Karoui, R.; Laguet, A.; Dufour, E. Fluorescence spectroscopy: A tool for the investigation of cheese melting - Correlation with rheological characteristics. *Lait* **2003**, 83 (3), 251-264.
75. Karoui, R.; Mazerolles, G.; Dufour, E. Spectroscopic techniques coupled with chemometric tools for structure and texture determinations in dairy products. *International Dairy Journal* **2003**, 13 (8), 607-620.
76. Kissmeyernielsen, A.; Jensen, S. A.; Munck, L. The Botanical Composition of Rye and Rye Milling Fractions Determined by Fluorescence Spectrometry and Amino-Acid Composition. *Journal of Cereal Science* **1985**, 3 (3), 181-192.

77. Kubista, M.; Sjoback, R.; Eriksson, S.; Albinsson, B. Experimental Correction for the Inner-Filter Effect in Fluorescence-Spectra. *Analyst* **1994**, *119* (3), 417-419.
78. Kulmyrzaev, A.; Levieux, D.; Dufour, E. Front-Face Fluorescence Spectroscopy Allows the Characterization of Mild Heat Treatments Applied to Milk. Relations with the Denaturation of Milk Proteins. *Journal of Agricultural and Food Chemistry* **2005**, *53* (3), 502-507.
79. Kyriakidis, N. B.; Skarkalis, P. Fluorescence spectra measurement of olive oil and other vegetable oils. *Journal of Aoac International* **2000**, *83* (6), 1435-1439.
80. Lakowicz, J. R. *Principles of Fluorescence Spectroscopy*; 2nd ed.; Kluwer Academics: 1999.
81. Leclere, J.; Birlouez-Aragon, I. The fluorescence of advanced Maillard products is a good indicator of lysine damage during the Maillard reaction. *Journal of Agricultural and Food Chemistry* **2001**, *49* (10), 4682-4687.
82. Lee, D.; Hoon Song, S.; Kim, J. H.; Yoo, Y. J. On-line monitoring of the denitrification process by measurement of NADH fluorescence. *Biotechnology Letters* **2002**, *24* (11), 949-952.
83. Leurgans, S. E.; Ross, R. T. Multilinear models: applications in spectroscopy. *Statistical Science* **1992**, *7*, 289-319.
84. Lindemann, C.; Marose, S.; Nielsen, H. O.; Scheper, T. 2-dimensional fluorescence spectroscopy for on-line bioprocess monitoring. *Sensors and Actuators B-Chemical* **1998**, *51* (1-3), 273-277.
85. Lopez, C.; Dufour, E. The composition of the milk fat globule surface alters the structural characteristics of the coagulum. *Journal of Colloid and Interface Science* **2001**, *233* (2), 241-249.
86. Lorber, A. Quantifying chemical composition from two-dimensional data arrays. *Anal. Chim. Acta* **1984**, *164*, 293-297.

87. Marchiarullo, M. A.; Ross, R. T. Factor-Analysis of Chlorophyll Fluorescence in Photosynthetic Systems. *Biophysical Journal* **1982**, 37 (2), A233.
88. Marose, S.; Lindemann, C.; Scheper, T. Two-dimensional fluorescence spectroscopy: A new tool for on-line bioprocess monitoring. *Biotechnology Progress* **1998**, 14 (1), 63-74.
89. Massart, D. L.; Vandeginste, B. G. M.; Buydens, L. M. C.; De Jong, S.; Lewi, P. J.; Smeyers-Verbeke, J. *Handbook of Chemometrics and Qualimetrics: Part A*; 1st ed.; Elsevier: 1997.
90. Mazerolles, G.; Devaux, M. F.; Duboz, G.; Duployer, M. H.; Riou, N. M.; Dufour, E. Infrared and fluorescence spectroscopy for monitoring protein structure and interaction changes during cheese ripening. *Lait* **2001**, 81 (4), 509-527.
91. McNaught, A. D.; Wilkinson, A. *IUPAC Compendium of Chemical Terminology*; 2nd ed.; Blackwell Science: 1997.
92. Moberg, L.; Robertsson, G.; Karlberg, B. Spectrofluorimetric determination of chlorophylls and pheopigments using parallel factor analysis. *Talanta* **2001**, 54 (1), 161-170.
93. Moller, J. K. S.; Parolari, G.; Gabba, L.; Christensen, J.; Skibsted, L. H. Monitoring chemical changes of dry-cured parma ham during processing by surface autofluorescence spectroscopy. *Journal of Agricultural and Food Chemistry* **2003**, 51 (5), 1224-1230.
94. Morel, E.; Santamaria, K.; Perrier, M.; Guiot, S. R.; Tartakovsky, B. Application of multi-wavelength fluorometry for on-line monitoring of an anaerobic digestion process. *Water Research* **2004**, 38 (14-15), 3287-3296.
95. Mortensen, G.; Sorensen, J.; Stapelfeldt, H. Response surface models used for prediction of photooxidative quality changes in havarti cheese. *European Food Research and Technology* **2003**, 216 (2), 93-98.

96. Moshou, D.; Wahlen, S.; Strasser, R.; Schenk, A.; Ramon, H. Apple mealiness detection using fluorescence and self-organising maps. *Computers and Electronics in Agriculture* **2003**, *40* (1-3), 103-114.
97. Munck, L.; Norgaard, L.; Engelsen, S. B.; Bro, R.; Andersson, C. A. Chemometrics in food science - a demonstration of the feasibility of a highly exploratory, inductive evaluation strategy of fundamental scientific significance. *Chemometrics and Intelligent Laboratory Systems* **1998**, *44* (1-2), 31-60.
98. Norgaard, L. Classification and prediction of quality and process parameters of thick juice and beet sugar by fluorescence spectroscopy and chemometrics. *Zuckerindustrie* **1995**, *120* (11), 970-981.
99. Norgaard, L. A multivariate chemometric approach to fluorescence spectroscopy. *Talanta* **1995**, *42*, 1305-1324.
100. Pearson, K. On lines and planes of closest fit to points in space. *Philosophical Magazine* **1901**, *2*, 559-572.
101. Pedersen, D. K.; Munck, L.; Engelsen, S. B. Screening for dioxin contamination in fish oil by PARAFAC and N-PLSR analysis of fluorescence landscapes. *Journal of Chemometrics* **2002**, *16* (8-10), 451-460.
102. Ram, M. S.; Seitz, L. M.; Dowell, F. E. Natural fluorescence of red and white wheat kernels. *Cereal Chemistry* **2004**, *81* (2), 244-248.
103. Rhee, J. I.; Lee, K. I.; Kim, C. K.; Yim, Y. S.; Chung, S. W.; Wei, J. Q.; Bellgardt, K. H. Classification of two-dimensional fluorescence spectra using self-organizing maps. *Biochemical Engineering Journal* **2005**, *22* (2), 135-144.
104. Rinnan, Å. Application of PARAFAC on Spectral Data. PhD thesis, The Royal Veterinary and Agricultural University, Denmark, May 2004.

105. Ross, R. T.; Lee, C. H.; Davis, C. M.; Ezzeddine, B. M.; Fayyad, E. A.; Leurgans, S. E. Resolution of the Fluorescence-Spectra of Plant Pigment-Complexes Using Trilinear Models. *Biochimica et Biophysica Acta* **1991**, *1056* (3), 317-320.
106. Russell, M. D.; Gouterman, M. Excitation-Emission-Lifetime Analysis of Multicomponent Systems .1. Principal Component Factor-Analysis. *Spectrochimica Acta Part A-Molecular and Biomolecular Spectroscopy* **1988**, *44* (9), 857-861.
107. Sanchez, E.; Kowalski, B. R. Tensorial resolution: a direct trilinear decomposition. *Journal of Chemometrics* **1990**, *4*, 29-45.
108. Sanchez, E.; Kowalski, B. R. Generalized Rank Annihilation Factor-Analysis. *Analytical Chemistry* **1986**, *58* (2), 496-499.
109. Schreiber, U.; Groberman, L.; Vidaver, W. Portable, Solid-State Fluorometer for Measurement of Chlorophyll Fluorescence Induction in Plants. *Review of Scientific Instruments* **1975**, *46* (5), 538-542.
110. Schulman, S. G. Luminescence spectroscopy: An overview. In *Molecular luminescence spectroscopy*, 1st ed.; Schulman, S. G., Ed.; John Wiley & sons: 1985; pp 1-29.
111. Seiden, P.; Bro, R.; Poll, L.; Munck, L. Exploring fluorescence spectra of apple juice and their connection to quality parameters by chemometrics. *Journal of Agricultural and Food Chemistry* **1996**, *44* (10), 3202-3205.
112. Selli, E.; Zaccaria, C.; Sena, F.; Tomasi, G.; Bidoglio, G. Application of multi-way models to the time-resolved fluorescence of polycyclic aromatic hydrocarbons mixtures in water. *Water Research* **2004**, *38* (9), 2269-2276.
113. Sharma, A.; Schulman, S. G. *Introduction to Fluorescence Spectroscopy*; 1st ed.; John Wiley & sons: 1999.

114. Sikorska, E.; Gorecki, T.; Khmelinskii, I. V.; Sikorski, M.; De Keukeleire, D. Fluorescence Spectroscopy for Characterization and Differentiation of Beers. *Journal of the Institute of Brewing* **2004**, *110* (4), 267-275.
115. Sikorska, E.; Gorecki, T.; Khmelinskii, I. V.; Sikorski, M.; Koziol, J. Classification of edible oils using synchronous scanning fluorescence spectroscopy. *Food Chemistry* **2005**, *89* (2), 217-225.
116. Sikorska, E.; Romaniuk, A.; Khmelinskii, I. V.; Herance, R.; Bourdelande, J. L.; Sikorski, M.; Koziol, J. Characterization of edible oils using total luminescence spectroscopy. *Journal of Fluorescence* **2004**, *14* (1), 25-35.
117. Skibsted, E.; Lindemann, C.; Roca, C.; Olsson, L. On-line bioprocess monitoring with a multi-wavelength fluorescence sensor using multivariate calibration. *Journal of Biotechnology* **2001**, *88* (1), 47-57.
118. Skjervold, P. O.; Taylor, R. G.; Wold, J. P.; Berge, P.; Abouelkaram, S.; Culioli, J.; Dufour, E. Development of intrinsic fluorescent multispectral imagery specific for fat, connective tissue, and myofibers in meat. *Journal of Food Science* **2003**, *68* (4), 1161-1168.
119. Smilde, A. K.; Doornbos, D. A. 3-Way Methods for the Calibration of Chromatographic Systems - Comparing Parafac and 3-Way Pls. *Journal of Chemometrics* **1991**, *5* (4), 345-360.
120. Solle, D.; Geissler, D.; Stark, E.; Scheper, T.; Hitzmann, B. Chemometric modelling based on 2D-fluorescence spectra without a calibration measurement. *Bioinformatics* **2003**, *19* (2), 173-177.
121. Song, J.; Deng, W. M.; Beaudry, R. M.; Armstrong, P. R. Changes in chlorophyll fluorescence of apple fruit during maturation, ripening, and senescence. *Hortscience* **1997**, *32* (5), 891-896.
122. Stedmon, C. A.; Markager, S.; Bro, R. Tracing dissolved organic matter in aquatic environments using a new approach to fluorescence spectroscopy. *Marine Chemistry* **2003**, *82* (3-4), 239-254.

123. Strasburg, G. M.; Ludescher, R. D. Theory and Applications of Fluorescence Spectroscopy in Food Research. *Trends in Food Science & Technology* **1995**, 6 (3), 69-75.
124. Swatland, H. J. Autofluorescence of Adipose-Tissue Measured with Fiber Optics. *Meat Science* **1987**, 19 (4), 277-284.
125. Swatland, H. J. Measurement of the Gristle Content in Beef by Macroscopic Ultraviolet Fluorometry. *Journal of Animal Science* **1987**, 65 (1), 158-164.
126. Swatland, H. J. Evaluation of Probe Designs to Measure Connective-Tissue Fluorescence in Carcasses. *Journal of Animal Science* **1991**, 69 (5), 1983-1988.
127. Swatland, H. J. Physical Measurements of Meat Quality - Optical Measurements, Pros and Cons. *Meat Science* **1994**, 36 (1-2), 251-259.
128. Swatland, H. J. Prediction of Physical-Properties of Turkey Meat from Ultraviolet Fluorescence Measured Through A Hypodermic Needle. *Archiv fur Tierzucht-Archives of Animal Breeding* **1995**, 38 (4), 437-444.
129. Swatland, H. J. Connective tissue distribution patterns in beef detected by ultraviolet fibre optics. *Food Science and Technology-Lebensmittel-Wissenschaft & Technologie* **1996**, 29 (3), 272-277.
130. Swatland, H. J. Relationships between the back-scatter of polarised light and the fibre-optic detection of connective tissue fluorescence in beef. *Journal of the Science of Food and Agriculture* **1997**, 75 (1), 45-49.
131. Swatland, H. J. Connective and adipose tissue detection by simultaneous fluorescence and reflectance measurements with an on-line meat probe. *Food Research International* **2000**, 33 (9), 749-757.
132. Swatland, H. J.; Barbut, S. Fluorometry via A Quartz-Glass Rod For Predicting the Skin Content and Processing Characteristics of Poultry Meat Slurry. *International Journal of Food Science and Technology* **1991**, 26 (4), 373-380.

133. Swatland, H. J.; Barbut, S. Optical Prediction of Processing Characteristics of Turkey Meat Using Uv Fluorescence and Nir Birefringence (Vol 28, Pg 227, 1995). *Food Research International* **1995**, 28 (4), 325-330.
134. Swatland, H. J.; Findlay, C. J. On-line probe prediction of beef toughness, correlating sensory evaluation with fluorescence detection of connective tissue and dynamic analysis of overall toughness. *Food Quality and Preference* **1997**, 8 (3), 233-239.
135. Swatland, H. J.; Gullett, E.; Hore, T.; Battenham, S. Uv Fiberoptic Probe Measurements of Connective-Tissue in Beef Correlated with Taste Panel Scores for Chewiness. *Food Research International* **1995**, 28 (1), 23-30.
136. Swatland, H. J.; Nielsen, T.; Andersen, J. R. Correlations of Mature Beef Palatability with Optical Probing of Raw Meat. *Food Research International* **1995**, 28 (4), 403-416.
137. Symons, S. J.; Dexter, J. E. Aleurone and pericarp fluorescence as estimators of mill stream refinement for various Canadian wheat classes. *Journal of Cereal Science* **1996**, 23 (1), 73-83.
138. Symons, S. J.; Dexter, J. E. Computer-Analysis of Fluorescence for the Measurement of Flour Refinement As Determined by Flour Ash Content, Flour Grade Color, and Tristimulus Color Measurements. *Cereal Chemistry* **1991**, 68 (5), 454-460.
139. Symons, S. J.; Dexter, J. E. Estimation of Milling Efficiency - Prediction of Flour Refinement by the Measurement of Pericarp Fluorescence. *Cereal Chemistry* **1992**, 69 (2), 137-141.
140. Symons, S. J.; Dexter, J. E. Relationship of Flour Aleurone Fluorescence to Flour Refinement for Some Canadian Hard Common Wheat Classes. *Cereal Chemistry* **1993**, 70 (1), 90-95.

141. Takhar, G.; King, M. Monitoring the colour and bitterness of beer. WO patent 95/21242, 1995.
142. Thygesen, L. G.; Rinnan, Å.; Barsberg, S.; Moller, J. K. S. Stabilizing the PARAFAC decomposition of Fluorescence Spectra by insertion of zeros outside the data area. *Chemometrics and Intelligent Laboratory Systems* **2004**, 71(2), 97-106.
143. Tomasi, G.; Bro, R. A comparison of algorithms for fitting the PARAFAC models. *Computational Statistics & Data Analysis* **2005**, *In press*.
144. Tomlinson, J. B.; Ormrod, I. H. L.; Sharpe, F. R. A Novel Method for Bitterness Determination in Beer Using A Delayed Fluorescence Technique. *Journal of the Institute of Brewing* **1995**, 101 (2), 113-118.
145. Warner, I. M.; Callis, J. B.; Davidson, E. R.; Christian, G. D. Multicomponent Analysis in Clinical-Chemistry by Use of Rapid Scanning Fluorescence Spectroscopy. *Clinical Chemistry* **1976**, 22 (9), 1483-1492.
146. Warner, I. M.; Callis, J. B.; Davidson, E. R.; Gouterman, M.; Christian, G. D. Fluorescence Analysis - New Approach. *Analytical Letters* **1975**, 8 (9), 665-681.
147. Warner, I. M.; Christian, G. D.; Davidson, E. R.; Callis, J. B. Analysis of Multicomponent Fluorescence Data. *Analytical Chemistry* **1977**, 49 (4), 564-573.
148. Warner, I. M.; Davidson, E. R.; Christian, G. D. Quantitative-Analyses of Multicomponent Fluorescence Data by Methods of Least-Squares and Nonnegative Least Sum of Errors. *Analytical Chemistry* **1977**, 49 (14), 2155-2159.
149. Wold, J. P.; Jorgensen, K.; Lundby, F. Nondestructive measurement of light-induced oxidation in dairy products by fluorescence spectroscopy and imaging. *Journal of Dairy Science* **2002**, 85 (7), 1693-1704.

150. Wold, J. P.; Kvaal, K. Mapping lipid oxidation in chicken meat by multispectral imaging of autofluorescence. *Applied Spectroscopy* **2000**, *54* (6), 900-909.
151. Wold, J. P.; Kvaal, K.; Egelanddal, B. Quantification of intramuscular fat content in beef by combining autofluorescence spectra and autofluorescence images. *Applied Spectroscopy* **1999**, *53* (4), 448-456.
152. Wold, J. P.; Lundby, F.; Egelanddal, B. Quantification of connective tissue (hydroxyproline) in ground beef by autofluorescence spectroscopy. *Journal of Food Science* **1999**, *64* (3), 377-383.
153. Wold, J. P.; Mielnik, M. Nondestructive assessment of lipid oxidation in minced poultry meat by autofluorescence spectroscopy. *Journal of Food Science* **2000**, *65* (1), 87-95.
154. Wold, J. P.; Mielnik, M.; Pettersen, M. K.; Aaby, K.; Baardseth, P. Rapid assessment of rancidity in complex meat products by front face fluorescence spectroscopy. *Journal of Food Science* **2002**, *67* (6), 2397-2404.
155. Wold, J. P.; Veberg, A.; Nilsen, A.; Iani, V.; Juzenas, P.; Moan, J. The role of naturally occurring chlorophyll and porphyrins in light-induced oxidation of dairy products. A study based on fluorescence spectroscopy and sensory analysis. *International Dairy Journal* **2005**, *15* (4), 343-353.
156. Wold, S. Spline Functions, A New Tool in Data-Analysis. *Kemisk Tidsskrift* **1972**, *84* (3), 34-37.
157. Wold, S. Chemometrics; What do we mean with it, and what do we want from it? *Chemometric and Intelligent Laboratory Systems* **1995**, *30* (1), 109-115.
158. Wold, S.; Martens, H.; Wold, H. The Multivariate Calibration-Problem in Chemistry Solved by the PLS Method. *Lecture Notes in Mathematics* **1983**, *973*, 286-293.

159. Wolfbeis, O. S. Fluorescence of organic natural products. In *Molecular Luminescence Spectroscopy*, 1st ed.; Schulman, S. G., Ed.; John Wiley & sons: 1985; pp 167-370.
160. Yamada, M.; Hidaka, T.; Fukamachi, H. Heat tolerance in leaves of tropical fruit crops as measured by chlorophyll fluorescence. *Scientia Horticulturae* **1996**, *67* (1-2), 39-48.
161. Zandomeneghi, M. Fluorescence of cereal flours. *Journal of Agricultural and Food Chemistry* **1999**, *47* (3), 878-882.
162. Zandomeneghi, M.; Carbonaro, L.; Caffarata, C. Fluorescence of Vegetable Oils: Olive Oils . *Journal of Agricultural and Food Chemistry* **2005**, *53* (3), 759-766.
163. Zandomeneghi, M.; Carbonaro, L.; Calucci, L.; Pinzino, C.; Gallechi, L.; Ghiringhelli, S. Direct fluorometric determination of fluorescent substances in powders: The case of riboflavin in cereal flours. *Journal of Agricultural and Food Chemistry* **2003**, *51* (10), 2888-2895.

Appendix A: List of Fluorophores

This appendix contains fluorescence landscapes of a number of pure fluorophores, frequently appearing in food products. Pure solutions of the 11 fluorophores listed below were measured. Appropriate concentration levels were chosen for each fluorophore in order to avoid concentration quenching.

An overview of the measured fluorescence landscapes will be presented, and the excitation and emission profiles for each of the compounds will be shown, calculated from a linear decomposition of each of the landscapes, separately.

Table 3. List of compounds measured

Fluorophore	Conc.	EX λ_{\max}	EM λ_{\max}	I_{\max}^*	Measuring range (Ex)	Solvent
Phenylalanine	10^{-3} M	258	284	32	250-320	Water
Tyrosine	10^{-5} M	276	302	28	250-320	Water
Tryptophan	10^{-5} M	280	357	100	250-320	Water
Vitamin A (Retinol)	10^{-5} M	346	480	16	250-380	Iso-octane
Vitamin B2 (Riboflavin)	10^{-5} M	270 (382,448)	518	167	250-510	Water
Vitamin B6 (Pyridoxin)	10^{-5} M	328	393	51	250-360	Water
Vitamin E (α -Tocopherol)	10^{-4} M	298	326	167	250-320	Iso-octane
NADH	10^{-4} M	344	465	16	260-470	Water
ATP	10^{-3} M	292	388	33	260-320	Water
Chlorophyll A	10^{-6} M	428	663	56	340-650	Iso-octane
Hematoporphyrin	10^{-5} M	396	614	27	300-550	Iso-octane

* normalized according to tryptophan

Measuring conditions

Fluorescence landscapes were measured on Perkin Elmer LS50B spectrofluorometer in cuvette with the traditional right-angle sampling geometry. Water was used as solvent, iso-octane when the compound is not soluble in water.

The fluorescence landscapes were measured in different spectral ranges according to Table 3, using an obey-file in the FLDM instrument controlling software. Common measurement parameters:

- Slit width: 5 nm for both excitation and emission light
- Step size: 2 nm for excitation
- Step size: 1 nm for emission

Fluorescence emission was recorded between 1st and 2nd order Rayleigh scatter only. However, no emission above 700 nm was recorded. If any minor Rayleigh scatter appeared in the recorded fluorescence data, it was removed in the preliminary signal processing, before further data analysis.

The measured spectral ranges are selected from full landscapes in order to increase the speed of measurement. For several of the compounds, the complete edges of the fluorescence peak were not recorded due to this selection procedure, meaning that some of the derived spectral profiles are affected by this cut off. As a result the excitation profiles of hematoporphyrin and chlorophyll shows some rather abrupt drops at the edge of the spectra, which can be entirely ascribed to the measuring conditions.

Results

The recorded fluorescence characteristics of all the fluorophores are depicted in Figure 23 and Figure 24, which shows the fluorescence landscapes and the derived excitation and emission profiles, respectively for each of the eleven compounds.

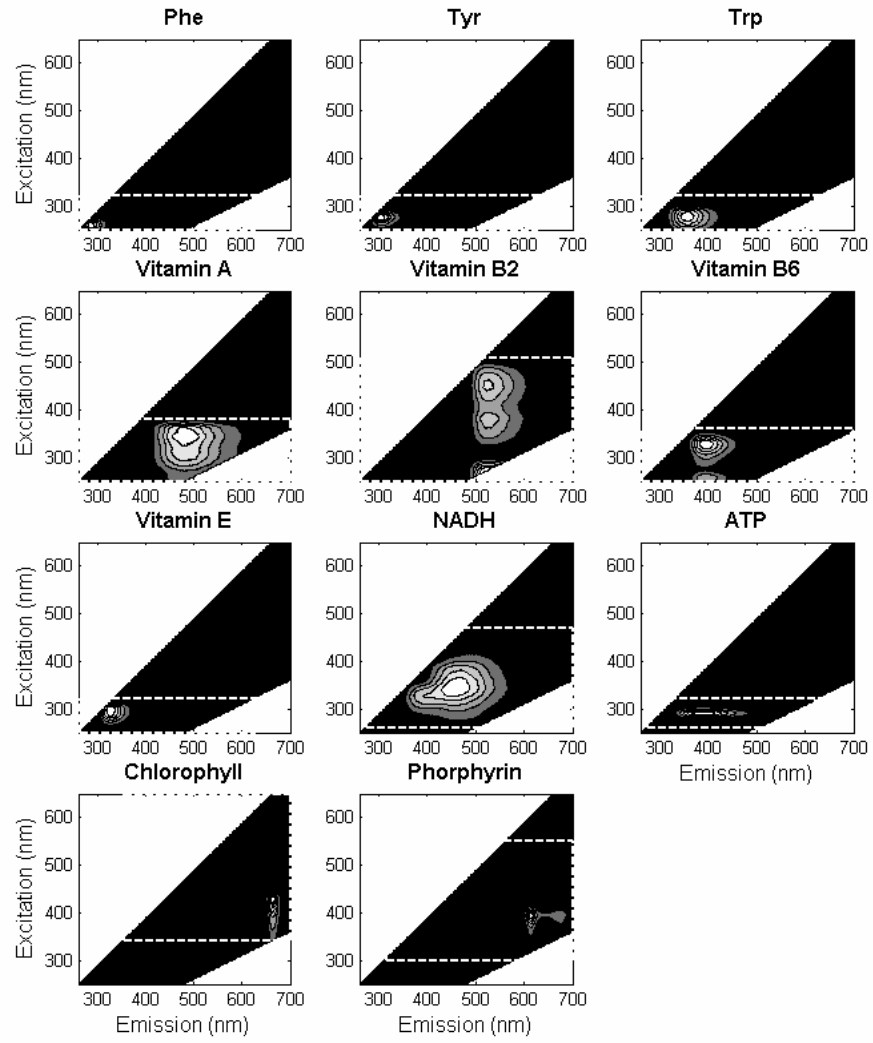


Figure 23. Fluorescence landscapes of each of the 11 pure fluorophores measured. The dotted lines encircle the actual measuring area. The remaining part is simply filled with zeros.

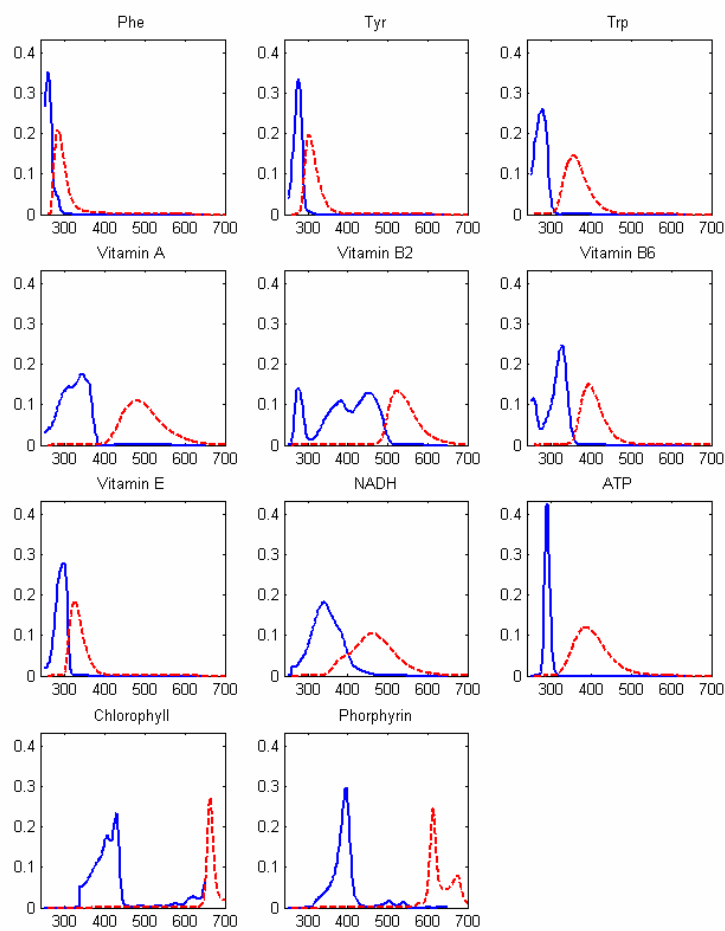


Figure 24. Overview of excitation (full line) and emission (dotted line) profiles of each of the 11 pure fluorophores measured. The profiles (loadings) are derived from a decomposition of each measurement, separately.

Appendix B: Fluorescence landscapes of food products

This appendix contains a list of documentation and the primary results of fluorescence measurements performed on a wide range of food products as well as results from PARAFAC models performed on the complete data set of fluorescence landscapes of 26 food samples.

Measuring conditions

Fluorescence landscapes of a variety of intact food samples – liquid as well as solid - were measured on Perkin Elmer LS50B spectrofluorometer using a front-face solid sample accessory with 60° sampling geometry. Liquid samples were measured in quartz cuvettes and solid samples in small sample cups.

The landscapes were recorded using an obey-file in the FLDM instrument controlling software with following measurement parameters:

- Slit width, excitation: 5 nm
- Slit width, emission: 10 nm
- Step size: 5 nm for excitation
- Step size: 1 nm for emission
- Excitation range: 250-650 nm
- Fluorescence emission was recorded between 1st and 2nd order Rayleigh scatter only. No emission above 700 nm was recorded.

The size of slit widths were chosen in order to obtain a useful fluorescence signal for all samples, but an emission 1% attenuation filter was used for samples yielding too high fluorescence intensity. If any minor Rayleigh scatter appeared in the recorded fluorescence data, it was removed in the preliminary signal processing, before further data analysis.

Samples

Table 4 contains a list of the 26 food products measured, including 10 liquid samples and 16 solid samples.

Table 4. List of samples for fluorescence measurements

Sample	Producer/ Brand	Notes
Milk	Arla	1.5 % fat
Yogurt, plain	Arla	3.5 % fat
Rape seed oil	Coop X-tra	Refined
Olive oil	Svansø organic	Extra virgin, pressed cold
Orange juice	Rynkeby, organic	
Apple juice	Rynkeby	
Soy sauce	Irma	Produced in Japan
Beer, lager	Carlsberg pilsner	4,6 % alc.
Beer, Elephant	Carlsberg Elephant	7.2 % alc.
White wine	Gato Blanco, Chile	Chardonnay, 2003
Rice	Doris	Parboiled
Wheat flour	Fakta	Germany
Cane sugar	Danisco	
Oatmeal	Cerealia, for Fakta	
Emmental	Le fromager	45+ (29 % fat)
Gorgonzola	Galbani	48+ (27 % fat)
Butter	Arla Lurpak	Medium salted
Beef meat		Denmark
Porcine meat		Denmark
Olive, green	Angel Camacho	Spain
Marzipan	Anthon Berg	
Chocolate	Milk chocolate	
Carrot	Lammefjord	Denmark
Potato	Ditta	Denmark
Pear	Conference	Holland
Tomato		Spain
Apple	Pink Lady	Holland

Results

Table 5. List of fluorescence maxima and maximum intensity recorded for all food samples measured

Sample	Filter	EX λ_{\max}	EM λ_{\max}	I_{\max}^*
Milk (1.5 % fat)	√	285	340	6900*
Yogurt, plain (3.5 %)	√	285	341	6200*
Rape seed oil		360	444	812
Olive oil		610	681	643
Orange juice		510	530	53
Apple juice		390	461	57
Soy sauce**		640	685	8
Carlsberg		390	465	242
Elephant		400	489	221
White wine		385	456	199
Rice		410	488	584
Wheat flour		285	338	185
Cane sugar		345	462	56
Oatmeal		285	338	18
Emmental	√	295	354	4500*
Gorgonzola	√	290	346	4300*
Butter		325	407	923
Beef meat		285	326	135
Porcine meat		296	334	888
Olive, green		420	677	170
Marzipan		460	517	488
Chocolate		285	338	20
Carrot		285	360	101
Potato		290	377	218
Pear		290	371	100
Tomato		635	655	46
Apple		510	530	60

*Calculated value; recorded with 1% attenuation, so $I * 100$ is listed

** The soy sauce was not included in the further data analysis, because of the very low and noisy fluorescence signal obtained.

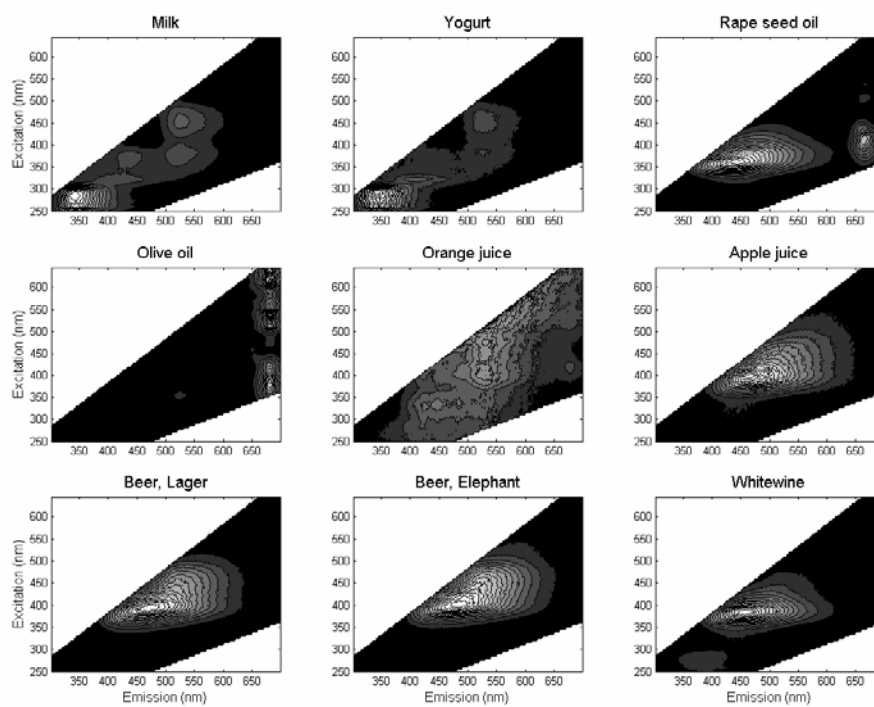


Figure 25. Contour plot of fluorescence landscapes of all liquid food samples. All landscapes are normalized according to maximum intensity. White indicate the maximum fluorescence intensity in arbitrary units.

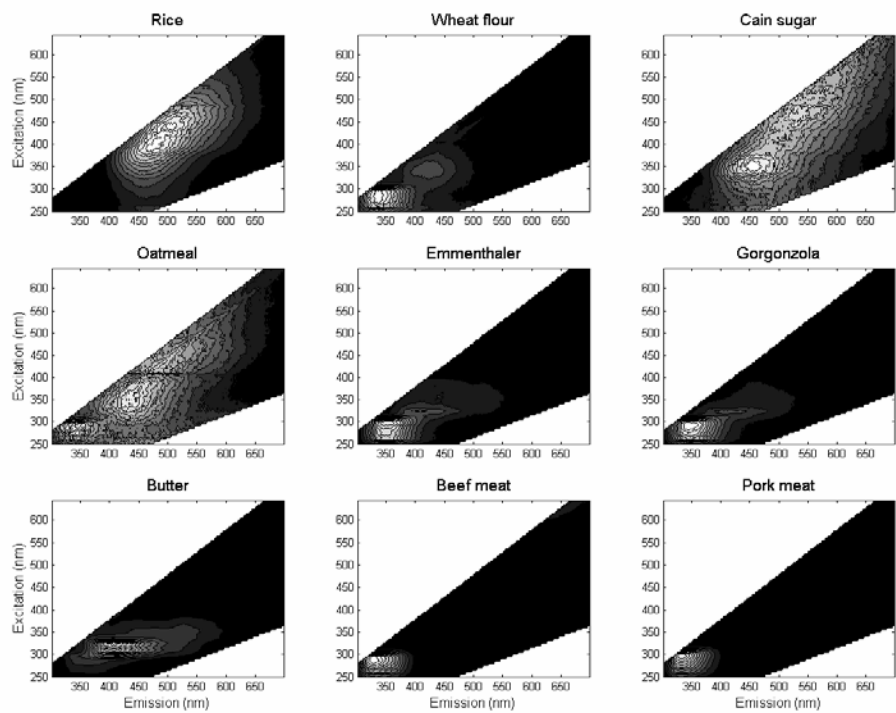


Figure 26. Contour plot of fluorescence landscapes of 9 solid food samples. All landscapes are normalized according to maximum intensity. White indicates the maximum fluorescence intensity in arbitrary units.

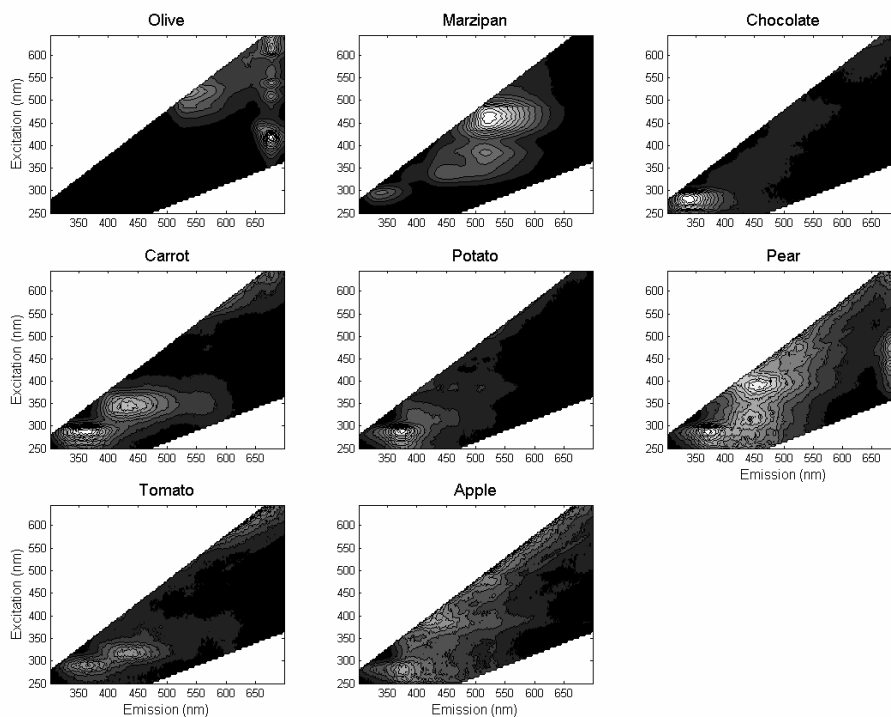


Figure 27. Contour plot of fluorescence landscapes of the remaining 8 solid food samples. All landscapes are normalized according to maximum intensity. White indicates the maximum fluorescence intensity in arbitrary units.

PARAFAC modelling

PARAFAC models were developed from the data array with 26 samples, 80 excitation wavelengths and 400 emission wavelengths. Because of computational problems the emission dimension was reduced to the half giving a final data matrix of 26*80*200. PARAFAC models with 1-13 components were calculated, using the N-way toolbox⁵. Non negativity constraint was applied in all 3 modes. Zeros were inserted instead of missing values for all emission more than 10 nm below the excitation wavelength and 10 nm above the double excitation wavelength, as suggested in literature¹⁴² and Paper II²⁹.

PARAFAC model results

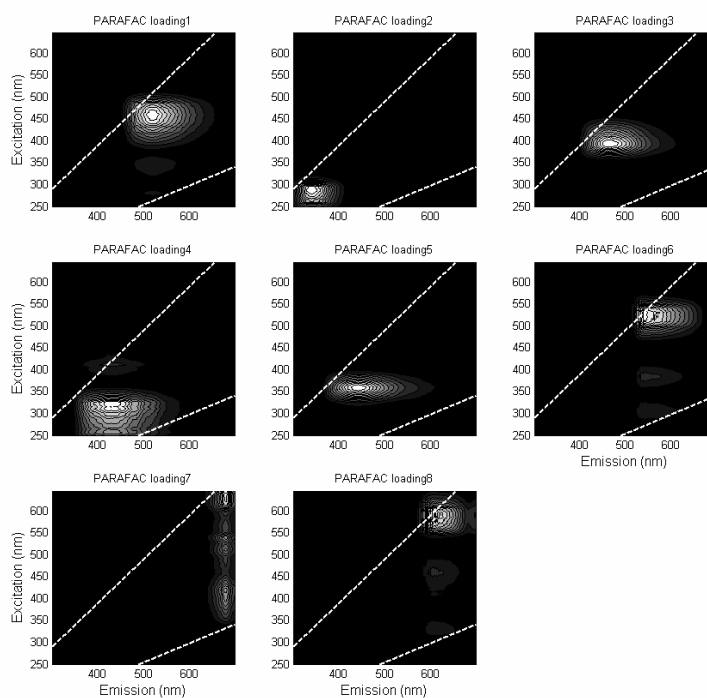


Figure 28. PARAFAC loading 1 to 8 of a model on 26 fluorescence landscapes of intact food samples with 8 PARAFAC factors. The shown "fluorescence loadings" is the product of each of the excitation and emission loadings. The white dotted lines indicate the area in which fluorescence is measured.

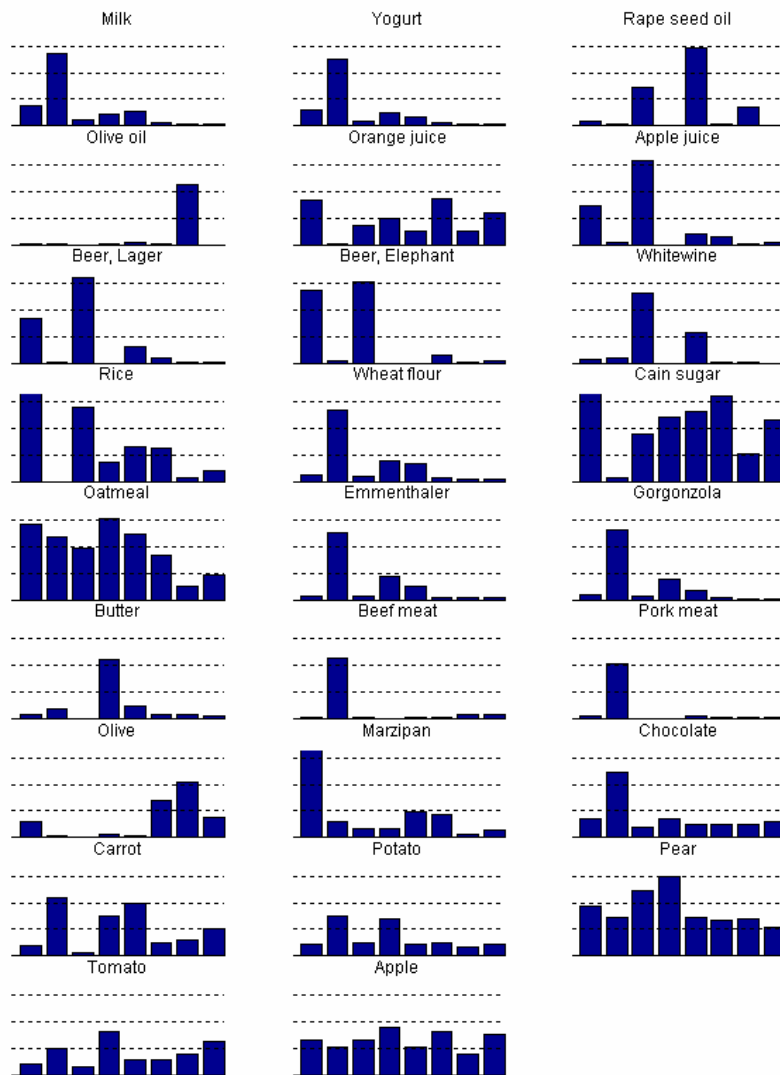


Figure 29. Score values for factor 1 to 8 (bars) for all 26 food samples (names on top) from a PARAFAC model with 8 factors based on the fluorescence landscapes of all samples. Dotted lines indicate score values of 5, 10 and 15 in arbitrary units.

Paper I

Determination of bitterness in beer using fluorescence spectroscopy and chemometrics

Jakob Christensen, Anne Marie Ladefoged and Lars Nørgaard

Journal of the Institute of Brewing 111 (1), 2005, in press.

Preliminary page mockup version.

Rapid Determination of Bitterness in Beer Using Fluorescence Spectroscopy and Chemometrics

Jakob Christensen¹, Anne Marie Ladefoged², and Lars Nørgaard¹⁻³

ABSTRACT

J. Inst. Brew. 111(1), 3–10, 2005

Two fluorescence spectroscopic methods with the aim to develop a fast quantitative determination of bitterness in beer were tested. The first method was based on autofluorescence of the diluted and degassed beer samples without any further processing. A total of 21 dark and light beer samples were analyzed and multivariate Partial Least Squares (PLS) regression models to bitterness in form of international bitter units (IBU) were performed. A prediction error in the form of Root Mean Square Error of Cross-Validation (RMSECV) of 2.77 IBU was obtained using six PLS components. Focusing only on the light beer samples the RMSECV was reduced to 1.81 IBU. The second method developed was based on addition of europium to induce delayed fluorescence signals in the beer samples. PLS models yielded an RMSECV of 2.65 IBU for all beers, while a model on the light beer samples gave an RMSECV of 1.75 IBU. The obtained prediction errors were compared to the errors given in the literature for the traditional extraction method of determining IBU.

Key words: Bitterness, chemometrics, europium, fluorescence spectroscopy.

INTRODUCTION

Bitterness is an essential quality parameter in modern breweries, and analysis of bitterness in beer and wort is conducted as a routine analysis throughout the brewing industry. The bitterness in beer is largely determined by alpha acids, which are resinous constituents of the hops. In the wort boiling they undergo an isomerisation reaction to produce iso-alpha acids, which are dominating for the bitter taste in beer. Analysis of bitterness in beer is thus based on a quantification of these bitter acids, which has been a subject to a variety of methods, as reviewed by Verzele and Keukelere in 1991²⁶. The traditional and international recommended analysis of bitterness in beer^{1,16} in terms of international bitter units (IBU), is carried out by a spectrophotometric measurement at 275 nm of an acidic

solvent extract of beer. The technique is a costly, time-consuming, and involves the use of undesirable organic solvents; also a high uncertainty is introduced in the manual extraction step. The absorbance at 275 nm is the sum of all species extracted from beer into iso-octane that absorb UV light, and minor contributions from species not contributing to the bitterness, such as polyphenols can appear²¹. The IBU method can thus be considered as a rather crude technique, which also lacks the ability to discriminate between different iso-alpha acid species. Although all iso-alpha acids possess the same chromophore, their UV spectra are not exactly the same. Furthermore different stereo-isomers have been shown to possess different absorptivities and absorption maxima wavelengths²⁶.

Despite the limitations, the IBU method is widely used as an indicator of the bitterness in quality control. Several efforts towards an automation and reducing the time of analysis has been performed throughout the last three decades^{11,23} and by applying flow injection techniques to the analysis²². The analysis precision reported from the modified methods analyses has been acceptable and in accordance with the IBU method^{2,15}. High performance liquid chromatography (HPLC) techniques can also be used to measure the amount of iso-alpha acids in beer⁹. HPLC methods can provide more detailed chemical information on the composition of bitter acids compared with the IBU method²⁶. However, the time of analysis plus the technical experience and instrumentation required to operate the HPLC, does not at first makes the technique well-suited for routine production use. Stir Bar Sorptive Extraction applied to HPLC has been suggested to improve the technique with respect to handling and costs¹⁴.

Autofluorescence spectroscopy

Fluorescence spectroscopy is an analytical method with high sensitivity and specificity. It can be used as a non-destructive analytical technique to provide information on the presence of fluorescent molecules and their environment in all sorts of biological samples

In food research, the presence of fluorophors in the form of aromatic amino acids, vitamins, cofactors and a variety of flavouring compounds makes the technique relevant and interesting. The application of autofluorescence in analysis of food has increased during the last decade, probably due to the propagated use of chemometrics, as first proposed in a food application study in 1982 by Jensen et al.¹⁷. Autofluorescence of food systems can

¹Chemometrics & Spectroscopy Group, Food Quality & Technology, Department of Food Science, The Royal Veterinary and Agricultural University, 1958 Frederiksberg, Denmark.

²Arla Foods Rødkærsbro, 8840 Rødkærsbro, Denmark.

³Corresponding author. E-mail: lan@kvl.dk

make up a complex chemical fingerprint of the sample, comprising both fluorescence and quenching phenomena. The use of chemometrics in the form of multivariate analysis has proven beneficial to this kind of data with respect to noise reduction, handling of interferences and outlier control⁸. Fluorescence spectroscopy applied directly on food samples evaluated with chemometrics, has among others been suggested for analysis of sugar^{7,19} and the oxidative stability of various dairy products^{5,10,27}.

The intrinsic fluorescence or autofluorescence of undiluted as well as diluted beer was investigated in 2002 by Apperson et al.⁴. Inner-filter effects were shown to appear in the fluorescence signal from the undiluted beer samples, expressed by the fact that protein fluorescence was only obtained upon dilution with distilled water. Similar observations were found in the present study, which is why fluorescence measurements were performed on diluted beer samples, in order to obtain the most ideal fluorescence signal with respect to dependency of the concentration of the intrinsic fluorophores. The complex fluorescence characteristics of diluted beer obtained by Apperson and coworkers was suggested to arise from complex polyphenols, protein and iso-alpha-acids. The idea of using the fluorescence signal from the iso-alpha acids to determine the bitterness, was first reported in a 1995 patent²⁴, where multivariate analysis was used to separate the relevant bitterness fluorescence from the background signal. In the patent no dilutions were suggested; in this way, a rapid bitterness determination was possible, with no need for sample preparation. However, in Apperson et al.⁴, no multivariate analysis was performed to calibrate the signals to the reference values and in the patent²⁴ no results are given regarding the performance of the method.

Europium-delayed fluorescence

An alternative to measure the intrinsic fluorescence of beer is delayed fluorescence induced by adding a lanthanide to the beer sample. This approach implies an extra, but simple and easily automated sample preparation step. However, the technique holds several advantages to the intrinsic fluorescence methods with respect to handling of interferences and separating the relevant fluorescent signal from the background fluorescence signal. Thus, the delay in time and the fluorescence emission characteristics of the lanthanide-induced fluorescence separates it from the autofluorescence signal.

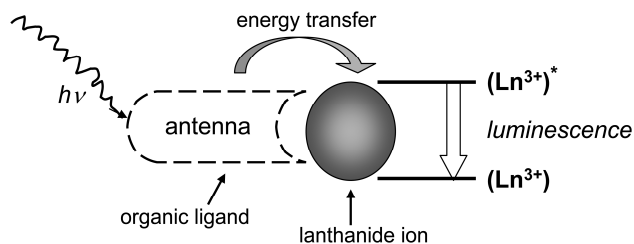


Fig. 1. The basic principles in lanthanide complex formation that exhibit efficient fluorescence. The europium (lanthanide) ion forms a complex with organic ligands, which in this case are the iso- α -acids. The ligands absorb light at specific wavelength. The energy is then transferred to the europium ion, which emits characteristic delayed fluorescence.

The delayed fluorescence method is dependent of the selective chelation of the lanthanide, europium to the β -carbonyl structure in the iso- α -acids and the unique fluorescent properties of the resultant europium complex. As illustrated in Fig. 1, radiation is absorbed at a wavelength characteristic of the iso- α -acids, which acts as "antenna" in the complex. Energy is then transferred from the excited state of the iso- α -acids to the europium ion. The europium ion emits its characteristic delayed fluorescence with emission of Eu (III) around 613 nm. Europium will not fluoresce unless it is bound to a ligand. The complex has fluorescent decay times in the order of milliseconds compared to the nanoseconds decay time of the background fluorescence. When the time-resolved or time-gated fluorescence is measured the background fluorescence has already decayed while the europium complex is still emitting.

This technique was first introduced for bitterness determination in beer by Tomlison et al.²⁵. However, a satisfactory correlation between the intensity of the delayed fluorescence (only one wavelength) and the content of iso- α -acids was not found. This study was based on a univariate approach and a calibration standard curve performed on a set of model solutions. By measuring whole emission spectra, evaluating them with multivariate data analysis and performing the calibration on real beer samples, we explore the method further and hope to improve its performance. Harms et al.¹³ and Nitzsche & Harms (2001)¹⁸ also used europium in a HPLC post column reagent in order to get a better separation of the iso- α -acids, still univariate, though.

The present study

The purpose of the present study was to explore the possibilities for a new rapid determination of bitterness in beer, which could make up an alternative to the widespread method based on extraction and a spectrophotometric determination although still using this method as a reference method. The presented analytical techniques were applied in order to investigate two different approaches:

1. Autofluorescence with multivariate evaluation, as suggested but not documented in a patent by Takhar et al.²⁴
2. Europium delayed fluorescence with multivariate evaluation.

MATERIALS AND METHODS

Beer samples and bitterness determination

A sample set of 21 lager beer samples provided from Carlsberg Breweries was investigated. The sample set included 16 light beers and five dark beers. Colour and bitterness in terms of international Bitter Units (IBU) was determined in duplicates according to Analytica EBC³. All analyses were performed the same day; spectral measurements were performed the following day.

Autofluorescence

Three hundred μ l degassed beer and 2.7 mL water were mixed in a 5 mL quartz vial. Fluorescence landscapes (excitation-emission matrices) were measured on a Varian

Cary Eclipse Fluorescence Spectrofluorometer with excitation from 230–400 nm, and a step size of 10 nm. Emission spectra were recorded for every nm from 240 to 600 nm. Excitation and emission slits were set to 5 nm.

Europium-induced delayed fluorescence

A 0.050 M aqueous solution of europium (III) chloride hexahydrate (Aldrich Chem. Co.) was prepared. Three hundred μ l europium solution and 2.7 mL degassed beer were mixed in a 5 mL quartz vial. The europium concentration and mixture ratio used were in agreement with the optimal findings of Tomlinson et al., 1995²⁵. Front face fluorescence emission spectra were measured on a Varian Cary Eclipse Fluorescence Spectrofluorometer using the accessory solid sample holder equipped with a cuvette holder and an incident light angle of 60 degrees. The measurement was started exactly 30 s after mixing of the sample and the europium solution. Delayed fluorescence measurements were performed with excitation 275 nm. The delay time was 0.10 ms with a gate time of 2.0 ms and total decay time of 0.1 s. Emission spectra were recorded for every nm from 575 to 715 nm. Excitation and emission slits were set to 5 nm.

Data analysis

Partial Least Squares (PLS) regression models²⁹ were applied for the comparison of autofluorescence spectra and europium-induced delayed fluorescence spectra with traditional determination of IBU, respectively. PLS is a predictive two-block regression method based on estimated latent variables and it is applied to the simultaneous analysis of the two data sets \mathbf{X} (spectra, independent variables) and \mathbf{y} (reference analysis, dependent variable).

Interval PLS (iPLS)²⁰ was applied in order to compare different spectral sub-regions in the autofluorescence measurements. In this study the spectral sub-regions according to each excitation wavelength were chosen for the iPLS calculations. The prediction performance of each of the local models and the global (full spectrum) model was compared.

Full cross-validation was applied for all regression models. Cross-validation²⁸ is a strategy for validating calibration models based on systematically leaving out groups of samples in the modeling and testing the left out samples in a model based on the remaining samples. In this case each of the samples was left out one by one (full cross-validation), meaning that 21 sub-models were calculated based on 20 samples plus one global model based on all 21 samples. For each of the models, the bitterness of the sample left out was predicted, and the prediction was compared with the reference value and used as a term for the validated performance of the regression model. The regression model was evaluated using the correlation coefficient (r), and the validation parameter, Root Mean Square Error of Cross-Validation (RMSECV) as a term to indicate the error of the model. The RMSECV is defined as in equation (1):

$$\text{RMSECV} = \sqrt{\frac{\sum_{i=1}^N (y_i^{\text{pred}} - y_i^{\text{ref}})^2}{N}} \quad (1)$$

where y_i^{pred} is the predicted value for sample i in the cross-validation, y_i^{ref} is the corresponding reference value and N is the number of samples.

Data analysis were performed in MATLAB 6.5 (MathWorks, Inc.) with the iToolbox 1.0 (www.models.kvl.dk), and Unscrambler 9.1 (CAMO, Norway).

RESULTS AND DISCUSSION

Traditional analyses

In Table I the results of the reference measurements on the 21 beer samples are given. The IBU values are in the range 3.1–31.5 representing large variation for lager beers, but within normal occurring values. The beer colours can be divided into two major groups; 16 light beers with values around 5 colour units and 5 darker beers with colour values above 20. The darker beers can be used to illuminate the effect of different colours on the fluorescence signal and its correlation to bitterness in beer.

Autofluorescence

The autofluorescence spectra of three selected samples are given as landscapes and contour plots in Fig. 2. The three samples span the bitterness level with sample A having a value of 8.8 IBU and sample B having a value of 28.5 IBU as well as the color with sample A and B being light beers while sample C is a dark beer. In all three samples two distinct peaks are seen with excitation/emission maxima around 290/350 nm and 340/430 nm, respectively. The first peak probably arise from protein fluorescence, mainly attributed to tryptophan, while the second peak can be related to fluorescence from complex polyphenols or iso- α -acids, as suggested by Apperson et al.⁴. Sample B has a significant higher IBU value than sample A, and thus was expected to contain a higher amount of iso- α -acids. However the intensity of the peak around 340/430 nm are not very different for the two samples, indicating that the bitter acids are not the main contributors to the fluorescence signal obtained in this area. Thus,

Table I. IBU and color values for 21 beer samples.

Beer ID	IBU	Colour, EBC
1	16.3	5.7
2	20.9	5.8
3	25.6	5.8
4	31.5	5.7
5	21.4	5.5
6	17.8	5.0
7	22.1	4.9
8	18.1	4.5
9	23.2	4.6
10	28.5	4.4
11	3.1	4.8
12	6.0	5.5
13	8.8	5.1
14	11.9	5.1
15	8.0	4.9
16	9.2	5.3
17	3.2	23.1
18	6.7	23.5
19	9.8	23.9
20	13.3	23.9
21	16.1	20.3

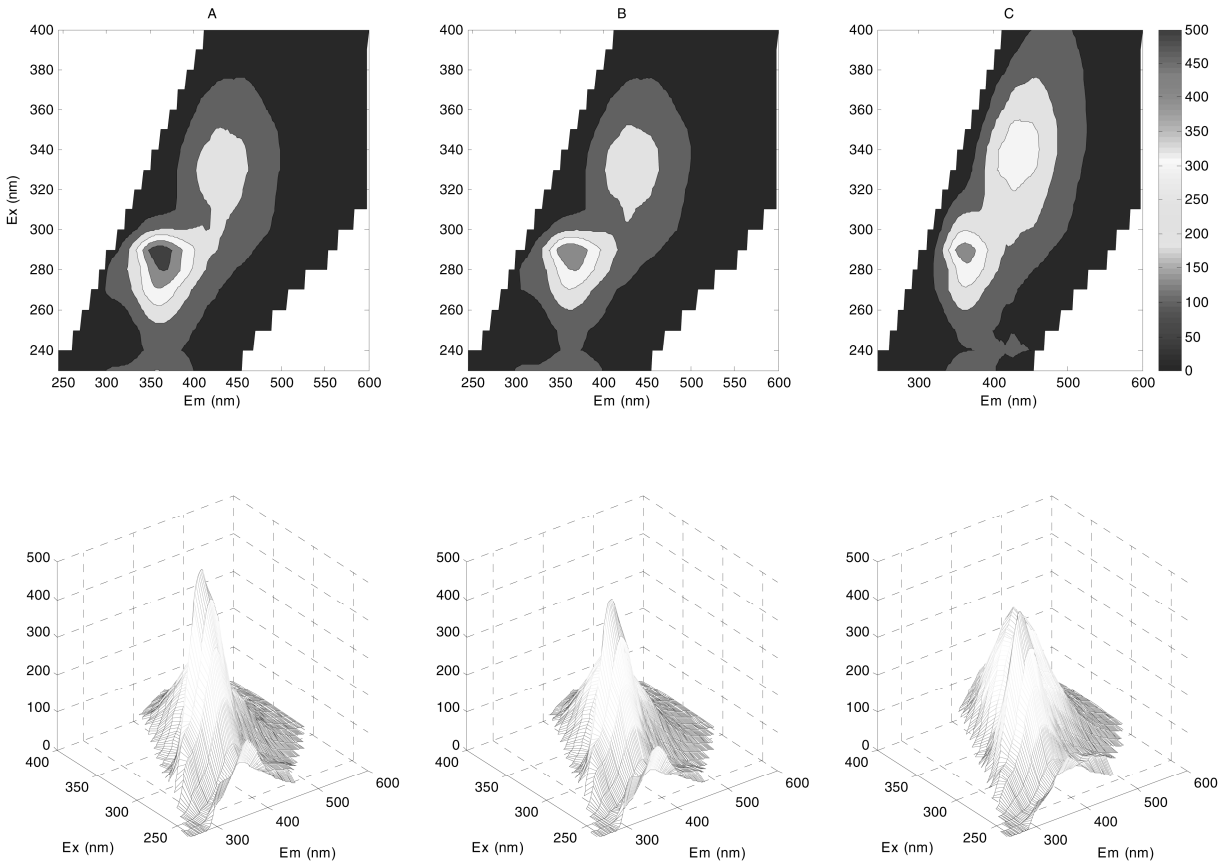


Fig. 2. Landscapes of the intrinsic fluorescence of the three diluted beer samples, A, B and C, depicted as contour plot (top) and 3D spectra (bottom). The bitterness level of the three beers was found to 8.8, 28.5 and 16.1, respectively. Sample A and B represent light beer samples, and sample C is a darker beer sample.

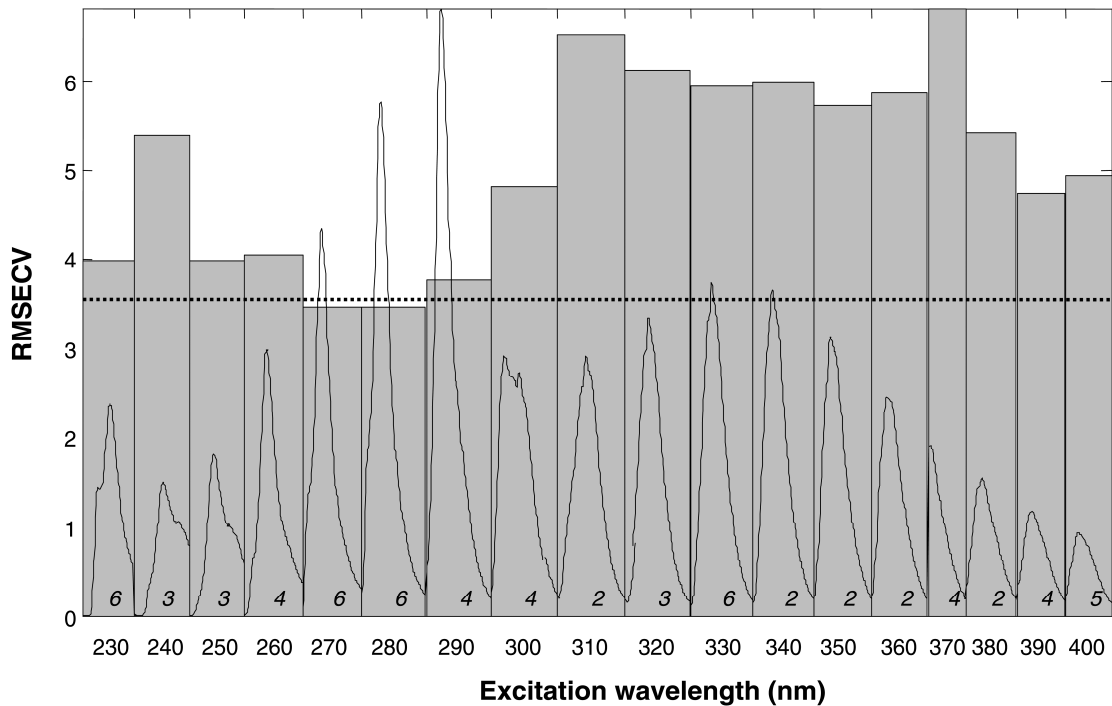


Fig. 3. Output result plot from interval-PLS analysis. Cross-validated prediction performance (RMSCEV) of PLS regression models on IBU values is plotted from a full-spectrum (“global”) model with 5 PLS components (dotted line) and from 20 interval models (bars) with the optimal number of components for the given interval. The mean spectrum is shown.

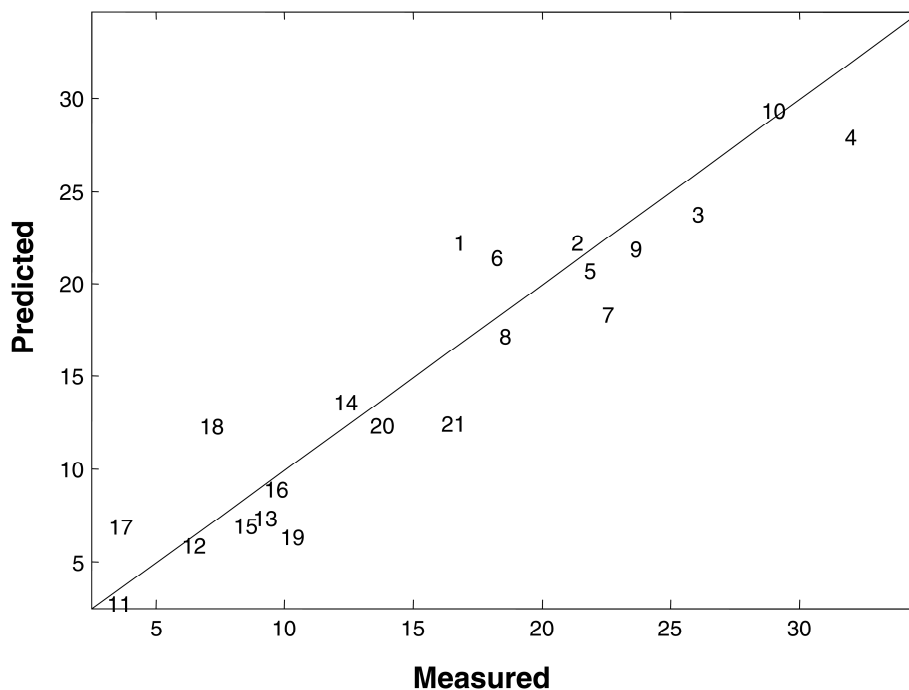


Fig. 4. Predicted versus measured IBU values of all 21 beer samples, based on a PLS regression model with 6 PLS components of autofluorescence measurement. Intervals 4, 5 and 7 of the fluorescence measurements from the iPLS analysis were included in the regression model. A multivariate regression coefficient, r of 0.94 and RMSECV of 2.77 IBU was obtained for the presented model.

polyphenols might be a better suggestion. The dark sample, C yields a little lower but broader shaped fluorescence signal. The lower intensity could suggest that inner-filter effects take place, but the differences observed are to be investigated through regression models to the assessed bitterness levels in the beer samples

A full spectrum PLS regression model between the concatenated autofluorescence spectra and the IBU reference values yielded an RMSECV of 3.56 IBU (Table II). In this model the independent variables had the dimension 21×2111 variables since the data were unfolded. The optimal number of PLS components to apply as determined by full cross-validation was five and the correlation

coefficient between the predicted values and the reference values is 0.90.

To investigate the performance of each excitation wavelength, i.e. from 230 nm to 400 nm with 10 nm steps, an iPLS was calculated. The result is given in Fig. 3 where the bars indicate the RMSECV obtained by a full cross-validation PLS model for each excitation wavelength, i.e. in total 18 local models have been developed. Due to the limited number of samples it was decided not to use more than six PLS components in all models even though the cross-validated results indicated a higher number of components for some models. The iPLS showed that intervals corresponding to excitation 270 nm and 280 nm performed slightly better than the full spectrum model using one more PLS component. A model on the emission spectra from excitation at 270 nm gave an RMSECV of 3.46 IBU and a correlations coefficient of 0.90. As judged by an F-test¹² this is a non-significant difference from the RMSECV of the full spectrum model ($p = 0.45$). All possible combinations of two and three intervals were also calculated and the best performing combinations of intervals were excitations 260 nm, 270 nm and 280 nm with an RMSECV of 2.77 IBU, lower than the full spectrum RMSECV ($p = 0.13$) and all individual intervals. The Predicted versus Measured plot for this PLS model based on six PLS components is given in Fig. 4. Inspecting this model revealed that the autofluorescence spectra of the dark samples deviated from the corresponding light beer spectra; this was also observed in the raw data as given in Fig. 2. Models without dark samples gave the results compiled in Table II. The full spectrum model is in the level

Table II. Results from PLS regression models between autofluorescence measurements and bitterness determined according to the IBU method. Fluorescence emission spectra from all excitation wavelengths (230–400 nm) or selected excitation wavelengths were used, as noted in brackets.

	RMSECV (IBU)	# PLSC	r
All beer samples (n = 21):			
Unfold PLS	3.56	5	0.90
Unfold PLS [Ex. 270 nm]	3.46	5	0.90
Unfold PLS [Ex. 260, 270, 290 nm]	2.77	6	0.94
Only light colored beers (n = 16):			
Unfold PLS	3.42	3	0.91
Unfold PLS [Ex. 230 nm]	2.71	5	0.94
Unfold PLS [Ex. 230 nm] without samples 1 & 4	1.81	5	0.97
Unfold PLS [Ex. 260, 270, 290 nm]	2.65	5	0.95

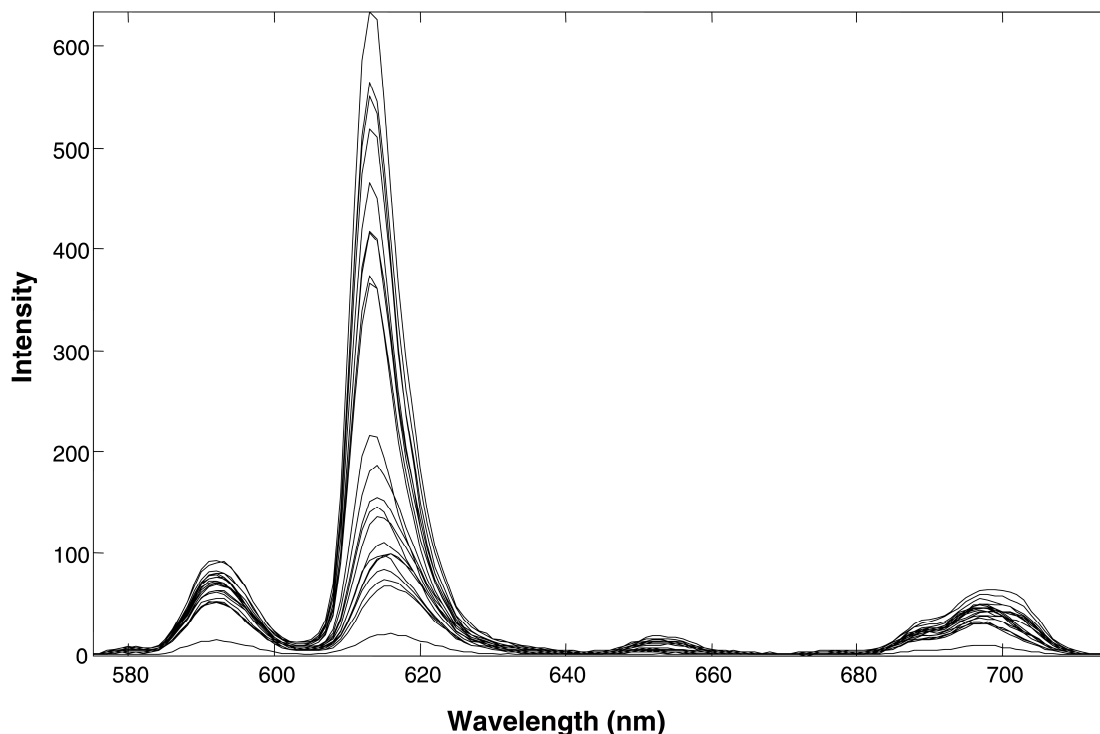


Fig. 5. Europium-induced delayed fluorescence emission spectra of all 21 beer samples. Excitation wavelength 275 nm.

regarding the RMSECV while the interval model now shows that excitation 230 nm (interval 1) is the one with optimum performance. Furthermore, attention was drawn to samples 1 and 4 and excluding these gave an RMSECV of 1.81 IBU ($p = 0.01$ compared to RMSECV = 3.56). Samples 1 and 4 were only excluded based on their poor fit to the regression model for the remaining model; no obvious causality was found and therefore the result should be addressed rather cautiously. It was not possible to further improve the model by combinations of intervals; the optimal combination gave an RMSECV of 2.65 IBU as seen in Table II.

Europium-induced delayed fluorescence

The europium-induced delayed fluorescence spectra of all samples are given in Fig. 5. The spectra holds the typical spectral characteristic of europium with four peaks corresponding to different electron transitions and with the main peak around 615 nm, where large variations in intensity between the samples can be observed.

A full spectrum PLS model on all 21 samples gave an RMSECV of 2.69 using two PLS components. The predicted versus measured plot for this model is shown in Fig. 6. The distribution of the samples does not appear linear; it seems that the samples are almost divided into two levels with either low or high IBU value, split between 15 and 20 IBU. The lower number of components in the PLS model based on delayed fluorescence can be explained by the fact that the signal is induced by the addition of europium and the model only needed one component to compensate for interferences as opposed to the autofluorescence case where up to six PLS components were necessary to perform this compensation.

A PLS model on only light beer samples further reduced the RMSECV to 2.05 IBU while excluding samples 1 and 4 gave an RMSECV of 1.75 IBU for the remaining fourteen samples, as listed in Table III.

In the preliminary experiments replicates were measured and it turned out that it was difficult to obtain reproducible measurements for the replicates for the induced experiment. After addition of the europium, a precipitate was formed, leading to a rather unstable chemical system. It was decided to measure exactly after 30 s in order to standardize the procedure and minimize the replicate deviations. However, the problem with precipitation needs to be addressed, before further implementation.

Discussion on uncertainties of bitterness determinations

The reproducibility of the traditional method for bitterness determination has been evaluated several times, estimating the terms for repeatability (r_{95}) and reproducibility (R_{95}) as defined in ISO Standard 5725, stating that the probability that two analyses deviate up to the value of

Table III. Results from PLS regression models between europium-induced delayed fluorescence measurements and bitterness determined according to the IBU method.

	RMSECV (IBU)	# PLSC	r
All beer samples (n = 21):			
PLS	2.69	2	0.94
Only light colored beers (n = 16):			
PLS	2.05	2	0.97
PLS without samples 1 & 4	1.75	3	0.97

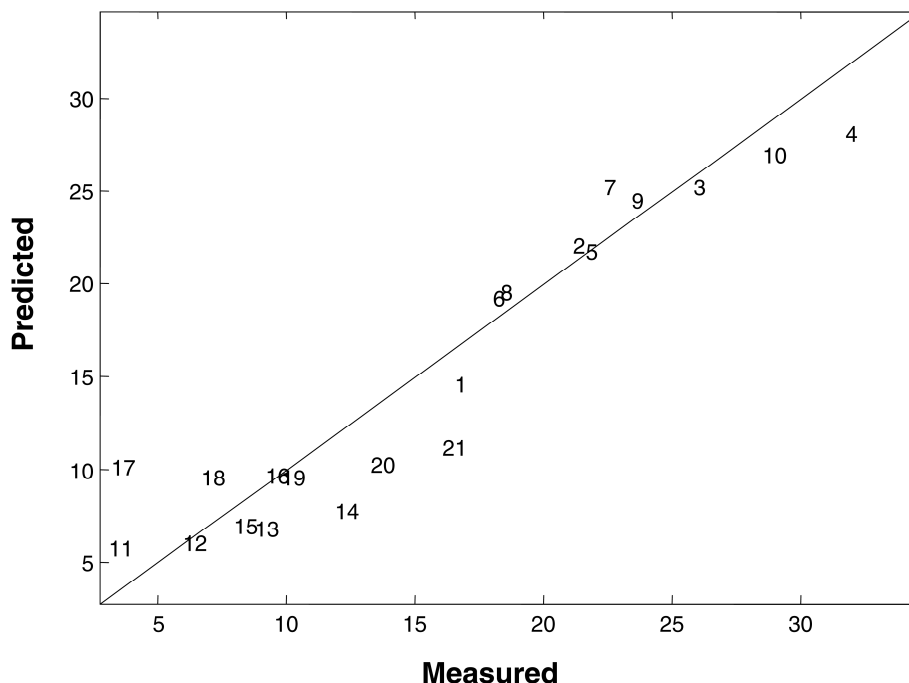


Fig. 6. Predicted versus measured IBU values of all 21 beer samples, based on a PLS regression model with 2 PLS components of europium-induced delayed fluorescence measurements. A multivariate regression coefficient, r of 0.94 and RMSECV of 2.69 IBU was obtained for the presented model.

r_{95}/R_{95} is approximately 95%, within one laboratory (r_{95}) or within all tested labs (R_{95}), respectively. The mean precision values of the IBU method in a major UK brewing company showed a repeatability of 1.0 IBU and a reproducibility of 4.1 IBU for 33 samples in the range 18–32 IBU, on the basis of 16 laboratories²⁵. In 2000, the EBC Analytical Committee found the precision of the bitterness analysis somewhat lower in a ring test of six beers in the range 13–36 IBU, analysed in 13 laboratories, that resulted in mean values of 0.8 IBU for repeatability, and 3.5 for reproducibility, with both r_{95} and R_{95} proportional to the measured IBU values⁶. The optimal models for predicting the bitterness from fluorescence in the present study yielded prediction errors below 2 IBU. These findings may not seem precise enough for implementation in breweries, but compared with the reproducibility of the reference method, they appear to be in the same order of magnitude. However, the reported repeatability of the IBU method, i.e. the precision within one laboratory seems to be superior to the findings in the present study.

CONCLUSIONS

A fast reliable method for bitterness determination is needed, and it is documented that both autofluorescence spectra and europium induced delayed fluorescence spectra by the aid of multivariate modeling holds the potential to be used to predict the bitterness in beers with an error comparable to that of the reference method. Both these methods are faster than the traditional method because the extraction step is avoided. Future work should delve into the uncertainty of the reference method as well as testing

the developed methods on a larger number of samples in order to reveal if local models (for example light beers) can be developed. Also methods for handling the precipitation observed in the europium induced delayed fluorescence method should be investigated.

ACKNOWLEDGEMENT

Carlsberg Breweries in Valby, Denmark and Steen Bech Sørensen from Carlsberg Research Center is acknowledged for providing the beer samples and performing the IBU bitterness determinations.

REFERENCES

1. Anonymous, Institute of Brewing Analysis Committee – Recommended Methods of Analysis. *J. Inst. Brew.*, 1971, **77**(2), 181.
2. Anonymous, Bitterness units of beer and wort. *J. Am. Soc. Brew. Chem.*, 1996, **54**(3), 186–187.
3. Anonymous, *European Brewery Convention: Analytica EBC*. Verlag Hans Carl Getränke-Fachverlag: Nurnberg, 1998, p. 125.
4. Apperson, K., Leiper, K.A., McKeown, I.P and Birch, D.J.S., Beer fluorescence and the isolation, characterisation and silica adsorption of haze-active beer proteins. *J. Inst. Brew.*, 2002, **108**(2), 193–199.
5. Becker, E.M., Christensen, J., Frederiksen, C.S., Haugaard, V.jK., Front-face fluorescence spectroscopy and chemometrics in analysis of yogurt: Rapid analysis of riboflavin. *J. Dairy Science*, 2003, 2508–2515.
6. Benard, M., Determination of repeatability and reproducibility of EBC accepted methods: V – Beer. *J. Inst. Brew.*, 2000, **106**(3), 135–138.
7. Bro, R., Exploratory study of sugar production using fluorescence spectroscopy and multi-way analysis. *Chemometrics and Intelligent Laboratory Systems*, 1999, **46**(2), 133–147.

8. Bro, R., Multivariate calibration – What is in chemometrics for the analytical chemist? *Analytica Chimica Acta*, 2003, **500**(1–2), 185–194.
9. Buckee, G.K., Estimation of iso-alpha-acids in beer by HPLC-collaborative trial. *J. Inst. Brew.*, 1990, **96**(3), 143–148.
10. Christensen, J., Povlsen, V.T., Sorensen J. Application of fluorescence spectroscopy and chemometrics in the evaluation of processed cheese during storage. *J Dairy Science*, 2003, **86**(4), 1101–1107.
11. Fisher, A., Semiautomatic method for determination of beer bitterness. *J. Inst. Brew.*, 1972, **78**(5), 407.
12. Haaland, D.M. and Thomas, E.V., Partial Least-Squares Methods for spectral analyses. 1 Relation to other quantitative calibration methods and the extraction of qualitative information. *Analytical Chemistry*, 1988, **60**(11), 1193–1202.
13. Harms, D. and Nitzsche, F., New ways to determine bitter substances in beer and wort. *Monatsschrift fur Brauwissenschaft*, 2000, **53**(7–8), 143–146.
14. Harms, D. and Nitzsche, F., The analysis of the bitter and other flavour compounds in beer and wort by stir bar sorptive extraction (SBSE) followed by HPLC. *AppNote*, 2001, p. 5.
15. Hassinger, T., Cattanaach, D., Gearhart, J., Mclinn, C., Ono, M. and Otterson, T, Bitterness in beer by automated flow-analysis. *J. Am. Soc. Brew. Chem.*, 1994, **52**(4), 182–183.
16. Howard, G.A., Estimation of bitterness of beer. *J. Inst. Brew.*, 1968, **74**(3), 249.
17. Jensen, S.A., Munck, L. and Martens, H., The botanical constituents of wheat and wheat milling fractions 1. Quantification by autofluorescence. *Cereal Chemistry*, 1982, **59**(6), 477–484.
18. Nitzsche, F. and Harm, D., Iso-alpha acids in beer and wort: Novel detection methods for routine and research applications. *ASBC Annual Meeting*, 2001.
19. Norgaard, L., Classification and prediction of quality and process parameters of thick juice and beet sugar by fluorescence spectroscopy and chemometrics. *Zuckerindustrie*, 1995, **120**(11), 970–981.
20. Norgaard, L., Saudland, A., Wagner, J., Nielsen, J.P., Munck, L. and Engelsen, S.B. Interval partial least-squares regression (iPLS): A comparative chemometric study with an example from near-infrared spectroscopy. *Applied Spectroscop*, 2000, **54**(3), 413–419.
21. Philpott, J., Taylor, D.M. and Williams, D.R., Critical assessment of factors affecting the accuracy of the IoB Bitterness Method. *J. Am. Soc. Brew. Chem.*, 1997, **55**(3), 103–106.
22. Sakuma, S., Kikuchi, C., Kowake, M. and Mawatari, M., A flow injection analyzer for determining the bitterness unit of wort and beer. *Tech. Q. Master Brew. Am.*, 1993, **30**, 45–47.
23. Seaton, J.C., Hutcheson, J.M., Moir, M., A practical method for enhancement of beer bitterness using beta-acids. *J. Inst. Brew.*, 1985, **91**(3), 126.
24. Takhar, G. and King, M., Monitoring the colour and bitterness of beer. Whitbread PLC. Patent PCT/GB95/00219[WO 95/21242] 1995.
25. Tomlinson, J.B., Ormrod, I.H.L. and Sharpe, F.R., A novel method for bitterness determination in beer using a delayed fluorescence technique. *J. Inst. Brew.*, 1995, **101**(2), 113–118.
26. Verzele, M. and De Keukeleire, D., Chemistry and analysis of hop and beer bitter acids. Elsevier: Amsterdam, 1991.
27. Wold, J.P., Jorgensen, K. and Lundby, F., Nondestructive measurement of light-induced oxidation in dairy products by fluorescence spectroscopy and imaging. *Journal of Dairy Science*, 2002, **85**(7), 1693–1704.
28. Wold, S., Cross-validators estimation of number of components in factor and principal components models. *Technometrics*, 1978, **20**(4), 397–405.
29. Wold, S., Martens, H. and Wold, H., The multivariate calibration-problem in chemistry solved by the PLS method. *Lecture Notes in Mathematics*, 1983, **973**, 286–293.

(Manuscript accepted for publication February 2005)

Paper II

Fluorescence spectroscopy and PARAFAC in the analysis of yogurt

Jakob Christensen, Eleonora Miquel Becker and Charlotte S. Frederiksen
Chemometrics and Intelligent Laboratory 75 (2), 201-208, 2005

Fluorescence spectroscopy and PARAFAC in the analysis of yogurt

J. Christensen^{a,*}, E. Miquel Becker^b, C.S. Frederiksen^b

^a*Food Technology, Department of Food Science, The Royal Veterinary and Agricultural University, Rolighedsvej 30, DK-1958 Frederiksberg C, Denmark*

^b*Food Chemistry, Department of Food Science, The Royal Veterinary and Agricultural University, Rolighedsvej 30, DK-1958 Frederiksberg C, Denmark*

Received 10 March 2004; received in revised form 6 July 2004; accepted 13 July 2004
Available online 11 September 2004

Abstract

Parallel factor (PARAFAC) analysis and fluorescence spectroscopy were applied in the evaluation of yogurt during storage. Fluorescence landscapes with excitation wavelengths from 270 to 550 nm and emission wavelengths in the range 310–590 nm were obtained from front-face fluorescence measurements directly on yogurt samples during two storage experiments over a period of 5 weeks at 4 °C. PARAFAC analysis of the fluorescence landscapes exhibited three fluorophores present in the yogurt, all strongly related to the storage conditions. The fluorescence signal was resolved into excitation and emission profiles of the pure fluorescent compounds, which are suggested to be tryptophan, riboflavin and lumichrom. Thus, it is concluded that fluorescence spectroscopy in combination with chemometrics has a potential as a fast method for monitoring the oxidative stability and quality of yogurt. Regression models between fluorescence landscapes and riboflavin content, determined by the traditional chemical analysis, were performed, yielding a root mean square error of cross-validation of 0.09 ppm riboflavin, corresponding to 7% of the mean riboflavin content in the yogurt samples. Regression models based on PARAFAC scores, Partial Least Squares (PLS) and N-PLS were compared and yielded only minor differences with respect to prediction error. Several missing values appear in the fluorescence data matrices, for all emission wavelengths below the excitation wavelength. Substituting some of the missing values with zeros was observed to have a large impact on the model solution and the computation time. It is concluded that at least 43% of the missing values in the present data set need to be substituted in order to obtain meaningful PARAFAC models.

© 2004 Elsevier B.V. All rights reserved.

Keywords: Fluorescence spectroscopy; PARAFAC; Yogurt

1. Introduction

Fluorescence spectroscopy is a rapid and sensitive method for characterising molecular environments and events. It can be used as a non-destructive analytical technique to provide information on the presence of fluorescent molecules and their environment in all sorts of biological samples. In food research, the presence of fluorophores in the form of aromatic amino acids, vitamins, cofactors, etc. makes the technique highly relevant and interesting. The application of autofluorescence in analysis

of food has increased during the last decade, probably due to the propagated use of chemometrics, as first proposed in a food application study by Jensen et al. back in 1982 [1].

In dairy research, fluorescence spectroscopy evaluated with chemometrics has previously been investigated in a few studies to monitor structural changes in milk proteins and their physico-chemical environment during milk heating [2], milk coagulation [3], cheese manufacture [4,5] and in the evaluation of oxidative changes in processed cheese during storage [6]. Changes in vitamin A in dairy products have also been monitored in several fluorescence studies [7,8], and front-face fluorescence spectroscopy has been used for measuring light-induced oxidation in various dairy products [9], as well as proposed as a new method for rapid quantification of riboflavin [10].

* Corresponding author. Tel.: +45 35 28 33 23; fax: +45 35 28 32 45.
E-mail address: jach@kvl.dk (J. Christensen).

In most of the latter studies, bilinear models as principal component analysis (PCA) and Partial Least Squares (PLS) have been used for evaluation of the fluorescence measurements. With the use of PARAFAC [11], it is possible to handle fluorescence landscapes (excitation–emission matrices) keeping intact the original two-dimensional data structure of each measurements. Thus, the trilinearity of the data can ideally be utilized in a unique decomposition of the fluorescence data into scores, excitation and emission loadings according to the concentration and the physical properties of each of the fluorophores present in the analysed sample.

Several studies have explored the use of fluorescence spectroscopy evaluated by multiway data analysis, such as PARAFAC. Within food research, applications can be found in analysis of sugar, meat, fish oil and cheese. In analysis of sugar and sugar solutions [12–15], information on sugar quality at a molecular level, ascribed to the impurities in sugar, has been thoroughly investigated with fluorescence landscapes. Fluorescence spectroscopy and PARAFAC have also been suggested in a potential screening method for dioxin contamination in fish oil [16], however, based on an indirect correlation. Furthermore, the technique has been demonstrated to hold relevant information when monitoring chemical changes of Parma ham during maturation [17] and the stability of processed cheese during storage [6].

In the present study, yogurt samples stored under different light and packaging conditions were measured by front-face fluorescence spectroscopy applied directly on the yogurt samples, with the purpose to monitor the oxidative stability and chemical changes during storage in order to compare the packaging materials. The underlying fluorescence structure of the fluorescence landscapes was investigated using PARAFAC. PARAFAC ideally decomposes the fluorescence landscapes presented in a three-way array into trilinear components according to the number of fluorophores present in the yogurt samples. The retrieved scores and loadings can then be directly related to the relative concentration (scores) and the fluorescence characteristics of the present fluorophores, which means that the excitation and emission loadings can be used in interpretation and identification of the found fluorescence phenomena. The obtained fluorescence PARAFAC results were compared with the riboflavin content as a chemical validation of the model results. Riboflavin—a strong fluorophore—plays a key role in the photo-oxidation of dairy products, and can be considered an important marker of early oxidation in milk and dairy products.

A few studies have recently focussed on some practical aspects of PARAFAC modeling of fluorescence data [18,19]. Especially light scattering effects and the large amount of missing values in fluorescence landscapes due to the fact that emission below the excitation wavelength does not give any physical meaning can be a challenge in the PARAFAC modeling. In this study, the strategy of inserting

zeros instead of missing values, as suggested by Ref. [19] in order to stabilize the decomposition, will be explored.

Thus, the present study aims at three investigations:

- The potential of using PARAFAC models of fluorescence data from measurements applied directly to an untreated complex food system like yogurt.
- Handling missing values by inserting zeros in fluorescence data in the PARAFAC analysis
- The potential of front-face autofluorescence spectroscopy as a new rapid method for riboflavin quantification.

2. Materials and methods

2.1. Yogurt storage and packaging materials

Plain yogurt (3.5% fat) was obtained from Arla Foods amba (Viby, Denmark). The yogurt was filled into cups of two rigid packaging materials, polylactate (PLA) and polystyrene (PS), with PS having the higher oxygen permeability and light transmission. The packages contained 180 and 155 g yogurt for PLA and PS, respectively, resulting in a headspace volume of 35 ml for each package. The cups were sealed by a transparent and colorless laminate. The packed samples were stored at 4 °C for 5 weeks under a radiant flux of approximately 3500 lx of fluorescent light (Philips fluotone, TLD 18W/830) or in darkness. The samples stored in light were illuminated both from above through the lid and from the sides. Throughout the storage period, the samples were randomly interchanged to minimize unequal temperature fluctuations and light conditions. For further details on packaging materials, see Becker et al. [10].

2.2. Experimental design

Two batches of yogurt were examined in two identical storage experiments. Analyses were performed after 0, 7, 14, 21, 28 and 35 days of storage, giving a total of 21 different samples (5 days×2 light conditions×2 packaging materials+1 starting sample) for each batch. Thus, 42 independent samples were studied in all. Three cups from identical conditions for each of the two batches were selected and considered as triplicates. All analyses were carried out in duplicate. Prior to the measurements, the yogurt was mixed in the cup.

2.3. Fluorescence spectroscopy

Fluorescence landscapes were measured directly on the yogurt by filling 15 g of yogurt in a 30-ml plastic cup and recording fluorescence by dipping the measuring probe 1 mm into the yogurt sample. All samples were measured on a BioView spectrofluorometer (Delta Light & Optics, Denmark) using a pulsed xenon lamp for excitation and

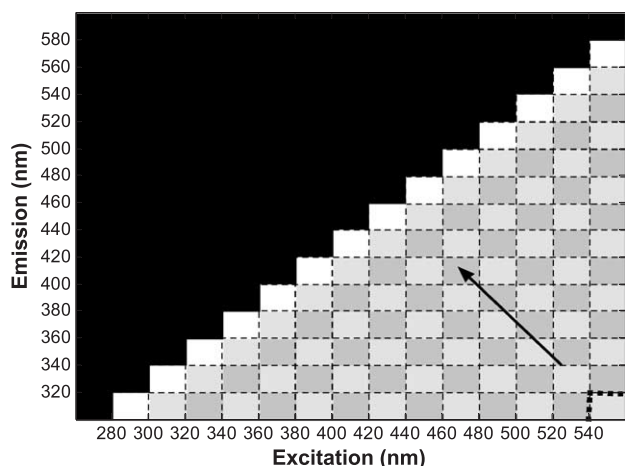


Fig. 1. Diagram of the recorded fluorescence data matrices. The black area indicates the range in which the fluorescence signal is recorded. The rest of the data points remain as missing values during the measurement. The colours indicate the strategy of inserting zeros in the modelling phase from the lower right corner and up to the diagonal line, stepping one diagonal data point at a time. This approach gives a total of 15 different amounts of inserted zeros.

equipped with an optical light conductor and a measuring probe, giving an open-end 180° measuring geometry. Fluorescence landscapes were obtained with excitations from 270 to 550 nm and emission wavelengths from 310 to 590 nm, with intervals and bandwidths of 20 nm, giving a total of 15 excitation and 15 emission wavelengths. Only emission wavelengths 40 nm above the excitation wavelength were recorded, resulting in 120 data points obtained for each measurement, as indicated in black in Fig. 1.

3. PARAFAC

PARAFAC decomposes the fluorescence landscapes into a number of trilinear components or factors, f . The principle behind the PARAFAC decomposition is to minimize the sum of squares of the residual e_{ijk} , according to Eq. (1).

$$x_{ijk} = \sum_{f=1}^F a_{if} b_{jf} c_{kf} + e_{ijk} \quad (i = 1, \dots, I; \\ j = 1, \dots, J; k = 1, \dots, K; f = 1, \dots, F) \quad (1)$$

The element x_{ijk} represents the fluorescence intensity for sample, i , excitation wavelength, j , and emission wavelength, k . The fluorescence landscapes are thus decomposed into sample scores, a_{if} , excitation loadings, b_{jf} , and emission loadings, c_{kf} , for each factor, f , also called PARAFAC components. The residual, e_{ijk} , contains the variation not captured by the PARAFAC model.

Split-half analysis of PARAFAC models [11] was performed for validation. The idea of this strategy is to divide the data set into two halves and make a PARAFAC model on both halves. Due to the uniqueness of the PARAFAC model, one will obtain the same result—same

loadings in the non-split mode, e.g. excitation and emission mode—on both data sets, if the correct number of components is chosen. The split-half analysis was performed by calculating PARAFAC models for each batch at a time, subsequently comparing the results and ensuring that more or less identical excitation and emission loadings were obtained.

PARAFAC modelling was performed on all 42 samples in triplicates. One single replicate sample was removed as spectral outlier, giving a total of 125 yogurt samples in the modelling. Thus, a three-way data array of $125 \times 15 \times 15$ was analysed.

3.1. Handling missing values—inserting zeros

The recorded fluorescence data matrices contain 47% missing values, as shown in Fig. 1, where the measuring area is indicated in black; the rest represent data points with missing values. Insertion of zeros to replace the missing values was tested. PARAFAC models were calculated from fluorescence data without any zeros inserted to replace the missing values as well as from fluorescence data with zeros completely inserted until the emission wavelength equals the excitation wavelength. All intermediate data matrices with zeros inserted up to a diagonal line were also used for calculations as indicated with the diagonal dotted lines in Fig. 1, giving a total of 15 different solutions. Thus, a gradient from 0 to 100% of zeros incorporated instead of missing values was compared. All PARAFAC models were calculated both with no constraints, and with non-negativity applied in all modes.

3.2. Chemical determination of riboflavin

The riboflavin content in the yogurt was measured by the fluorometric method established by AOAC (1990) using an Aminco Bowman series 2 luminescence spectrophotometer (SLM-Aminco, Urbana, IL, USA). This method implies a chemical extraction and cleanup of riboflavin prior to the fluorometric measurement, making the method time-consuming and the use of organic solvent necessary. The selected wavelengths were 446/525 nm for excitation/emission.

3.3. Riboflavin calibration

Regression models were performed between traditionally determined riboflavin content and fluorescence landscapes of 42 averaged samples. Leave-one-out cross-validation was performed. Regression models were evaluated using the validation parameter, Root Mean Square Error of Cross-Validation (RMSECV), as a term to indicate the prediction error of the model. Score values derived from the PARAFAC decomposition were used for regression models using Partial Least Squares (PLS) and multiple linear regression (MLR). Also, multiway calibration in the form

of N-PLS regression was performed on the fluorescence landscapes kept as three-way array, and PLS regression was performed on unfolded fluorescence emission spectra.

3.4. Software

Data analyses were performed in MatLab 6.5 (Math-Works) with the N-way Toolbox [20] (www.models.kvl.dk) and the PLS Toolbox 2.0 (www.Eigenvector.com). In the N-way Toolbox, missing values in the PARAFAC modelling are handled by expectation maximization.

Spectral data and reference riboflavin values can be downloaded in MatLab format from: <http://www.models.kvl.dk>.

4. Results and discussion

4.1. Fluorescence spectroscopy

The fluorescence landscapes of two yogurt samples are shown in Fig. 2 in the form of contour plots. The two samples represent the extremes in the experimental plan, i.e.

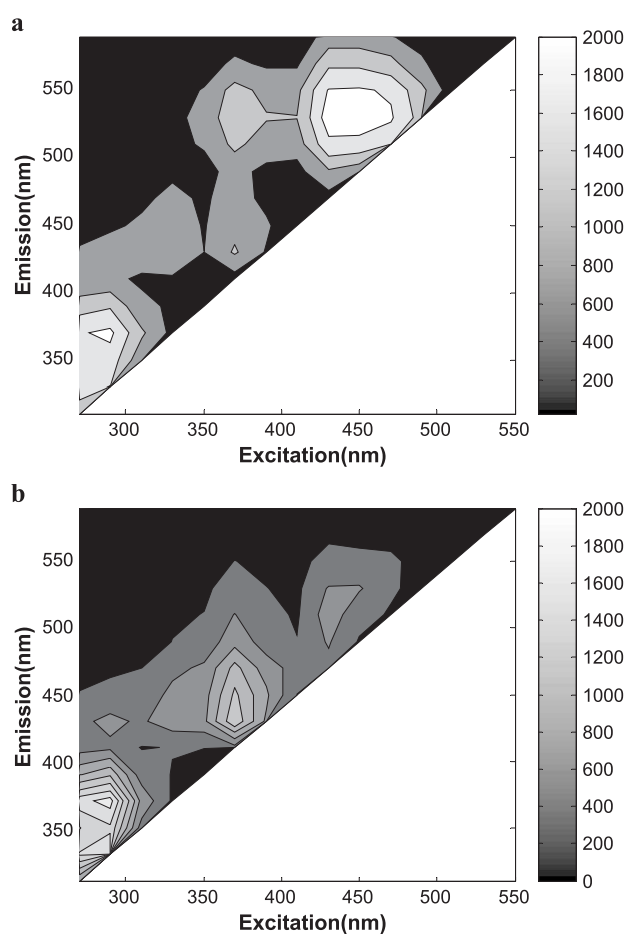


Fig. 2. Contour plot of a fluorescence landscape of a yogurt samples. (a) Fresh yogurt sample and (b) yogurt sample stored in light for 35 days and packed in polystyrene.

a fresh yogurt sample (a) and a yogurt sample stored under the most severe conditions (b). The highest fluorescence peaks for the fresh sample are seen with excitation below 300 nm and emission around 370 nm as well as for excitations between 370 and 490 nm, and emission wavelengths around 500 to 550 nm. The excitation and emission characteristics indicate that the fluorescence peaks arise from tryptophan and riboflavin, which are both expected to be present in yogurt. Tryptophan was reported to have excitation/emission wavelength maximum at 285/365 nm in pure solutions, and riboflavin to have emission maximum at 520 nm for excitations at 270, 370 and 445 nm [21]. Apparently, the excitation around 270 nm of riboflavin is not observed in this case, probably due to absorption by other molecules. The suggested tryptophan fluorescence still seems present in the yogurt sample stored in light for 35 days (Fig. 2b), whereas the riboflavin signal seems considerably decreased. Furthermore, a peak with excitation/emission maxima around 370/430 nm seems to have increased, and the fluorescence profile could correspond to the photo-chemical degradation product from riboflavin, lumichrome, with excitation/emission maxima reported somewhere around 360/450 nm in a model system [22]. These observations were further investigated by the use of PARAFAC.

4.2. PARAFAC results

PARAFAC models of fluorescence landscapes were estimated with one to four factors. Based on split-half experiments and investigation of any systematics in the residuals, the PARAFAC model with three components was considered optimal, i.e. three different fluorescence phenomena were found present in the yogurts in this investigation.

The results from a PARAFAC model are shown in Figs. 3 and 4, in the form of PARAFAC loadings and scores, respectively. This result is based on fluorescence data with zeros inserted instead of the missing values for all emission wavelengths below the given excitation wavelength, corresponding to 74% of the missing data replaced with zeros (the missing data subject will be more thoroughly discussed in the next passage). In Fig. 3, the fluorescence profiles of the three resolved fluorophores are shown as fluorescence landscapes, formed by products of the derived excitation (b) and emission (c) loading vectors. The profiles of the three PARAFAC components are in agreement with the first inspection of the fluorescence data, and further indicate the fact that the obtained fluorescence signal from the yogurt samples arises from riboflavin (Fig. 3a), tryptophan (Fig. 3b) and lumichrom (Fig. 3c). The concentration level of these three PARAFAC components can be followed in the score plots (Fig. 4a and b), displaying the distribution of the samples. Thus, the development in riboflavin (score 1) and tryptophan (score 2) fluorescence are seen in Fig. 4a, showing a decrease in riboflavin throughout time for the

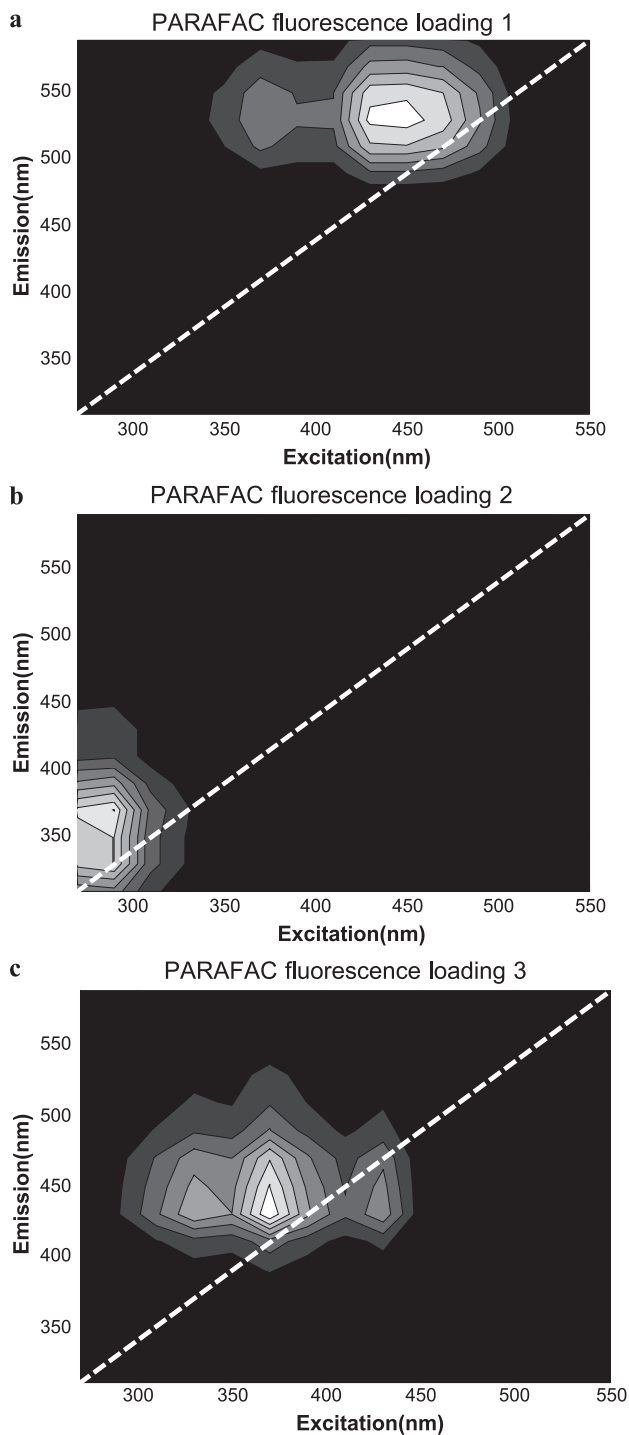


Fig. 3. PARAFAC fluorescence loadings (excitation times emission loading vectors) for the first three components (a+b+c) of a PARAFAC model based on fluorescence measurements of 125 yogurt samples and developed with zeros inserted instead of the missing values for all emission wavelengths below the given excitation wavelength, meaning that 74% of the missing values were replaced with zeros, corresponding with two steps in the diagonal line from the black measuring area in Fig. 1.

yogurt samples stored in light, and a general decrease in tryptophan throughout the storage, more or less independent of the storage conditions. The observed decrease in

riboflavin fluorescence is the most pronounced for yogurts stored in polystyrene cups, which also has the highest oxygen permeability and light transmission, and therefore expected to induce a higher level of oxidation. All in all, the experimental plan is very evident in this score plot, as indicated with the dotted lines, separating the different packaging materials and light exposure, and indicating the direction of samples according to storage time.

The lumichrom and riboflavin fluorescence can be followed in the score plot in Fig. 4b, which shows a decreasing trend in lumichrom throughout storage. Comparing each of the storage times, a negative correlation to riboflavin fluorescence is seen, though, as indicated with the dotted trend lines in the score plot. Thus, for a given storage

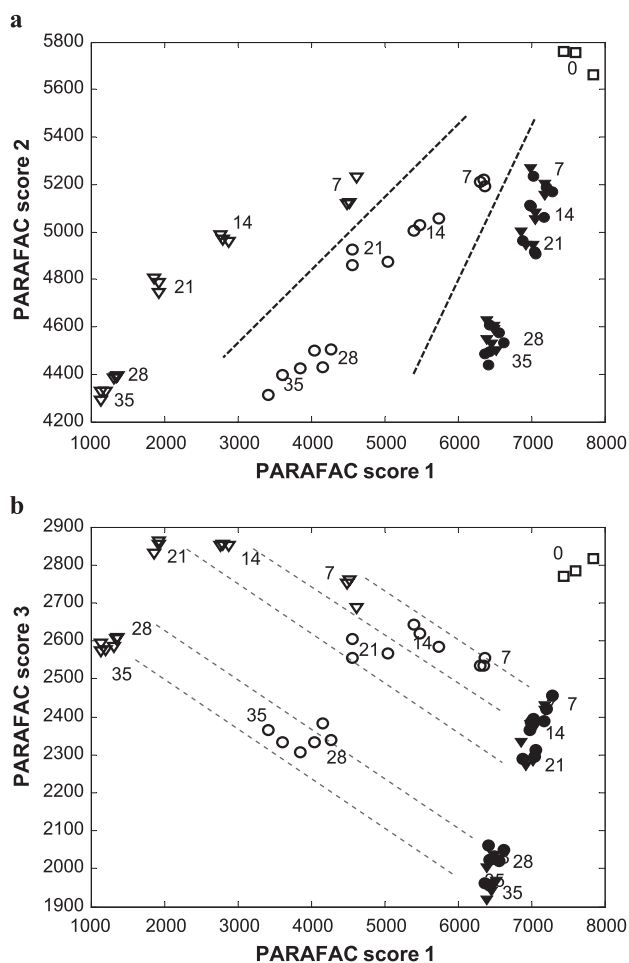


Fig. 4. Score plot of (a) scores 1 and 2, (b) scores 1 and 3 from a PARAFAC model based on fluorescence landscapes of 125 yogurt samples packaged in PLA (○) or PS (▽) at 4 °C under continuous light exposure at 3500 lx (open symbol) or in darkness (dark symbol). Samples are numbered according to days of storage, Day 0=(□). The dotted lines indicate the differences between the storage conditions (a) and the trend line for each time of storage (b). The PARAFAC model was developed with zeros inserted instead of the missing values for all emission wavelengths below the given excitation wavelength. Only samples from the first storage experiment are shown. Similar score plots were obtained for the second experiment (result not shown), with a little difference in offset, but with similar trends, comparing the two identical storage experiments.

time, the level of lumichrom fluorescence increases with decreasing riboflavin content and with storage conditions expected to induce the higher level of oxidation.

4.3. Handling missing data—inserting zeros

The measured excitation–emission matrix (landscape) contains 47% missing values, due to the physical limitations of the fluorescence measurements. The large amount of missing values can be a potential problem in the PARAFAC decomposition [19]. In order to facilitate the decomposition, insertion of zeros instead of missing values was tested.

PARAFAC component 1 is used as an example to illustrate the impact on the decomposition, when comparing PARAFAC models with different amounts of zeros replacing the missing values. In Fig. 5, contour plots of the fluorescence loadings for the first PARAFAC component are shown, based on the different PARAFAC models developed with increasing amount of zeros inserted, from the upper left corner to the lower right. It is evident that meaningful fluorescence profiles, corresponding to the fluorescence characteristics of riboflavin, only appear for the last three models, indicating that a certain amount of zeros is needed to perform a proper decomposition of these data. As indicated with the grey background, the three apparently satisfactory fluorescence loading profiles represent models with zeros inserted, leaving a band of four, two and no missing values, respectively, in the diagonal line, according to Fig. 1 (52%, 74% and 100% of zeros inserted instead of missing values). The rest of the obtained PARAFAC models yield loadings which are difficult to interpret and they all contain major artefacts in the sense that

fluorescence profiles appear for emission wavelengths shorter than the excitation wavelength.

Only every second of the calculated PARAFAC models are included in Fig. 5. The overall results are that models on data with zeros inserted and leaving a band of up to five data points of missing values result in satisfactory decomposition and meaningful loadings, which means that at least 43% of the missing values need to be substituted. Similar results were obtained for PARAFAC loadings 2 and 3 (results not shown), underlining that the missing values need to be handled in order to obtain a valid PARAFAC decomposition of these kind of fluorescence data.

Since fluorescence emission at wavelengths below the excitation wavelengths is physically impossible, it makes sense to insert zeros in this area of the excitation–emission matrix in order to facilitate the decomposition by reducing the amount of missing values to be handled in the PARAFAC algorithm. However, it is previously shown that zeros inserted for emission wavelengths slightly below the excitation wavelengths can hinder an adequate mathematical decomposition, due to the required trilinearity in the fluorescence data [18]. Apparently, this does not make up a problem in the present investigation; even zeros inserted for all the missing values (also including one emission wavelength above the given excitation wavelength) seem to facilitate a meaningful decomposition, as seen in the lower right corner of Fig. 5.

As an alternative to the insertion of zeros, one could try to cut off some of the extreme wavelengths (high excitation or low emission wavelengths) which contain many missing values, as seen by Ref. [17]. In this way, the part of missing values can be significantly reduced, but also the measuring

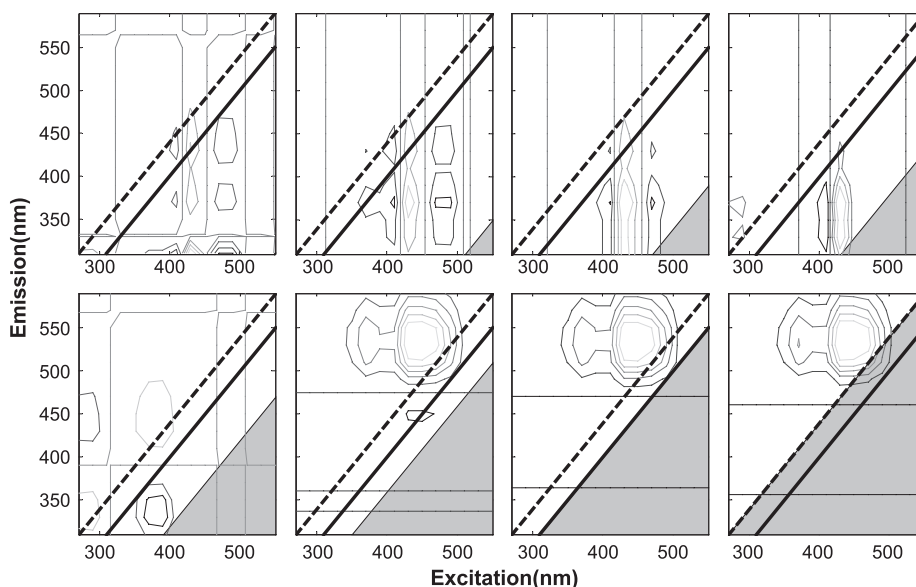


Fig. 5. Contour plots of fluorescence loadings (excitation times emission loadings) of the first component from PARAFAC models based on data with different amounts of inserted zeros, going from modelling with no insertion of zeros (upper left) to all missing values completely substituted with zeros (lower right corner). The grey-filled area represents where zeros are inserted. Loadings from every second intermediate model result according to Fig. 1 are shown. The solid diagonal lines indicate when emission equals the excitation wavelength. Fluorescence is only measured in the area above the dotted line.

spectral range will be restricted. Applying constraints to the PARAFAC model parameters has also proven to be helpful in the curve resolution and model stability [18]. However, when applying non-negativity in the PARAFAC modelling in the present study, similar results were obtained, with respect to the amount of zeros needed for a meaningful decomposition.

4.4. Riboflavin calibration

To verify the dependency between riboflavin and fluorescence signal, various regression models were developed. At first, the score values of PARAFAC component 1, which is expected to be due to riboflavin fluorescence, are compared with the traditional determined riboflavin content. A linear regression between the PARAFAC score and riboflavin content yields a correlation coefficient, R^2 of 0.94, confirming the assumption. However, a regression model for predicting the riboflavin content from the fluorescence landscapes can be further optimized, including the other PARAFAC scores in the regression model, as listed in Table 1 and shown in Fig. 6. This is probably due to the fact that the resolved fluorescence signal of riboflavin still is somewhat influenced by the fluorescence from other fluorophores or by differences in the sample matrix.

In Table 1, the results of different regression models are shown in the form of correlation coefficient and prediction errors, RMSECV. Comparing MLR on PARAFAC scores with PLS regression of PARAFAC scores as well as unfolded fluorescence spectra and multiway PLS regression of the fluorescence landscapes, only minor differences are found in this study. Only the univariate regression model of PARAFAC score 1 proved to perform significantly poorer ($p \leq 0.015$), compared with the best performing regression model, when evaluated with an F -test of the RMSECV values [23].

Even though three fluorescent components were found in the PARAFAC model, only two components were apparently needed to obtain the optimal regression. This is both evident for the PLS and MLR models in Table 1. Thus, for MLR between PARAFAC scores of the expected riboflavin and lumichrom components and riboflavin

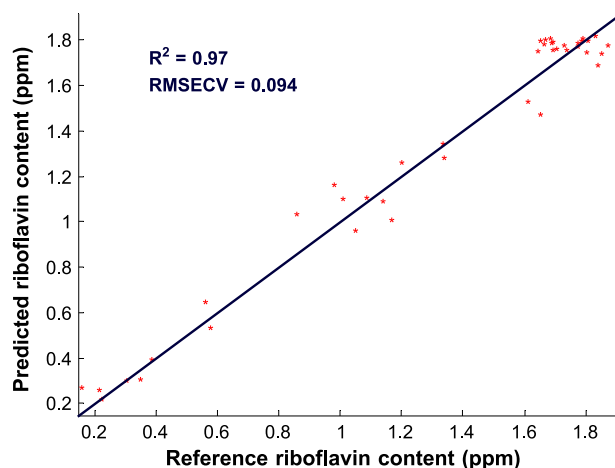


Fig. 6. Predicted vs. reference riboflavin content of 42 yogurt samples, based on a PLS regression model with two components of the scores values (1–3) from a PARAFAC model of fluorescence landscapes.

content, a regression model was obtained with a correlation of 0.97 (R^2), and a prediction error of 0.094 ppm, corresponding to 7% of the mean riboflavin content in the yogurt samples.

The results further indicate that the investigated non-destructive fluorescence measurements have the potential to substitute the traditional AOAC method for determination of riboflavin. The AOAC fluorometric method involves a chemical extraction while the investigated method makes use of a “mathematical extraction” of the riboflavin contribution to the fluorescence signal from the yogurt.

5. Conclusions

The present study represents an example of the application of fluorescence spectroscopy and PARAFAC to follow the oxidative quality of a food product. Thus, yogurt was monitored with rapid and non-destructive fluorescence spectroscopy, yielding information about the yogurt throughout storage at a molecular level, in the form of the development in fluorescence signal assigned to riboflavin, tryptophan, and the oxidative product of riboflavin, lumichrom.

The fluorescence landscapes in the present study contained a large amount of missing values, which make up a problem in the PARAFAC modelling, leading to model solution, which did not make sense, physically and chemically. Substituting a certain amount of the missing values with zeros facilitated a satisfactory decomposition. Thus, it was shown that at least 43% of the missing values had to be substituted in order to obtain meaningful PARAFAC models with the present data.

Regression models between the fluorescence landscapes and the riboflavin content of the yogurts confirmed the chemical causality, and underlined the potential of the method to be used for rapid determination of riboflavin.

Table 1
Results from different regression models between fluorescence landscapes and riboflavin content of 42 yogurt samples

Data	Method	# Comp.	R^2	RMSECV (ppm)
PARAFAC score 1	MLR	1	0.94	0.13
PARAFAC scores 1–3	MLR	3	0.97	0.096
PARAFAC scores 1–2	MLR	2	0.97	0.096
PARAFAC scores 1+3	MLR	2	0.97	0.094
PARAFAC scores 1–3	PLS	2	0.97	0.094
Unfolded emission spectra	PLS	2	0.97	0.092
Fluorescence landscapes	N-PLS	2	0.97	0.094

Acknowledgments

This study was partly sponsored by an EU innovation programme with the acronym OPUS (IN30905I). The aim of this project was to adapt and apply advanced fluorescence measurement techniques for on-line analysis to traditional food industries. Dr. Lars Nørgaard is acknowledged for rewarding discussions.

References

- [1] S.A. Jensen, L. Munck, H. Martens, *Cereal Chemistry* 59 (1982) 477–484.
- [2] E. Dufour, A. Riaublanc, *Lait* 77 (1997) 657–670.
- [3] S. Herbert, A. Riaublanc, B. Bouchet, D.J. Gallant, E. Dufour, *Journal of Dairy Science* 82 (1999) 2056–2062.
- [4] E. Dufour, M.F. Devaux, P. Fortier, S. Herbert, *International Dairy Journal* 11 (2001) 465–473.
- [5] G. Mazerolles, M.F. Devaux, G. Duboz, M.H. Duployer, N.M. Riou, E. Dufour, *Lait* 81 (2001) 509–527.
- [6] J. Christensen, V.T. Povlsen, J. Sorensen, *Journal of Dairy Science* 86 (2003) 1101–1107.
- [7] E. Dufour, G. Mazerolles, M.F. Devaux, G. Duboz, M.H. Duployer, M.N. Riou, *International Dairy Journal* 10 (2000) 81–93.
- [8] S. Herbert, N.M. Riou, M.F. Devaux, A. Riaublanc, B. Bouchet, D.J. Gallant, E. Dufour, *Lait* 80 (2000) 621–634.
- [9] J.P. Wold, K. Jorgensen, F. Lundby, *Journal of Dairy Science* 85 (2002) 1693–1704.
- [10] E.M. Becker, J. Christensen, C.S. Frederiksen, V.K. Haugaard, *Journal of Dairy Science* 86 (2003) 2508–2515.
- [11] R. Bro, *Chemometrics and Intelligent Laboratory Systems*. 38 (1997) 149–171.
- [12] D. Baunsgaard, L. Munck, L. Norgaard, *Applied Spectroscopy* 54 (2000) 438–444.
- [13] D. Baunsgaard, C.A. Andersson, A. Arndal, L. Munck, *Food Chemistry* 70 (2000) 113–121.
- [14] R. Bro, *Chemometrics and Intelligent Laboratory Systems*. 46 (1999) 133–147.
- [15] D. Baunsgaard, L. Norgaard, H.A. Godshall, *Journal of Agricultural and Food Chemistry* 49 (2001) 1687–1694.
- [16] D.K. Pedersen, L. Munck, S.B. Engelsens, *Journal of Chemometrics* 16 (2002) 451–460.
- [17] J.K.S. Moller, G. Parolari, L. Gabba, J. Christensen, L.H. Skibsted, *Journal of Agricultural and Food Chemistry* 51 (2003) 1224–1230.
- [18] C.M. Andersen, R. Bro, *Journal of Chemometrics* 17 (2003) 200–215.
- [19] L.G. Thygesen, Å. Rinnan, S. Barsberg, J.K.S. Moller, *Chemometrics and Intelligent Laboratory Systems*. 71 (2004) 97–106.
- [20] C.A. Andersson, R. Bro, *Chemometrics and Intelligent Laboratory Systems*. 52 (2000) 1–4.
- [21] D.E. Duggan, R.L. Bowman, B.B. Brodie, S. Udenfriend, *Archives of Biochemistry and Biophysics* 68 (1957) 1–14.
- [22] J.B. Fox, D.W. Thayer, *International Journal for Vitamin and Nutrition Research* 68 (1998) 174–180.
- [23] D.M. Haal, E.V. Thomas, *Analytical Chemistry* 60 (1988) 1193–1202.

Paper III

Oxidative changes in pork scratchings, peanuts, oatmeal and muesli viewed by fluorescence, near-infrared and infrared spectroscopy

Pernille N. Jensen, Jakob Christensen and Søren B. Engelsen
European Food Research and Technology 219 (3), 294-304, 2004

Pernille N. Jensen · Jakob Christensen ·
Søren B. Engelsen

Oxidative changes in pork scratchings, peanuts, oatmeal and muesli viewed by fluorescence, near-infrared and infrared spectroscopy

Received: 8 January 2004 / Published online: 3 July 2004
© Springer-Verlag 2004

Abstract The possibility of using rapid spectroscopic methods to detect lipid oxidation of four standard food products—peanuts, pork scratchings, oatmeal and muesli—were investigated in a large screening experiment. Fluorescence, near-infrared [including visual (Vis/NIR)] and infrared (IR) spectra have been recorded during and beyond the normal shelf lives of the products and related by means of multivariate data analysis to reference oxidation measures of free radicals and hexanal, as well as to sensory evaluation. For pork scratchings, the three spectroscopic techniques were able to monitor the progressing level of oxidation: IR with good correlation to hexanal ($r^2=0.86$), Vis/NIR with good correlations to free radicals ($r^2=0.82$) and fluorescence with good correlations to both free radicals ($r^2=0.76$) and hexanal ($r^2=0.83$). In the case of IR, the best result was obtained using the region including the out-of-plane C–H of trans-fatty acids. For the other three products, the results were generally inferior except for good correlations between fluorescence spectra and free radicals in peanuts ($r^2=0.73$) and between Vis/NIR spectra and hexanal for muesli products ($r^2=0.8$).

Keywords Lipid oxidation · Infrared-spectroscopy · Visual/near-infrared · Fluorescence · Peanuts · Pork scratchings · Oatmeal · Muesli

Introduction

Peanuts, pork scratchings, oatmeal and muesli are susceptible to lipid oxidation due to a high content of unsaturated fatty acids. The oxidative processes involving oxygen are accelerated by light, and result in the formation of hydroperoxides, which are precursors of secondary oxidation products. The latter off-flavours cause rancidity, and thus deterioration of the foods. Prior to the formation of hydroperoxides, free radicals can be detected. Hence, the presence of free radicals is an early indication of lipid oxidation. To obtain products of high quality it is important that the quality is high prior to packaging. The quality is often determined by content of volatiles, but determination of the early stages of oxidation is naturally more advantageous and is becoming more common [1].

The oxidation products, of which some are unstable, react with other compounds. When illuminated by light some of these products are fluorescent and can be used as indicators of the degree of oxidation. The vibrational states of sample molecules can be detected in the mid-infrared (IR) and near-infrared (NIR) regions. The IR region is attractive, as it allows for qualitative determination of organic compounds. The characteristic vibrational modes of each molecular group cause a unique fingerprint, which may be distinguished from the absorption patterns of other compounds in the sample matrix. Compared to the IR region, the NIR region consists of broad and overlapping overtone and combination tone absorption bands of C–H, O–H and N–H vibrations. However, NIR is used worldwide for the rapid quantitative determinations of moisture, fat, protein, carbohydrate and fibre in cereals, grains, feeds, meat and dairy products [2]. Fluorescence, IR and visible (Vis)/NIR spectroscopy are rapid, non-destructive and sensitive techniques, which in combination with supervised multivariate data analysis such as partial least squares regression (PLSR), can be related to “hidden” chemical information.

P. N. Jensen
Centre for Advanced Food Studies, Department of Food Science,
Food Chemistry,
The Royal Veterinary and Agricultural University,
Rolighedsvej 30, 1958 Frederiksberg C, Denmark

J. Christensen · S. B. Engelsen (✉)
Centre for Advanced Food Studies, Department of Food Science,
Food Technology,
The Royal Veterinary and Agricultural University,
Rolighedsvej 30, 1958 Frederiksberg C, Denmark
e-mail: se@kvl.dk
Tel.: +45-3528-3205
Fax: +45-3528-3245

Fluorescence spectroscopy

To the best of our knowledge no investigations of fluorescence spectroscopy on peanuts, pork scratchings, oatmeal or muesli in order to predict their oxidation statuses have been made. Fluorescence spectroscopy has previously been shown to be useful in determining the riboflavin content in wheat flour [3] and stored dairy products [4, 5]. In addition, sensory off-flavours [5] and stability during storage [6] can be predicted in dairy products. In Parma ham, a good correlation was found between sensory evaluation and fluorescence, which also relates to major chemical/physical changes during processing [7]. This finding is in accordance with results obtained on other meat products where fluorescence was correlated to sensorially assessed rancidity with the same accuracy as for chemical determination of volatile compounds. Fluorescence was found to be rather non-specific with regard to the various oxidation products, as the different aldehydes resulted in very similar spectra. Moreover, the fluorescent compounds were formed during a period of 24 h at 4 °C, thereby suggesting that fluorescence was capable of detecting early oxidation [8]. Fluorescence spectroscopy has also found applicability in monitoring frying oil deterioration by prediction of anisidine values (AVs), oligomers, iodine values (IVs) and vitamin E [9]. In these investigations fluorescence was used to determine the oxidative status of different products, but other applications of fluorescence were also found. In wheat milling, fluorescence detected the physical separation of the plant tissue components pericarp, aleurone and endosperm, resulting in a percentage distribution [10, 11]. Analysis of sugar and sugar juices by fluorescence facilitated identification of different sugar factories and prediction of sugar quality. Sugar is non-fluorescent, but impurities such as amino acids react with reducing sugars and fluoresce. In the longer perspective, fluorescence can be used to provide a process signature that can be related to underlying process steps in sugar production [12].

Vis/NIR spectroscopy

Vis/NIR spectroscopy has been abundantly proven to be a stable and reliable method for monitoring the overall quality changes in different food products. Investigations on different oils have revealed good correlations between oxidative state [13, 14], fatty acid composition [15], peroxide value (PV) and conjugated dienes [16] and NIR. However, prediction of the PV by Vis/NIR was not successful in frying oils, whereas determinations of free fatty acids (FFA), AV, IV and vitamin E were [9]. In addition, FT-NIR could determine IV, saponification number and *cis* and *trans* contents in fats and oils [17]. In more complex food matrices such as mayonnaise, NIR has proven to be able to detect minor variations in oil content and quality [18], and in walnuts Vis/NIR could predict the sensory quality and hexanal content [19]. In analysis of wheat, NIR replaced the more traditional and time-con-

suming methods to identify varieties [20] or predict the chemical composition (dry matter, crude protein, ash, starch and oil) [21]. Near-infrared transmittance has shown an excellent ability to determine protein content in single wheat kernels [22].

FT-IR spectroscopy

Over the last decade the applicability of infrared spectroscopy to the study of oxidative changes in oils and other foods has increased. Some of the traditional chemical analyses for measuring oxidative stability can advantageously be replaced by Fourier-transformed infrared (FT-IR). Determination of PV [23, 24, 25], IV [9, 26, 27] and FFA [9, 28] in different oils and fats could all be performed by IR spectroscopy. In addition, determination of secondary oxidation products such as AV has also been performed by FT-IR [9, 29, 30]. IR has also characterized secondary oxidation products from photosensitized oxidation of methyl linoleate [31, 32] and classified edible oils, butters and margarines according to their degrees of esterification and unsaturation [33].

The oxidation process of safflower and cottonseed oils was monitored and evaluated by studying the spectral changes in FT-IR attenuated total reflectance (ATR) spectroscopy. The absorption bands associated with oxidation products were identified by standards and the oxidative status was thus determined by the content of hydroperoxides, alcohols and total carbonyls [34]. The oxidation process was also studied in 13 oil samples with different proportions of oleic, linoleic and linolenic acids. FT-IR was able to distinguish between the different stages of the oxidation process and establish the degree of oxidation of each oil sample. The differences among samples were basically due to the rate at which the primary and secondary oxidation products were produced. This depended on the fatty acid composition, as the higher the content of polyunsaturated fatty acids, the lower the oxidative stability [35, 36].

These investigations have all been performed on different oils, i.e. homogeneous materials, but FT-IR has also been applied to more complex foodstuffs such as potato chips. Deterioration of potato chips has been monitored by FT-IR photoacoustic spectroscopy (PAS). Identification of some of the spectral changes revealed, for example, an increase in the band at $1,717\text{ cm}^{-1}$ corresponding to saturated aldehyde functional groups or secondary oxidation products [37]. However, the band at approximately $1,717\text{ cm}^{-1}$ has also been assigned to FFA.

This paper presents the exploratory spectroscopy area of storage experiments on pork scratchings, peanuts, oatmeal and muesli in investigating the applicability of spectroscopic analyses to monitor deterioration of foods. The development of free radicals and hexanal and evaluation of sensory quality during storage is discussed in Jensen et al. [38]. The aim of the present study was to investigate whether fluorescence, Vis/NIR or FT-IR spectroscopy can replace or complement the oxidation anal-

yses mentioned, and thereby make quality control easier and faster. Interpretation of the obtained spectra is discussed.

Materials and methods

Products. Peanuts and pork scratchings were commercial products obtained from KiMs (Denmark); muesli I was from Nutana (Denmark) and oatmeal and muesli II were from Cerealia (Denmark). Muesli I was composed of rolled oats, wheat flakes, extruded rice, raisins, almonds and desiccated coconut. The ingredients were mixed, refined vegetable oil (4%) and honey were added and the mixture baked. Prior to analysis, the rolled oats and wheat flakes were separated from the other ingredients and only these two ingredients were analysed. Muesli II was composed of rolled oats, extruded rice and corn flakes, which were coated with a mixture of sugar, vegetable oil, glucose syrup and honey.

Experimental design and storage. The influence of the external factors (light, oxygen concentration and product-to-headspace (P/H) ratio) was investigated for pork scratchings, peanuts, oatmeal and muesli I in experiment I, whereas the effects of oxygen transmission rate of the packaging material combined with different oxygen concentrations were investigated for pork scratchings, peanuts and muesli I and II in experiment II. The time scale with indication of the time of sample withdrawal for analysis for both experiments is shown in Fig. 1. The quality changes in experiment I were monitored by electron spin resonance spectroscopy (ESR), gas

chromatography (GC)-headspace, and fluorescence and IR spectroscopies, whereas the quality changes were measured by ESR, GC-headspace, Vis/NIR spectroscopy and sensory evaluation in experiment II. Further description of the chemical and sensory analyses is found in Jensen et al. [38].

Fluorescence spectroscopy. Fluorescence landscapes were measured directly on the homogenized sample using a Bio View spectrofluorometer (Delta, Lyngby, Denmark). The instrument uses a pulsed xenon lamp for excitation and a surface area of approximately 6 mm in diameter was sampled in each measurement. The spectrofluorometer was equipped with a fibre optics probe with an open-end 180° measuring geometry. Different voltages were applied to the photo multiplier: 750 mV for pork scratchings and peanuts and 800 mV for oatmeal and muesli I. The landscapes were obtained using excitation wavelengths from 270 to 550 nm and emission wavelengths from 310 to 590 nm, with intervals and bandwidths of 20 nm, giving a total of 15 excitation and 15 emission wavelengths. The emission wavelengths were shifted by 40 nm from each excitation wavelength, resulting in a total of 120 data points for each measurement. For the data analysis, the 2D fluorescence landscapes were unfolded into a row of emission spectra.

Vis/NIR spectroscopy. Visible/NIR spectroscopic data were measured in the range 400–2,498 nm in 2-nm intervals using a NIRSystems spectrophotometer (Model 6500, Foss NIRSystems, Silver Spring, MD). The spectrophotometer used a split detector system with a silicon (Si) detector between 400 and 1,100 nm and a lead sulphide detector from 1,100 to 2,500 nm. The angle of incident light was 180° and reflectance was measured at a 45° angle. The Vis/NIR reflection spectra were recorded using a small ring cup and a Spinning Module (NR-6506). The collected spectral data were converted to $\log(1/R)$ units prior to data analysis.

FT-IR spectroscopy. The FT-IR data were collected with an Aridzone MB100 FT-IR (Bomem, Quebec, Canada) in the range 4,000 to 550 cm^{-1} using an ATR device with a tipple bounce diamond crystal (Durascope, SensIR Technologies). The homogenized samples were squeezed onto the ATR crystal with equal pressure of 1 N/cm^2 . The instrument was purged with dry air to minimize water vapour and carbon dioxide interference. A resolution of 4 cm^{-1} was employed and 32 spectra were accumulated, averaged and ratioed against a single-beam spectrum of the clean ATR crystal and converted into absorbance units.

Data handling. The results were evaluated by multivariate data analysis using principal component analysis (PCA) and PLSR. Prior to data analysis the fluorescence data were normalized, whereas the Vis/NIR and FT-IR spectra (without the region where the diamond absorbs (1,900–2,500 cm^{-1})) were transformed by multiplicative scatter correction (MSC) [39]. Owing to instrument errors, fluorescence data obtained from weeks 5–12 were excluded from the data analysis, as were the week 8 FT-IR data for pork scratchings. Chemometric models were performed on mean-centred and autoscaled (divided by the standard deviation) data and evaluated using segmented cross-validation. Each segment was constructed to include data from one storage time only, except one segment, which contains data from weeks 0–3, as day 0 consisted of only four measurements. The PCA models were constructed on an average of six measurements (average of two identical bags with three measurements on each bag), whereas all the individual measurements were used for the PLSR models. Only PLSR models with correlation coefficients (r^2) above approximately 0.6 are shown, i.e. those which can explain more than 60% of the total variation in the data. In order to optimize the models, interval partial least squares regression (iPLS) [40] models were developed on Vis/NIR and FT-IR data. Multivariate data analysis was performed using The Unscrambler version 7.8 (CAMO, Trondheim, Norway), whereas iPLS regression models were calculated in MatLab 6.5 (MathWorks) using the PLS-Toolbox 2.0 (Eigenvector) and the command line iPLS toolbox for MatLab, ver. 3.0 by L.

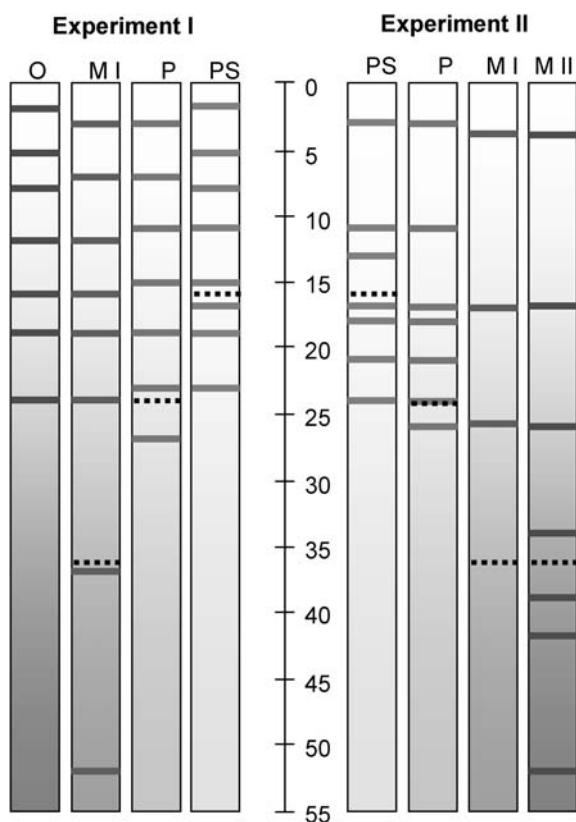


Fig. 1 Time scale (weeks) for experiments I and II for pork scratchings (PS), peanuts (P), oatmeal (O), muesli I (MI) and muesli II (MII). Time points where samples were withdrawn for analysis are marked by solid lines and the shelf life of the products is marked by dotted lines

Nørgaard. The iPLS toolbox is available at <http://www.mod-els.kvl.dk>.

Results and discussion

The oxidative stabilities of pork scratchings, peanuts, oatmeal and two different types of muesli were monitored in two storage experiments by ESR and GC-headspace, measuring the contents of free radicals and volatiles such as hexanal, respectively. The first storage experiment investigated the effects of light and oxygen availability (P/H ratio and oxygen concentration) on pork scratchings, peanuts, oatmeal and muesli I. The quality changes were followed by fluorescence and FT-IR spectroscopy and compared to the content of free radicals and volatiles. In the second experiment pork scratchings, peanuts and muesli I and II were packed in different packaging materials containing either <1%, 5% or 21% oxygen. Besides contents of free radicals and volatiles, the oxidative status was determined by Vis/NIR spectroscopy and sensory evaluation. The obtained reference results (free radicals, hexanal and sensory evaluation) from these storage experiments are described and discussed in detail in Jensen et al. [38]. However, during storage other aroma com-

ponents in addition to hexanal were developed, two of which (pentanal and acetaldehyde) are also discussed in the present paper.

Chemical reference data

The contents of water, protein, carbohydrate, fat (including the content of oleic acid and linoleic acid) and the total amount of vitamin E for the different products are listed in Table 1, from which it is possible to divide the products into high-fat samples (pork scratchings and peanuts) and high-carbohydrate samples (oatmeal, muesli I and muesli II). Pork scratchings deviate further by having an extremely high protein content. Table 2 gives an overview of the results (minimum, maximum and mean values) from the chemical and sensory reference analyses. It can be observed that the relative free radical concentration ranges from approximately 4.5 to 16 for pork scratchings and muesli whereas the range for oatmeal is 5.5–43. For peanuts, a narrow range is found for hexanal, as the content varies between 0.0 and 1.3 mg/kg for storage experiment I, whilst a variation of 0.0–7.3 mg/kg was observed for storage experiment II. The fact that the content of free radicals varies from experiment I to

Table 1 Composition of pork scratchings, peanuts, oatmeal and muesli I and II

	Fat ^a	Carbohydrate ^a	Protein ^a	Water	Oleic acid	Linoleic acid	Vitamin E content ^b
	(g/100 g)	(g/100 g)	(g/100 g)	(g/100 g)	(%)	(%)	(µg/g)
Pork scratchings	45	1	50	1	46	11	296
Peanuts	50	16	29	1	51	27	178
Oatmeal	7	68	13	1	42	38	3
Muesli I	14	62	10	7	48	31	54
Muesli II	15	65	9	4	49	20	19

^a From nutritional information label

^b Total amount of α -, δ - and γ -tocopherols

Table 2 Minimum, maximum and mean for the chemical and sensory analyses

Food	Content ^a	Experiment I			Experiment II		
		Min	Max	Mean	Min	Max	Mean
Pork scratchings ^a	Free radicals	4.4	15.0	10.9	6.1	12.2	9.5
	Hexanal ^b	0.0	394.3	36.6	0.0	43.8	3.7
	Pentanal ^b	0.0	118.8	16.0			
Peanuts ^a	Free radicals	8.2	13.1	10.5	13.1	19.3	15.3
	Hexanal ^b	0.0	1.3	0.2	0.0	7.3	1.3
Oatmeal ^a	Free radicals	5.5	43.2	19.6			
	Hexanal ^b	0.0	134.0	22.6			
	Pentanal ^b	0.0	11.7	2.5			
Muesli I ^a	Free radicals	4.8	16.3	8.7	9.2	75.7	47.1
	Hexanal ^b	0.0	55.5	5.2	0.9	141.9	20.5
	Acetaldehyde ^b	0.0	12.1	3.6			
Muesli II ^{a,c}	Free radicals				6.0	8.7	7.2
	Hexanal ^b				0.0	1.5	0.7
	Vanilla flavour				2.1	7.1	4.4
	Rancid flavour				1.3	6.0	3.5
	Overall impression				1.3	4.0	2.7

^a The content of free radicals is relative, whereas the volatiles (acetaldehyde, pentanal and hexanal) are expressed as milligrams per kilogram

^b Obtained from GC-headspace

^c The descriptors are rated on a 10-point scale, except "overall impression" which is on a 5-point scale

Table 3 Intercorrelation (r^2) between chemical and sensory analysis

		Hexanal	Pentanal	Rancid odour	Rancid flavour	Overall impression
Experiment II	Free radicals	0.28	0.23			
	Hexanal		0.99			
Experiment II	Free radicals	0.10		0.29	0.24	0.32
	Hexanal			0.11	0.08	0.08
	Rancid odour				0.90	0.96
	Rancid flavour					0.91

experiment II indicates natural product variation between batches. The relationship between the chemical and sensory analyses has been examined. Hexanal content was found to correlate to most of the sensory descriptors in peanuts, muesli I and II and it was further found that almost all the sensory descriptors intercorrelate, cf. Table 3. In muesli I and II, hexanal and free radicals were also found to intercorrelate. In pork scratchings, hexanal and pentanal were highly correlated in experiment I and in experiment II a strong intercorrelation was observed between the sensory descriptors.

Fluorescence

The unfolded fluorescence landscapes (plotted as concatenated emission spectra) are shown in Fig. 2. Two sample spectra for each product represent the extremes, i.e. a fresh (from day 0; grey spectra) and an oxidized (stored under the most severe conditions; solid line spectra) sample. A comparison of the products reveals that the fluorescence signal from the high-fat samples, pork scratchings and peanuts (a+b) look alike and that the high-carbohydrate samples, oatmeal and muesli (c+d) are comparable. The latter makes good sense, as muesli is mainly composed of oatmeal and wheat flakes. The differences between the fresh and oxidized samples are most evident for pork scratchings and oatmeal and these results will therefore be discussed in more detail.

The results of a PCA model on the unfolded fluorescence emission spectra of pork scratchings are shown in Fig. 3a. The distribution of samples according to the major variations in the fluorescence signal are displayed in the score plot, revealing the experimental design and the expected degree of oxidation. The first principal component (PC1) discriminates between the samples stored in light or in darkness, whereas PC2 to some extent represents the oxygen exposure with a distribution according to the oxygen concentration in headspace. However, the separation into light and darkness for 0% oxygen is not as clear as for 4% and 21% oxygen, as only negligible oxidation occurs when almost no oxygen is present.

The corresponding loading plot (Fig. 4) displays which fluorescence variables are responsible for the discriminative trends, i.e. which excitation and emission wavelengths are influenced by the expected oxidation. The fluorescence signals can be interpreted as a complex chemical fingerprint of the samples, as suggested by Munck et al. [12], comprising both fluorescence and quenching phe-

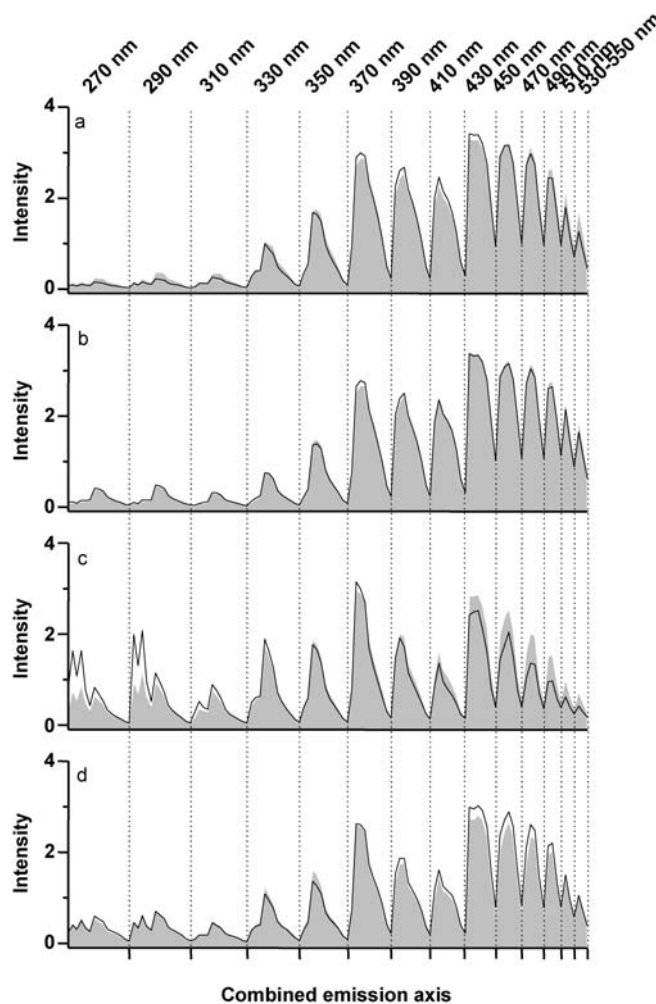


Fig. 2a–d Unfolded fluorescence emission spectra for a fresh (grey) and an oxidized (solid line) sample of **a** pork scratchings, **b** peanuts, **c** oatmeal and **d** muesli I. Excitation wavelengths are written above each emission spectrum, divided by the vertical dotted lines

nomena. In order to try to interpret and identify which compounds/fluorophores that can be responsible for the changes in the fluorescence signals, the fluorescence PCA loadings will be further discussed.

For the first PCA loading, an increase in fluorescence from excitation around 370 nm and a decrease at excitation above 470 nm can be observed. During lipid oxidation proteins cross-link with, for example, aldehydes leading to other fluorescent compounds. The observed in-

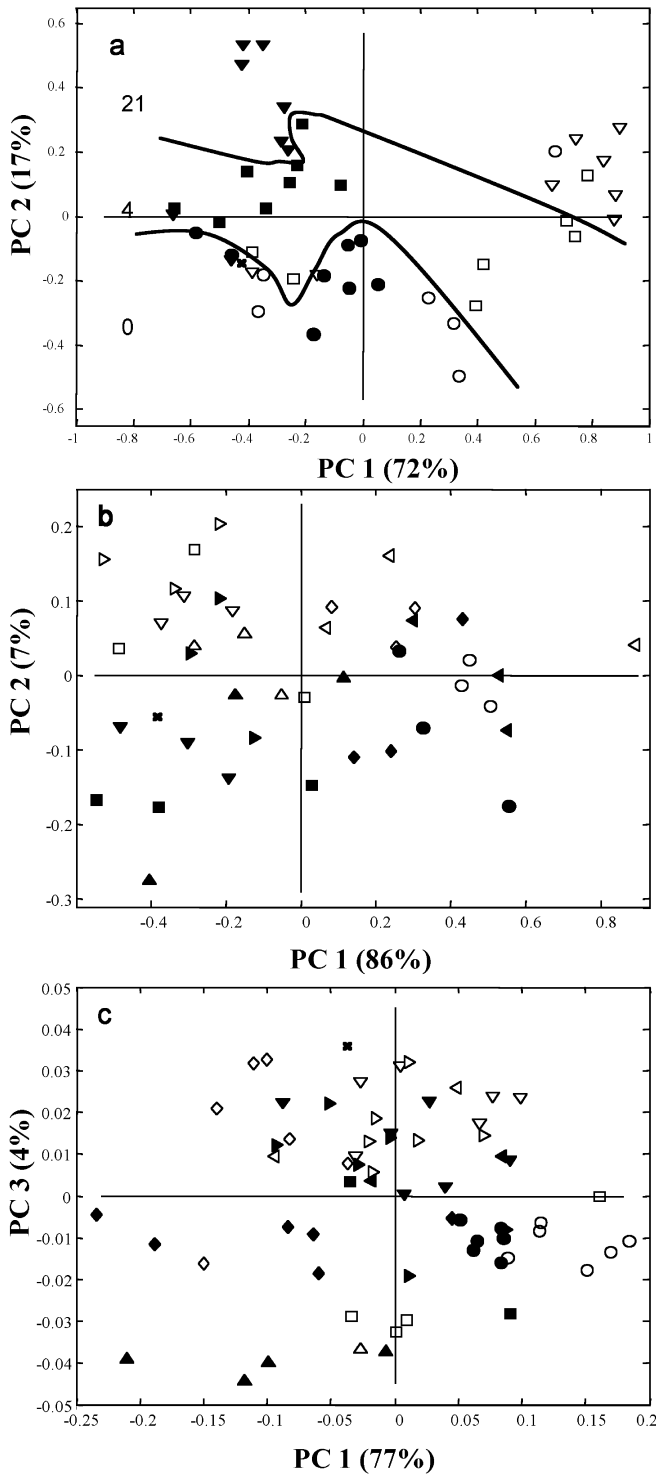


Fig. 3a–c Score plots for principal component analysis (PCA) models for pork scratchings. **a** Principal component 1 (PC1) vs. PC2 (explaining 72+17%) for fluorescence spectra with indication of O₂ concentration 0 (circles), 4 (squares), or 21% (triangles); open and solid points indicate storage in light and darkness, respectively. **b** PC1 vs. PC2 (explaining 86+7%) for visible/near-infrared (Vis/NIR) spectra with indication of <1% (open points) and 21% (solid points) O₂ and storage time [day 0 (cross), 2 (circles), 11 (squares), 13 (down triangles), 17 (right triangles), 18 (left triangles), 21 (up triangles) and 24 (diamond)]. **c** PC1 vs. PC3 (explaining 77+4%) for IR data with indication of storage time [day

crease at excitation/emission (ex/em) around 370/450 nm could thus be due to reported reactions of malondialdehyde with amino compounds (with ex=370–405 nm and em=450–470 nm) [41, 42], indicating increased level of lipid oxidation. The decrease in excitation above 470 nm (emission above 530 nm) could be related to riboflavin, which is known as a marker for photo-oxidation and has an ex/em peak of 445/520 nm in pure solutions [43].

The second PCA loading displays an increase in fluorescence with excitation around 430 nm and decreases at excitation below 300 nm and around 350 nm. The increase at excitation 430 nm (em=470–510 nm) could be due to increased oxidation, as this region has been shown to be related to fluorescent protein-bound lipid peroxidation products [44].

The results obtained for oatmeal (PCA model not shown) reveal some similar trends with an increase related to the suggested reactions of malondialdehyde with amino compounds (ex/em=370/450 nm) and a decrease in fluorescence intensity above excitation 470 nm. However, a marked intensity increase at lower excitation wavelengths is observed for oatmeal, whereas the intensity decreases for pork scratchings. The excitation characteristics at 270 and 290 nm (em=330 and 270) arise generally from proteins containing tryptophan and other aromatic amino acids [11, 45]. As the protein content or the amount of aromatic amino acids is not expected to change during storage, the decreasing trend can possibly be interpreted by differences in quenching effects in the sample. A decrease in fluorescence signals around excitation 450 nm is, for example, observed in the oatmeal samples throughout storage. This can be related to the presence of carotenoids, as reported by [45, 46], or riboflavin. In wheat flour, excitation of 470 nm and emission wavelength larger than 500 nm was found to be due to riboflavin [3] and this could also be the case for the oatmeal samples investigated in this study. The decreased intensity of carotenoids or riboflavin fluorescence could be caused by degradation during storage.

To investigate whether fluorescence is able to predict the oxidative status of the different food products, PLSR models were constructed between fluorescence data and content of free radicals and volatiles (acetaldehyde, pentanal, or hexanal). The results of the calculated PLSR models are listed in Table 4. They clearly show that prediction of quality by fluorescence results in the highest correlations for pork scratchings; this accounts for free radicals as well as volatiles. For peanuts only the content of free radicals can be predicted by fluorescence, while for oatmeal only the hexanal content can be predicted. As for pork scratchings, the contents of free radicals as well as volatiles in muesli can be described by the changes in fluorescence intensity.

0 (cross), 2 (circles), 15 (squares), 17 (down triangle), 19 (right triangle) and 23 (left triangle)]; open and solid points indicate storage in light and darkness, respectively

Fig. 4a, b Contour plot of the first (a) and second (b) loading from the PCA model on re-folded fluorescence emission spectra for pork scratchings

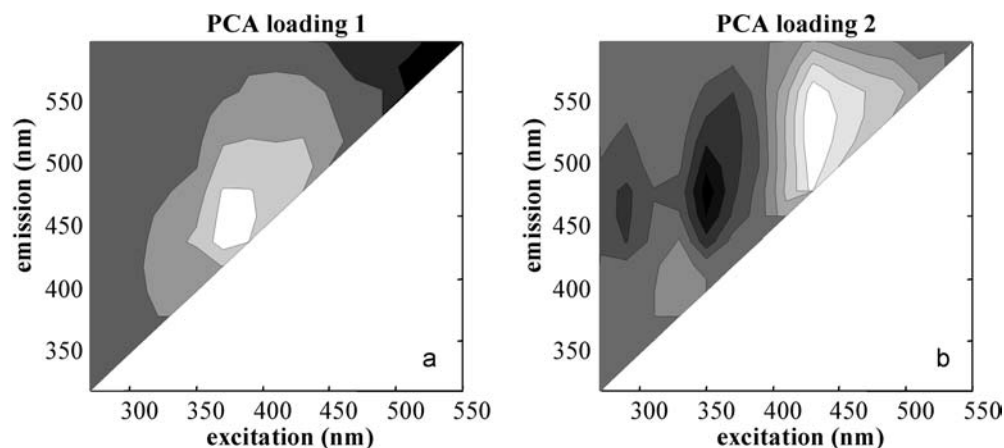


Table 4 Partial least squares regression (PLSR) correlations (r^2) between fluorescence and chemical analysis. *PC* Principal component, *RMSECV* root mean square error of cross validation

		Time/ samples ^a	PC ^b	RMSECV ^c	r^{2d}
Pork scratch- ings	Free radicals	5/235	4	1.1	0.76
	Hexanal	5/233	3	35.3	0.83
	Pentanal	4/184	3	10.8	0.81
Peanuts	Free radicals	5/261	6	0.6	0.73
Oatmeal	Hexanal	4/184	4	8.3	0.65
Muesli I	Free radicals	6/320	7	1.7	0.68
	Hexanal	6/320	7	7.1	0.63
	Acetaldehyde	6/320	6	1.1	0.71

^a Number of time points and samples used

^b Applied number of PCs

^c Prediction error

^d Correlation coefficients

A closer look at the regression coefficients (data not shown) reveals information about the most important wavelengths for the different models. When predicting free radicals in pork scratchings the spectral regions describing aromatic amino acids in proteins, reactions of malondialdehyde with amino compounds, protein-bound lipid peroxidation products and the unidentified peak at $\text{ex}=530$ nm are the most important. The model describing hexanal content also uses the spectral region of aromatic amino acids in proteins and the unidentified emission spectra at $\text{ex}=410$ nm and $\text{ex}=530$ nm. For prediction of hexanal in oatmeal the regions describing the reactions of malondialdehyde with amino compounds, the decrease in carotenoids and riboflavin and excitations above 510 nm are important.

Vis/NIR

The obtained Vis/NIR spectra for pork scratchings, peanuts and two kinds of muesli are shown in Fig. 5. The figure also displays a fresh (grey spectra) and an oxidized (solid spectra) sample for each product. A comparison of the spectra shows that the spectra for high-fat samples of pork scratchings and peanuts and high-carbohydrate sam-

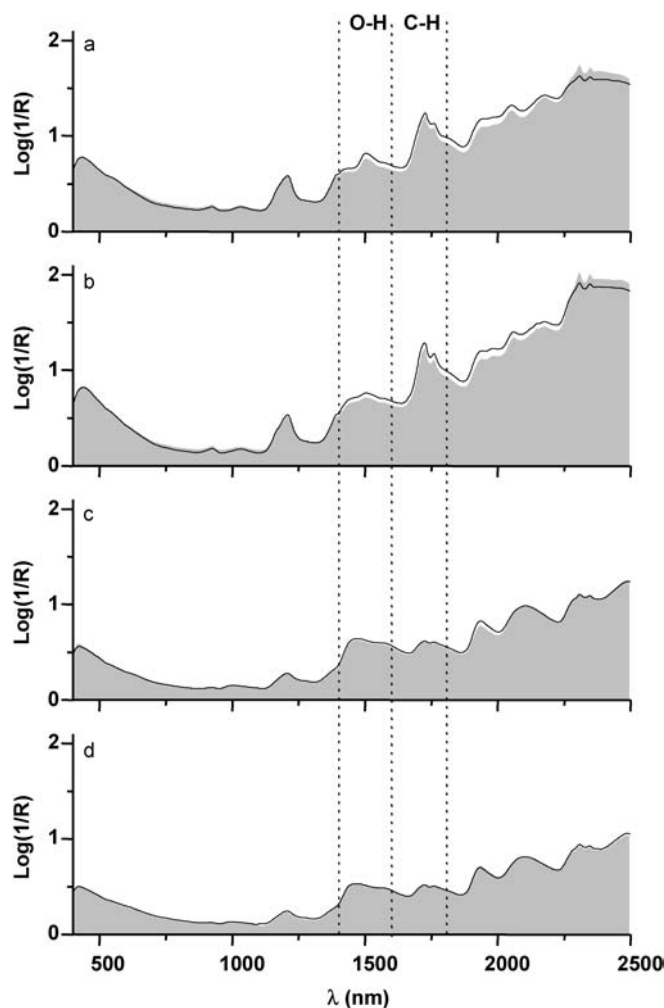


Fig. 5a–d Vis/NIR spectra for a fresh (grey) and an oxidized (line) sample of **a** pork scratchings, **b** peanuts, **c** oatmeal and **d** muesli I. Regions of overtones and combinations of the fundamental vibrational transitions of C–H and O–H are marked

ples of mueslis I and II are much alike. In addition, a higher absorbance level for pork scratchings and peanuts than for mueslis I and II is observed, especially in the visual region below 700 nm and the NIR combination

Table 5 PLSR correlations (r^2) between Vis/NIR data and chemical and sensory analysis. See Table 4 for explanations of abbreviations

		Spectral interval (nm)	Time/samples	PC	RMSECV	r^2
Pork	Free radicals	400–2,500	5/169	10	0.7	0.82
scratchings	Free radicals	718–8,22	5/169	7	0.8	0.82
Peanuts	Hexanal	400–2,500	7/170	11	0.7	0.64
	Hexanal	930–1,034	7/168	6	0.7	0.58
Muesli I	Hexanal ^a	400–2,500	3/58	4	1.0	0.70
	Hexanal ^a	1,668–1,770	3/60	4	0.8	0.80
Muesli II	Free radicals	400–2,500	7/171	8	0.4	0.63
	Hexanal	400–2,500	7/167	8	0.2	0.83
	Vanilla flavour	400–2,500	7/136	6	0.7	0.75
	Rancid flavour	400–2,500	7/133	4	0.9	0.62
	Overall impression	400–2,500	7/136	6	0.5	0.71

^a Transformed by $\ln(\text{hexanal}+1)$

tone region above 1,500 nm. Below 780 nm the difference between the products is due to simple colour differences, whereas differences above 1,500 nm are primarily due to the fat fraction [47]. The absorbance level for the oxidized samples for pork scratchings and peanuts is higher than the fresh samples in the combination tone region 1,400–2,250 nm.

The score plot from the PCA model of the Vis/NIR spectra on pork scratchings is shown in Fig. 3b. The score plot of PC1 versus PC2 displays separation according to O₂ concentration by PC2, whereas separation into storage time by PC1 is only a trend. The loadings for the second PC are dominated by information from the visible region. Examination of the loadings from PCA models of the Vis/NIR data (results not shown) reveals that the first and second overtone of C–H and the combination bands above 1,800 nm are primarily described by PC1, i.e. changes in the fat fraction. This accounts for pork scratchings, peanuts and muesli I, whereas muesli II is mainly described by changes in water and carbohydrate vibrations (O–H). For all products the second PC also describes changes related to the fat fraction, while the third PC explains the changes in colour (except for pork scratchings).

As was the case for the fluorescence spectra, it was investigated whether Vis/NIR can predict the oxidative changes in the products. Hence, PLSR models were constructed using the entire Vis/NIR spectrum or a selected spectral subregion (iPLS). iPLS compares the prediction performance of the full-spectrum model and the interval PLS models based on spectral subintervals of equal width (local models). The advantage of iPLS is the ability to focus on important spectral regions with fewer interferences, which leads to simpler parsimonious models [40]. The obtained PLSR models, cf. Table 5, reveal that Vis/NIR is especially good for describing changes in relative free radical concentration of pork scratchings; PLSR models with either the whole spectrum or a subregion resulted in the same correlation. However, the number of PCs was reduced from 10 to 7 using only the spectral range 718–822 nm. Prediction of the hexanal content in muesli I was improved using the spectral interval 1,668–1,770 nm (describing the first overtone of C–H) instead of the whole spectrum. Vis/NIR proved also to be able to predict the hexanal content in muesli II, but in this case

the whole spectrum led to a slightly better model. Neither the whole spectrum nor an interval of Vis/NIR proved able to describe the quality changes in peanuts, as only weak correlations (r^2) of 0.58 and 0.64 were obtained.

FT-IR

The FT-IR spectra of the four different products are displayed in Fig. 6, where a fresh (grey spectra) and an oxidized (solid line spectra) sample for each product are compared. As expected the patterns of FT-IR spectra for oatmeal and muesli I are very similar, but the high-fat samples of pork scratchings and peanuts also gave similar patterns. In the region 3,200–3,600 cm⁻¹ water (O–H) strongly absorbs and it is observed that the fresh oatmeal has the highest absorbance in this region. However, after storage the oxidized muesli has the highest O–H absorption. The latter reflects the higher water content for the oxidized samples (data not shown) (Table 1). The small peak observed at ~3,007 cm⁻¹ is characteristic for olefins and results from the *cis* (=C–H) stretching. A high proportion of linoleic or linoleic acyl groups shows higher absorbance at this band than oils with a high proportion of oleic acyl groups [48]. This is in good agreement with our results, as peanuts and oatmeal have higher absorbance and higher linoleic acid content than pork scratchings and muesli, respectively. However, this difference is not observed between the snack products and the cereals, probably due to the higher fat content in the snacks. In the region 2,800–3,000 cm⁻¹ oils and fats have very strong aliphatic C–H stretching absorption and a clear difference is also observed between the snack products and the cereals. The snack products have the highest fat content and thus the highest absorbance. Furthermore, oatmeal contains less fat than muesli (cf. Table 1) and has lower absorbance. The fundamental vibrations of O–H and C–H are observed as overtones and combination tones in Vis/NIR, cf. Fig. 5. The ester carbonyl group (C=O) of the triglycerides absorbs strongly at ~1,745 cm⁻¹ and reflects the total fat concentration in the samples. The absorbance at 1,745 cm⁻¹ decreases during storage for the cereals, in agreement with observations on potato chips [37]. The small shoulder at 1,713 cm⁻¹ is assigned to

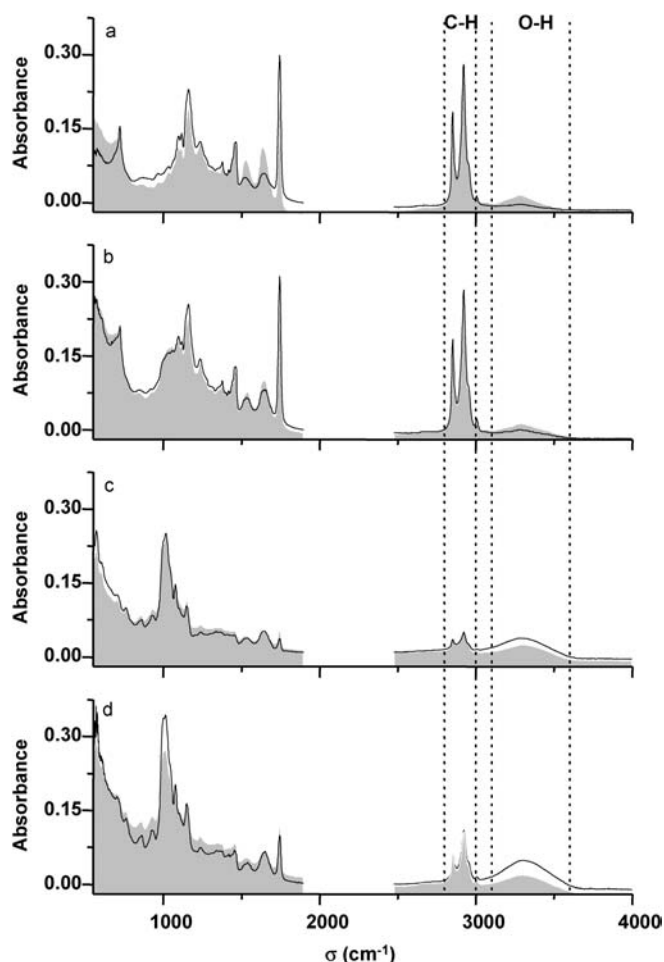


Fig. 6 IR spectra for a fresh (grey) and an oxidized (line) sample of **a** pork scratchings, **b** peanuts, **c** oatmeal and **d** muesli I. Regions of fundamental vibrational transitions of C–H and O–H are marked

FFA. As the water-bending vibration strongly absorbs at about $1,640\text{ cm}^{-1}$, the amide I band at $1,630\text{--}1,660\text{ cm}^{-1}$ is interfered by the presence of water. The oxidized pork scratchings have the highest amide I absorbance and the intensity increases with storage for both pork scratchings and peanuts, whereas the absorbance is almost constant for oatmeal and muesli. Stretching vibrations of the C–O bonds of the glycerol skeleton in triglyceride molecules occur between $1,000$ and $1,300\text{ cm}^{-1}$.

The PCA score plot (PC1 vs. PC3) based on the FT-IR spectra of pork scratchings is displayed in Fig. 3c. The samples are separated according to storage time and a clear separation of weeks 2, 5, 19 and 23 is observed. The

effect of storage time is dominant while separation of samples stored in light and darkness is absent.

Even though minor spectral differences exist between fresh and oxidized samples for peanuts, oatmeal and muesli, FT-IR is not able to predict the quality changes measured by ESR and GC-headspace. In contrast, very good PLSR models were obtained for pork scratchings, cf. Table 6, when predicting the oxidative changes measured by GC-headspace (hexanal and pentanal) but not ESR. As mentioned above, hexanal and pentanal are highly intercorrelated and therefore only results from predicting hexanal content are shown.

A comparison of the constructed PLSR models using the whole spectrum (except the region where the diamond absorbs) with the intervals $839\text{--}982$, $982\text{--}1,126$ or $1,701\text{--}1,850\text{ cm}^{-1}$ (optimized by iPLS) reveals higher correlation coefficients with lower root mean square error of cross validation (RMSECV) for hexanal. However, the model based on the region $982\text{--}1,126\text{ cm}^{-1}$ requires one PC more than the full model. The RMSECV's for the iPLS model (bars) and for the full-spectrum model (line) are plotted in Fig. 7a together with the MSC-transformed mean spectrum. Fig. 7b shows the predicted versus measured plot for the best interval (no. 3; $839\text{--}982\text{ cm}^{-1}$). This region can be assigned to out-of-plane bending vibrations of CH bonds of isolated *trans*-olefins. Oxidation of the unsaturated fatty acids results in various oxidation products and apparently some of these have *trans* configuration.

In the region $1,701\text{--}1,850\text{ cm}^{-1}$, the ester carbonyl (C=O stretching) of the FFA and triglycerides absorbs and apparently one of the dominating quality changes in the samples is in this region. This result was also observed for frying oil deterioration. The carbonyl peak, which is the most intense and stable peak in IR, was able to monitor the oxidative level by probing the thermal oxidation of triglycerides ($1,745\text{ cm}^{-1}$) into FFA ($1,713\text{ cm}^{-1}$) [9].

Comparison of the spectroscopic methods

A comparison of the performances of fluorescence, Vis/NIR and FT-IR to predict oxidative changes in food revealed a large dependence on the product and the reference method. Generally, the spectra for pork scratchings and peanuts obtained by fluorescence, Vis/NIR and FT-IR spectra exhibited very similar patterns. This is also the case for oatmeal and muesli I or muesli I and II.

In the unsupervised chemometric approach the score plots from PCA models based on fluorescence on pork scratchings revealed separation of the samples stored in light and darkness and according to O_2 concentration. Vis/

Table 6 PLSR correlations (r^2) between FT-IR spectra and hexanal for pork scratchings. See Table 4 for explanations of abbreviations

	Spectral interval (cm^{-1})	Time/samples	PC	RMSECV	r^2
Hexanal	$550\text{--}4,000^a$	6/343	7	31.7	0.84
	$839\text{--}982$	6/343	3	29.6	0.86
	$982\text{--}1,126$	6/343	8	30.5	0.85
	$1,701\text{--}1,850$	6/343	3	30.7	0.85

^a Without the region where the diamond absorbs ($1,900\text{--}2,500\text{ cm}^{-1}$)

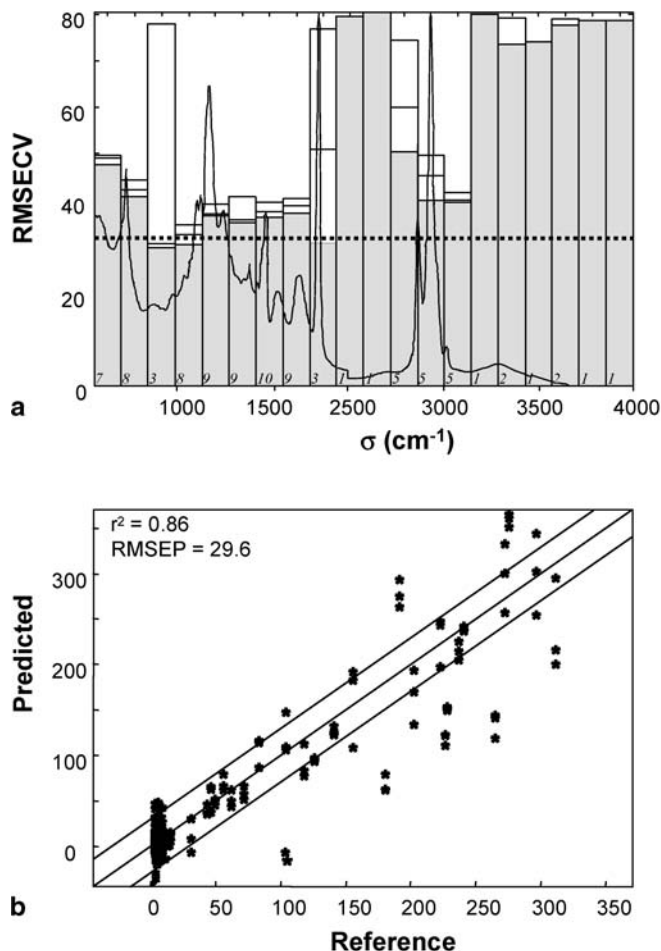


Fig. 7a, b Prediction of hexanal in pork scratchings by FT-IR. **a**) Interval partial least squares regression (iPLS) plot of a seven-component model based on 20 subintervals of the full FT-IR spectra (4,000–550 cm^{-1}). The prediction errors [root mean square error of cross validation (*RMSECV*)] for each subinterval are presented as bars: the *solid bars* correspond to *RMSECV* of models based on the number of PCs indicated at the bottom of the bars, whereas *RMSECV* for models based on the two preceding PC's are marked by *white bars*. **b**) Predicted versus measured hexanal contents for PLS model (3 PC) based on the FT-IR region 839–982 cm^{-1} . *RMSEP* Root mean square error of prediction

NIR displayed an effect of storage in light and darkness, whereas FT-IR showed a very dominant effect of storage time.

In the supervised approach all the spectroscopic methods proved able to predict the variations in pork scratchings with relatively good precision, but quality changes in peanuts, oatmeal and muesli I and II can be monitored as well. However, it is noteworthy that no single spectroscopic method proved able to predict both content of free radicals and hexanal in any of the products. PLSR models made on the basis of fluorescence and Vis/NIR spectra revealed the highest correlation coefficients (r^2) for pork scratchings for all the reference methods. Fluorescence spectroscopy proved able to predict free radicals in peanuts and muesli I, whereas Vis/NIR proved most useful for prediction of hexanal content. The opposite held for

pork scratchings, as Vis/NIR described the variation in free radicals very well, while fluorescence predicted the hexanal (and pentanal) content best. Both hexanal and pentanal, but not free radicals, were predicted well by FT-IR in pork scratchings, whereas FT-IR proved unable to predict the oxidative status of peanuts, oatmeal and muesli I. With respect to sensory attributes, only Vis/NIR proved able to predict oxidative changes in muesli II, whereas no serious regression models could be built for pork scratchings, peanuts or muesli I.

Scrutiny of the FT-IR spectra revealed a difference in the products according to, for example the aliphatic C–H stretching (2,800–3,000 cm^{-1}) band; this was most intense in pork scratchings and peanuts, which also have the highest fat content compared to oatmeal and muesli I. At wavenumber $\sim 1,745 \text{ cm}^{-1}$ the absorbance of ester carbonyl (C=O) stretching showed a decrease during storage for oatmeal and muesli I, indicating oxidative degradation of the triglycerides. The iPLS regression model for pork scratchings selected the carbonyl stretching region (1,701–1,850 cm^{-1}) or, even better, the *trans*-olefin region (839–982 cm^{-1}) to describe the quality changes during storage.

In conclusion, multivariate spectroscopic methods proved able to complement, but not replace traditional chemical analyses. The high throughput and the (in principle) non-invasive character of these methods makes it possible to screen a large number of samples and identify deviating samples (concentration faults in bulk components such as water, carbohydrate, protein and fat, including oxidation faults and other abnormalities) to be subjected to detailed chemical analysis. This study demonstrates that carefully selected and optimized spec-troscopic methods have the potential to rapidly and non-invasively monitor the oxidation level of several food products.

Acknowledgements The Directorate for Food, Fisheries and Agri Business supported this work. The authors are grateful to participants from Coop Danmark, AGA A/S, Cerealia Foods A/S, KiMs A/S, Nutana A/S, Ehrno Plast A/S and PBI-Dansensor A/S (Denmark) who provided technical assistance and to AGELESS for providing the oxygen absorbers. This study was also partly sponsored by an EU innovation programme with the acronym OPUS (IN30905I). The aim of this project was to adapt and apply advanced fluorescence measurement techniques for on-line analysis to traditional food industries. Gilda Kischinovsky is acknowledged for help with the manuscript.

References

- Andersen ML, Skibsted LH (2002) *Eur J Lipid Sci Technol* 104:65–68
- Dunmire DL, Williams RC (1990) *Cereal Foods World* 35:913, 915, 916, 918
- Zandomenighi M, Carbonaro L, Calucci L, Pinzino C, Galleschi L, Ghiringhelli S (2003) *J Agric Food Chem* 51:2888–2895
- Becker EM, Christensen J, Frederiksen CS, Haugaard VK (2003) *J Dairy Sci* 86:2508–2515
- Wold JP, Jørgensen K, Lundby F (2002) *J Dairy Sci* 85:1693–1704

6. Christensen J, Povlsen VT, Sørensen J (2003) *J Dairy Sci* 86:1101–1107
7. Møller JK, Parolari G, Gabba L, Christensen J, Skibsted LH (2003) *J Agric Food Chem* 51:1224–1230
8. Wold JP, Mielnik M, Pettersen MK, Aaby K, Baardseth P (2002) *J Food Sci* 67:2397–2404
9. Engelsen SB (1997) *JAOCS* 74:1495–1508
10. Jensen SA, Martens H (1983) Multivariate calibration of fluorescence data for quantitative analysis of cereal composition. In: Martens H, Russwurm H (eds) *Food research and data analysis*. Applied Science, Essex, UK, pp253–269
11. Jensen SA, Munck L, Martens H (1982) *Cereal Chem* 59:477–484
12. Munck L, Nørgaard L, Engelsen SB, Bro R, Andersson CA (1998) *Chemom Intell Lab Syst* 44:31–60
13. Bewig KM, Clarke AD, Roberts C, Unklesbay N (1994) *JAOCS* 71:195–200
14. Isengard H-D, Schmid M (2001) *Food Aust* 53:96–100
15. Sato T, Kawano S, Iwamoto M (1991) *JAOCS* 68:827–833
16. Yildiz G, Wehling RL, Cuppett SL (2001) *JAOCS* 78:495–502
17. Li H, van de Voort FR, Sedman J, Ismail AA (1999) *JAOCS* 76:491–497
18. Indahl UG, Sahni NS, Kirkhus B, Naes T (1999) *Chemom Intell Lab Syst* 49:19–31
19. Jensen PN, Sørensen G, Engelsen SB, Bertelsen G (2001) *J Agric Food Chem* 49:5790–5796
20. Bertrand D, Robert P, Loisel W (1985) *J Sci Food Agric* 36:1120–1124
21. Garnsworthy PC, Wiseman J, Fegeros K (2000) *J Agric Sci* 135:409–417
22. Pedersen DK, Martens H, Nielsen JP, Engelsen SB (2002) *Appl Spectrosc* 56:1206–1214
23. Ma K, van de Voort FR, Sedman J, Ismail AA (1997) *JAOCS* 74:897–906
24. Moh MH, Tang TS (1999) *J Food Lipids* 6:261–270
25. van de Voort FR, Ismail AA, Sedman J, Dubois J, Nicodemo T (1994) *JAOCS* 71:921–926
26. Che Man YB, Setiowaty G (1999) *Food Chem* 67:193–198
27. van de Voort FR, Sedman J, Emo G, Ismail AA (1992) *JAOCS* 69:1118–1123
28. Ismail AA, van de Voort FR, Sedman J (1993) *JAOCS* 70:335–341
29. Che Man YB, Setiowaty G (1999) *JAOCS* 76:243–247
30. Dubois J, van de Voort FR, Sedman J, Ismail AA, Ramaswamy HR (1996) *JAOCS* 73:787–794
31. Frankel EN, Neff WE, Selke E, Weisleder D (1982) *Lipids* 17:11–18
32. Neff WE, Frankel EN, Weisleder D (1982) *Lipids* 17:780–790
33. Safar M, Bertrand D, Robert P, Devaux MF, Genot C (1994) *JAOCS* 71:371–377
34. van de Voort FR, Ismail AA, Sedman J, Emo G (1994) *JAOCS* 71:243–253
35. Guillén MD, Cabo N (2000) *J Sci Food Agric* 80:2028–2036
36. Guillén MD, Cabo N (1999) *J Agric Food Chem* 47:709–719
37. Sivakesava S, Irudayaraj J (2000) *J Sci Food Agric* 80:1805–1810
38. Jensen PN, Bertelsen G, Danielsen B, Skibsted LH, Andersen ML (in press) *Food Chem*
39. Geladi P, MacDougall D, Martens H (1985) *Applied Spectrosc* 39:491–500
40. Nørgaard L, Saudland A, Wagner J, Nielsen JP, Munck L, Engelsen SB (2000) *Applied Spectrosc* 54:413–419
41. Kikugawa K, Machida Y, Kida M, Kurechi T (1981) *Chem Pharm Bull* 29:3003–3011
42. Wold JP, Mielnik M (2000) *J Food Sci* 65:87–95
43. Duggan DE, Bowman RL, Brodie BB, Udenfriend S (1957) *Arch Biochem Biophys* 68:1–14
44. Hasegawa K, Endo Y, Fujimoto K (1992) *J Food Sci* 57:1123–1126
45. Zandomenighi M (1999) *J Agric Food Chem* 47:878–882
46. Zandomenighi M, Festa C, Carbonaro L, Galleschi L, Lenzi A, Calucci L (2000) *J Agric Food Chem* 48:2216–2221
47. Osborn GS, Fearn T, Hindle PH (1993) *Practical NIR spectroscopy with applications in food and beverage analysis*, 2nd edn. Longman, Essex, UK
48. Guillén MD, Cabo N (1997) *JAOCS* 74:1281–1286

Paper IV

Front-Face Fluorescence Spectroscopy and Chemometrics for Analysis of Yogurt – Rapid Analysis of Riboflavin

Eleonora Miquel Becker, Jakob Christensen,
Charlotte S. Frederiksen and Vibeke K. Haugaard
Journal of Dairy Science 86 (8), 2508-2515, 2003

Front-Face Fluorescence Spectroscopy and Chemometrics in Analysis of Yogurt: Rapid Analysis of Riboflavin

E. Miquel Becker,* J. Christensen,† C. S. Frederiksen,* and V. K. Haugaard*

*Food Chemistry, Department of Dairy and Food Science,
The Royal Veterinary and Agricultural University,

Rolighedsvej 30, DK-1958 Frederiksberg C, Denmark

†Food Technology, Department of Dairy and Food Science,

The Royal Veterinary and Agricultural University,

Rolighedsvej 30, DK-1958 Frederiksberg C, Denmark

ABSTRACT

The present study demonstrates the use of front-face fluorescence spectroscopy and chemometrics for monitoring light-induced changes in plain yogurt during storage. Fluorescence analysis is suggested as a new rapid method for measuring riboflavin content in yogurt. Fluorescence landscapes with excitation wavelengths from 270 to 550 nm and emission wavelengths in the range 310 to 590 nm were obtained from front-face fluorescence measurements directly on yogurt samples during two storage experiments over a period of 5 wk at 4°C. Yogurts were stored in two different packaging materials (polylactate and polystyrene) and under fluorescent light (3500 lux) or in darkness. Principal Component Analysis of unfolded fluorescence emission spectra revealed systematic changes in fluorescence signal throughout the storage period, strongly related to the storage conditions, i.e. storage time and differences in packaging materials. Correlation between fluorescence spectra and riboflavin content determined by the standard AOAC fluorometric method was evaluated using a Partial Least Square Regression model. The regression model showed a good ability to predict riboflavin in plain yogurt with a high correlation ($R = 0.99$) and a prediction error of $0.092 \mu\text{g}$ riboflavin/g. Thus, it is concluded that nondestructive fluorescence spectroscopy can be used to monitor riboflavin content in yogurt, and that the suggested rapid method has the potential to substitute the standard method for analysis of riboflavin in yogurt.

(Key words: fluorescence spectroscopy, chemometrics, riboflavin, yogurt, light-induced oxidation)

Abbreviation key: PCA = principal component analysis, PC = principal component, PLSR = partial least squares regression, RMSECV = root mean square error of cross validation, PLA = polylactate, PS = polystyrene.

INTRODUCTION

Light-induced oxidation requires the presence of a light source, a photosensitizer and oxygen in order to occur. Riboflavin plays a key role in problems related to the photosensitivity and photodegradation of milk and dairy products like yogurt. The vitamin can absorb visual light and react as a photosensitizer, which involves oxygen activation and radical formation leading to protein and lipid degradation (Skibsted, 2000). Both light and oxygen have been found to induce riboflavin degradation (Singleton et al., 1963; Sattar et al., 1977; Bosset et al., 1994; Skibsted, 2000). These oxidative deterioration processes may lead to discoloration, formation of off-flavors and loss of nutrients in dairy products (Bosset and Flückinger, 1986; 1989; Bekbölet, 1990; Bosset et al., 1994; Skibsted, 2000; Kristensen et al., 2000). Therefore, design of packaging materials with optimal protection of the product against the combined action of light and oxygen is necessary to minimize light-induced changes.

Fluorescence spectroscopy is a rapid, nondestructive analytical technique with high sensitivity and specificity. The potential of using fluorescence in food research has increased during the last few years with the propagated application of chemometrics and with technical and optical developments of spectrofluorometers. Fluorescence spectroscopy applied on dairy products has previously been investigated in a few studies to monitor structural changes in milk proteins and their physicochemical environment during milk heating (Dufour and Riaublanc, 1997), milk coagulation (Dufour et al., 1998; Herbert et al., 1999), cheese manufacture (Dufour et al., 2001, Mazerolles et al., 2001) and in the evaluation of oxidative changes in processed cheese during storage (Christensen et al., 2002). Changes in vitamin A in dairy products have also been monitored in several fluorescence studies (Dufour et al., 2000; Herbert et al., 2000). Wold and coworkers (2002) showed that front-face fluorescence spectroscopy could be used to measure light-induced oxidation in various dairy products, and pro-

Received December 16, 2002.

Accepted February 18, 2003.

Corresponding author: J. Christensen; e-mail: jach@kvl.dk.

posed the method for rapid quantification of riboflavin, however, this was not verified by reference analyses. The aim of the present study is to illuminate the potential of fluorescence spectroscopy in nondestructive assessment of light-induced changes in plain yogurt.

Due to the importance on light-induced oxidation and the fact that riboflavin plays a key role in the photo-oxidation of dairy products, riboflavin can be considered an important marker of early oxidation in milk and dairy products. In addition, riboflavin is also an important nutrient. Therefore, a rapid analysis of riboflavin is expected to be of high interest. Riboflavin has so far been measured according to a standard fluorometric method (AOAC, 1990), which requires extraction and cleanup of riboflavin prior to the fluorometrically measurements, making the method time-consuming and the use of organic solvents necessary. The content of riboflavin is calculated by the fluorescence data recorded at one combination of excitation and emission wavelengths. In this study the potential of front-face fluorescence spectroscopy applied directly on the yogurt combined with multivariate data analysis (chemometrics) is investigated as a rapid alternative to the standard method. The proposed method offers several inherent advantages for riboflavin determination in yogurt: There is no sample preparation, since the fluorescence is recorded directly on the yogurt sample without prior riboflavin extraction. Furthermore, the whole excitation-emission matrix (fluorescence landscape) is used in the chemometric analysis and can therefore provide extra information about changes in the sample. Thus, a simultaneous analysis of more fluorescent compounds, for instance in the form of aromatic amino acids and vitamin A, can be performed.

MATERIALS AND METHODS

Yogurt and Packaging Materials

Plain yogurt (3.5% fat) was obtained from Arla Foods aamba (Viby, Denmark). Two rigid packaging materials were used: Polylactate (PLA) cups from Autobar, France (volume 215 ml, thickness 197 μm , oxygen permeability 0.21 $\text{ml}/\text{cup} \times \text{d}^{-1}$ at 0.21 atm O_2 , 23°C and 50% RH) (Petersen et al., 2001) and polystyrene (PS) cups from Danapak Plast A/S, Denmark (volume 190 ml, thickness 244 μm , oxygen permeability 1.49 $\text{ml}/\text{cup} \times \text{d}^{-1}$ at 0.21 atm O_2 , 23°C and 50% RH). The cups were sealed by bonding a transparent and colorless laminate from Amcor Flexible, Denmark (oxygen permeability 0.5 $\text{ml}/\text{m}^2 \times \text{d}^{-1}$ at 1 atm O_2 , 23°C and 5/95% RH) with a two component epoxy adhesive. The light transmission of the packages and the lid, as shown in Figure 1, was determined using a Cintra 40 spectrophotometer (CBC Scientific Equipment Pty Ltd, Victoria, Australia) equipped with an integrating sphere detector.

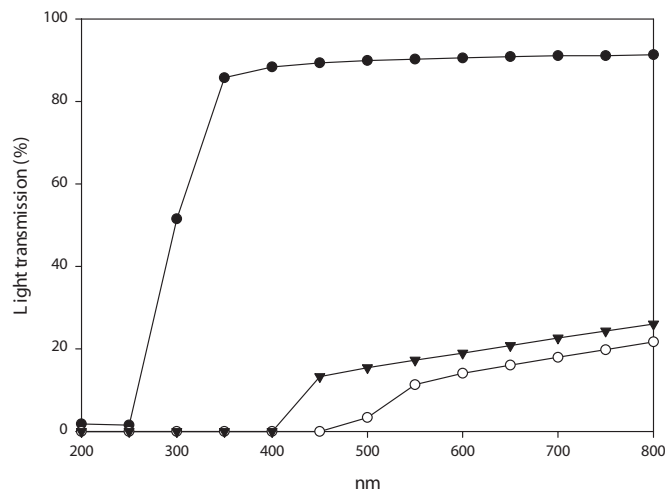


Figure 1. Light transmission spectra (%) of PLA cups (○), PS cups (▼) and lid (●).

Experimental Design

Two batches of yogurt were examined in two identical storage experiments. The amount of yogurt filled into the packages was 180 and 155 g for PLA and PS, respectively, resulting in a headspace volume of 35 ml for each package. The packed samples were stored at 4°C for five weeks under a radiant flux of approx. 3500 lux of fluorescent light (Philips fluotone, TLD 18W/830) or in darkness. The samples stored in light were illuminated both from above through the lid and from the sides. Throughout the storage period the samples were randomly interchanged to minimize unequal temperature fluctuations and light conditions. Analyses were performed after 0, 7, 14, 21, 28, and 35 d of storage, giving a total of 21 different samples (5 d \times 2 light conditions \times 2 packaging materials + one starting sample) for each batch. Thus, 42 independent samples were studied in all. Three cups from identical conditions for each of the two batches were selected and considered as triplicates. All analyses were carried out in duplicate. Prior to the measurements, the yogurt was mixed in the cup.

Fluorescence Spectroscopy

Fluorescence landscapes were measured directly on the yogurt by filling 15 g of yogurt in a 30 ml plastic cup and recording fluorescence by dipping the measuring probe 1 mm into the yogurt sample. All samples were measured on a BioView spectrofluorometer (Delta Light and Optics, Denmark) using a pulsed xenon lamp for excitation and equipped with an optical light conductor and a measuring probe, giving an open-end 180° measuring geometry. Fluorescence landscapes were obtained

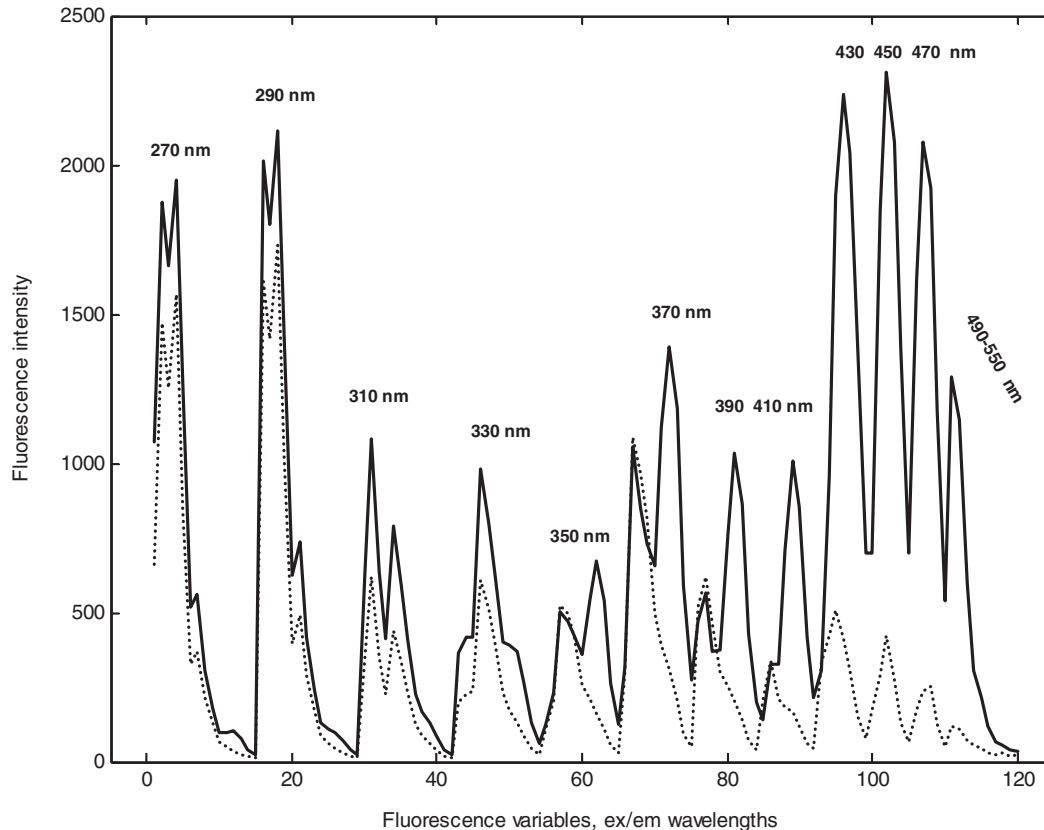


Figure 2. Unfolded fluorescence emission spectra for fresh yogurt sample (—) and yogurt sample stored in light for 35 d and packed in polystyrene (·····). Excitation wavelengths are noted in top of each emission spectrum.

with excitations from 270 to 550 nm and emission wavelengths from 310 to 590 nm, with intervals and bandwidths of 20 nm, giving a total of 15 excitation and 15 emission wavelengths. Only emission wavelengths 40 nm above the excitation wavelength were recorded, resulting in 120 data points obtained for each measurement. For the data analysis, the 2D fluorescence landscapes were unfolded into a row of emission spectra one after another, as seen in Figure 2.

Chemical Determination of Riboflavin

The riboflavin content in the yogurt was measured by the fluorometric method established by AOAC (1990) using an Aminco Bowman series 2 luminescence spectrophotometer (SLM-Aminco, Urbana, IL). The selected wavelengths were 446 nm/525 nm excitation/emission.

Data Analysis

Statistical analyses of the effects of the packaging materials, light conditions and storage time on the riboflavin content were evaluated by two-way analyses of vari-

ance by the general linear model procedure (SAS, version 6.12). Significant packaging and light treatment effects were further classified by Least Significant Difference ($P \leq 0.05$).

Principal Component Analysis (PCA), and Partial Least Squares Regression (PLSR) were the two chemometric tools used in the multivariate evaluation of the fluorescence data; both techniques based on a linear decomposition of data. PCA (Wold et al., 1987) provides an approximation of a data matrix, X into a few vectors, in terms of the product of two sets of vectors, T (scores) and P (loadings). These vectors capture the essential patterns of X, and are called latent variables or principal components (PC). PLSR (Martens and Naes, 1989) models the relationship between two data tables, X, and Y. PLSR is a predictive two-block regression method based on estimated latent variables and is applied to the simultaneous analysis of the two data sets, X (spectra) and Y (reference analysis).

PCA of the fluorescence data was applied in order to obtain the best possible overview of the spectral structure and distribution of samples. Score plots visualize the relationship between yogurt samples for each PC,

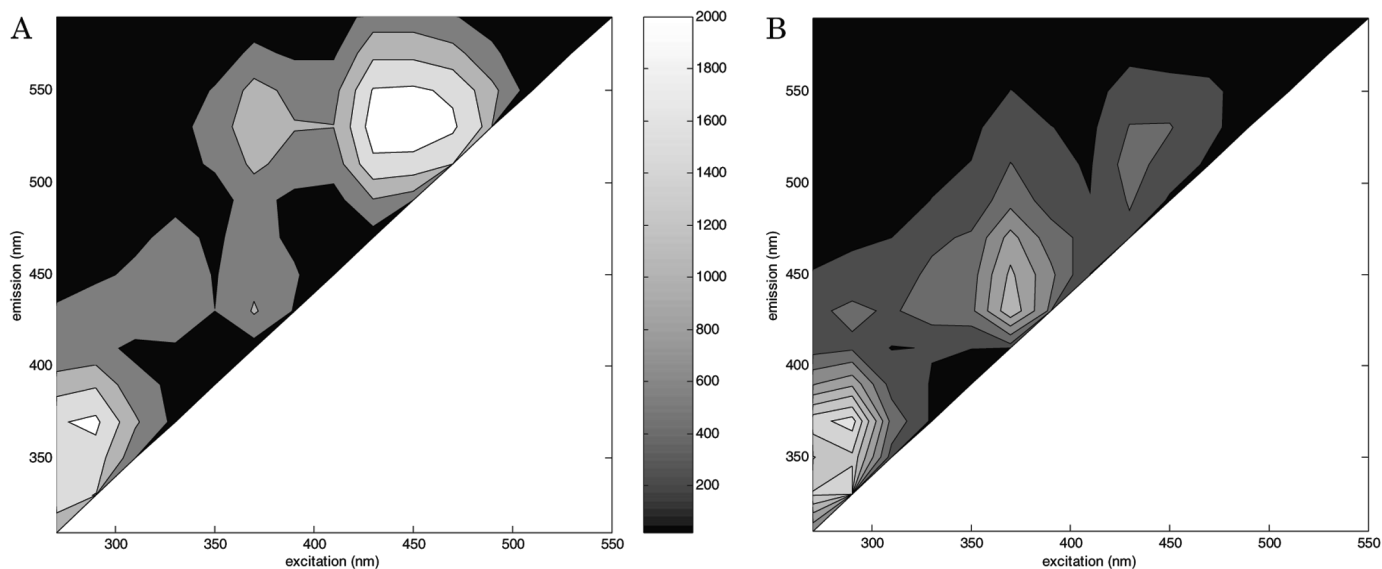


Figure 3. Contour plot of a fluorescence landscape for yogurt samples. a) fresh yogurt sample and b) yogurt sample stored in light for 35 d and packed in polystyrene.

while loadings plots were used for interpretation of the corresponding spectral variation. PLSR was used for investigating the dependency and making calibrations between fluorescence spectra and riboflavin content in the yogurt samples. The calibrations were performed on the average of the replicate samples. Full cross-validation was applied for all regression models. Cross-validation (Wold, 1978) is a strategy for validating calibration models based on systematically leaving out some samples in the modelling and testing them against the rest. In this case each of the samples was left out one by one, meaning that 42 submodels were calculated based on 41 samples plus one global model based on all 42 samples. For each of the models, the sample left out was predicted, and the prediction was compared with the reference values and used as a term for the validated performance of the calibration model. The regression model was evaluated using the multivariate correlation coefficient (R), and the validation parameter, Root Mean Square Error of Cross-Validation (**RMSECV**) as a term to indicate the error of the model. The RMSECV is defined as in equation (1):

$$\text{RMSECV} = \sqrt{\frac{\sum (y_{\text{pred}} - y_{\text{ref}})^2}{N}} \quad [1]$$

where y_{pred} is the predicted values from the cross-validated samples, y_{ref} is the reference values and N is the number of samples.

Data analyses were performed in Unscrambler 7.6 SR-1 (CAMO ASA) and MatLab 6.1 (MathWorks, Inc.) with the PLS-Toolbox 2.0 (Eigenvector Research, Inc.).

RESULTS AND DISCUSSION

The fluorescence landscapes of two yogurt samples are shown in Figure 3 in the form of contour plots. The two samples represent the extremes in the experimental plan, i.e. a fresh yogurt sample (a) and a yogurt sample stored under the most severe conditions (b). The highest fluorescence peaks for the fresh sample are seen with excitation below 300 nm and emission around 370 nm as well as for excitations between 370 to 490 nm and emission wavelengths around 500 to 550 nm. The excitation and emission characteristics indicate that the fluorescence peaks arise from tryptophan (Trp) and riboflavin. Trp was reported to have excitation/emission wavelength maximum at 285/365 nm in pure solutions, and riboflavin to have emission maximum at 520 nm for excitations at 270, 370 and 445 nm (Duggan et al., 1957). The suggested Trp fluorescence still seems present in the yogurt sample stored in light for 35 d (Figure 3b), whereas the riboflavin signal seems considerably decreased. Thus, this experiment supports the hypothesis that photochemical degradation of riboflavin causes major changes in fluorescence. Furthermore, in Figure 3 the peak with excitation/emission maxima around 370/430 nm seems to increase during storage, and the fluorescence profile could correspond to the photo-chemical degradation product from riboflavin, lumichrome, with

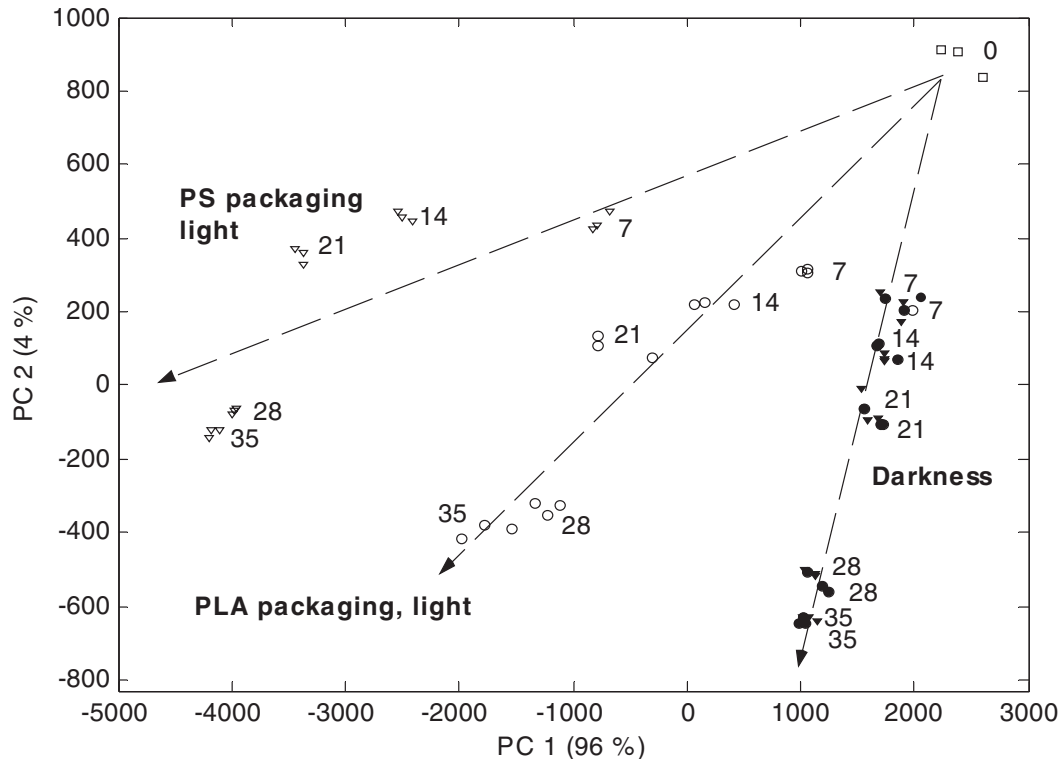


Figure 4. Score plot for PC1 vs. PC2 of a principal component analysis on unfolded fluorescence emission spectra of yogurt samples packaged in PLA (○) or PS (▽) at 4°C under continuous light exposure at 3500 lux (open symbol) or in darkness (dark symbol). Day 0 (□). Samples are numbered according to days of storage, and arrows indicate increasing storage time. Values in brackets note the degree of variation explained by each PC.

excitation/emission maxima reported somewhere around 360/450 nm in a model system (Fox and Thayer, 1998).

In Figure 2, the two same fluorescence landscapes as in Figure 3 are plotted as unfolded emission spectra in one joint plot, underlining the decrease in signal during

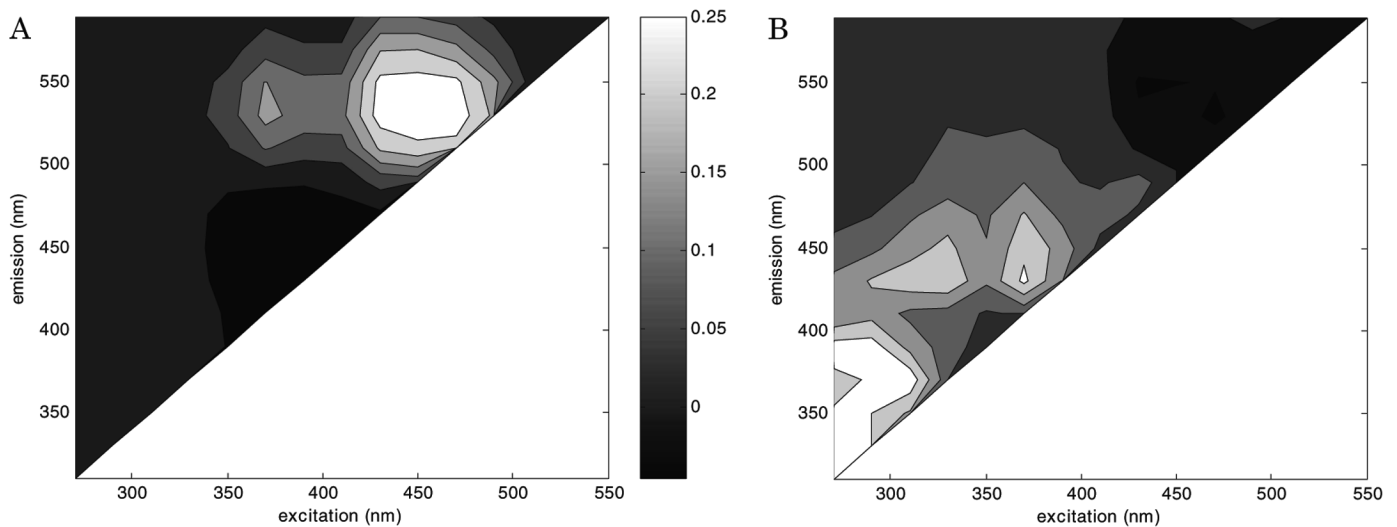


Figure 5. Contour plot of the first (a) and second (b) loading from PCA model on unfolded fluorescence emission spectra of yogurt samples.

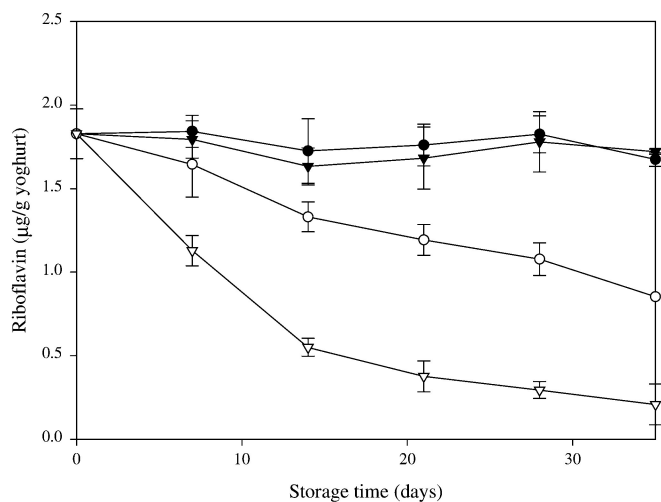


Figure 6. Riboflavin content in yogurt samples packaged in PLA (○) or PS (▽) at 4°C under continuous light exposure at 3500 lux (open symbol) or in darkness (dark symbol). Bars denote the standard deviations.

storage. It also displays the way the fluorescence data is handled in the chemometric analyses, which were applied in order to further investigate the above-mentioned trend using whole fluorescence landscapes. Figure 4 shows the score plot of PC1 versus PC2 of a PCA model performed on the first storage experiment; a similar result was obtained for the second storage experiment (result not shown). The distribution of samples in the score plot clearly displays the features in the experimental design, with PC1 mainly explaining variations caused by the degree of light exposure, while PC2 seems to separate samples according to storage time, as illustrated by the arrows for each of the storage conditions (darkness, PLA, PS) and the numbers that indicate the days of storage for the given sample. Similar trends were found in the work of Wold et al. (2002), for light-exposed goat cheese and sour cream in comparison to dark storage. Differences between packaging materials are also obvious in the score plot with yogurt samples exposed to light and packed in PLA situated closer to the samples stored in darkness, in agreement with the differences between light transmission (Figure 1) and oxygen permeability of the packaging materials. Figure 5 shows the corresponding loading plot for the PCA model displaying the spectral structure of the first two PC's, in the form of refolded fluorescence spectra displayed in contour plots. The importance of the wavelengths with excitation from 370 to 470 nm and emission around 530 nm is evident in PC1 (representing 96% of the variation), which corresponds very well with the fluorescent properties of riboflavin, indicating that the major variation in fluorescence is due to degradation of

this vitamin. Furthermore a systematic negative peak with excitation/emission maxima around 370/450 nm is seen, which could be caused by formation of lumichrome throughout storage, as previously suggested. The second loading shows high values for excitation 290 nm and emission around 350 nm, suggesting that this component is dominated by the variation in Trp fluorescence. However, fluorescence peaks with emission around 430 nm is also seen in PC2. Thus, the overall trend from the PCA is that a significant decrease in riboflavin fluorescence is observed due to light exposure throughout the storage period, and a decrease in Trp fluorescence is observed with increasing storage time, practically independent of light exposure. The spectral features found in PC1 and PC2 for excitation around 370 nm, resembles those found by Wold et al. (2002) on various dairy products, suggesting that the proposed method can be applied to other dairy products.

The observed sample grouping in the score plot (Figure 4) of the fluorescence spectra seems to be in agreement with the chemical analysis of riboflavin (Figure 6). Continuous exposure to light resulted in a pronounced decrease in riboflavin content compared to the dark-stored yogurts. Yogurts stored in darkness showed no significant changes in riboflavin content during storage and there was no effect of the packaging materials. Yogurt exposed to light was better protected against riboflavin degradation in PLA packages than in PS packages. On d 21, 60 to 65% of the riboflavin originally present in the yogurt was retained in light-stored PLA packages, whereas only 20% was retained in yogurt packed in PS. After 21 d of storage there was no further decrease in riboflavin content. Similar results were obtained for the second storage experiment (result not shown). Riboflavin degradation in yogurt exposed to light was in agreement with other findings in the literature (Bosset and Flückinger, 1986, 1989).

To verify the dependency between riboflavin and fluorescence, a PLSR model was constructed with data from both storage experiments with fluorescence spectra as x-variables and chemical analysis of riboflavin as the y-variable. The result of the PLSR (Figure 7) underlines the strong correlation between fluorescence and riboflavin content. A multivariate correlation coefficient of $R = 0.99$ and a prediction error (RMSECV) of $0.092 \mu\text{g}$ riboflavin/g yogurt for a 2 component model was obtained, corresponding to 7% of the mean riboflavin content in the yogurt samples. The multivariate regression was compared with a univariate one in order to investigate the advantage of the multivariate approach in the analysis of riboflavin. A linear regression model between the fluorescence data of excitation 450 nm/emission 530 nm and riboflavin content was constructed with identical validation conditions as for the PLSR. The univariate

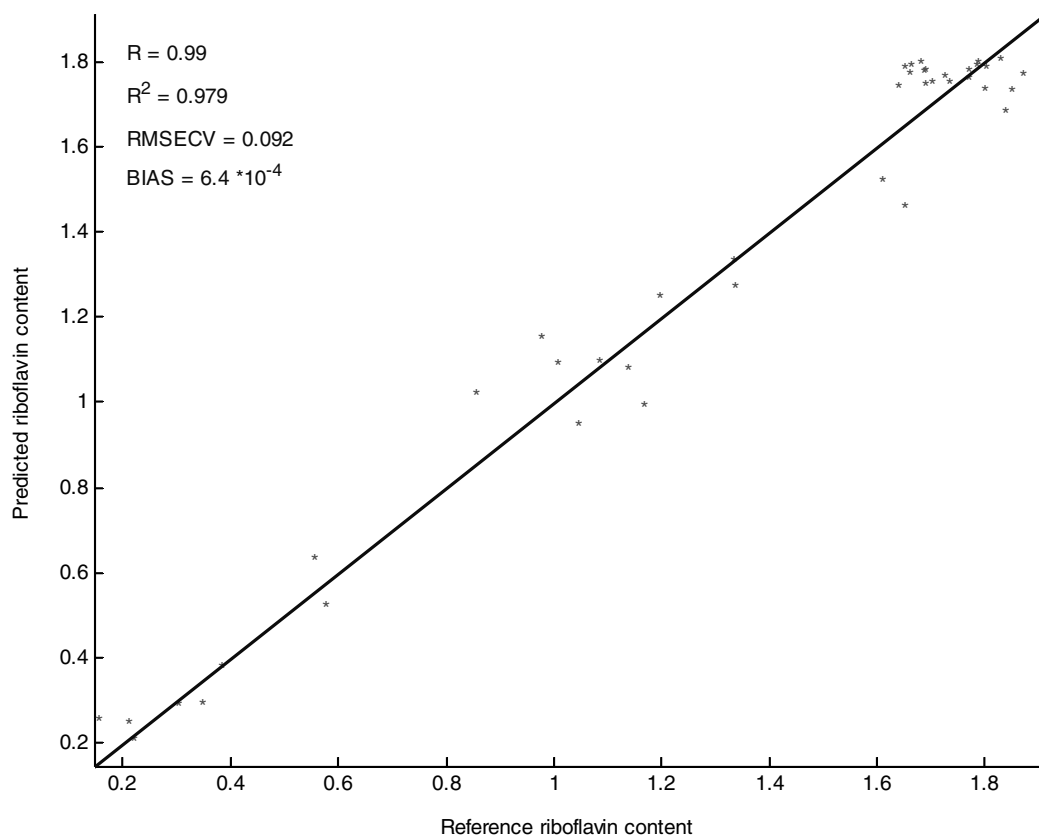


Figure 7. Predicted vs. reference riboflavin content of 42 yogurt samples, based on full cross-validation of a 2-component PLSR model on unfolded fluorescence emission spectra.

regression yielded a correlation of 0.97 and a RMSECV of 0.13 μg riboflavin/g yogurt, and also proved to perform rather well for analysis of riboflavin. The multivariate regression model performed significantly better ($P = 0.015$), when evaluated with an F-test of the RMSECV values, as suggested by Haaland and Thomas (1988). Furthermore, it is expected that a model based on the multivariate signal will be more robust against larger possible differences in the background fluorescence, and that it will improve detection of potential outliers considerably (Martens and Naes, 1989).

CONCLUSIONS

The present study demonstrates the potential of fluorescence spectroscopy and chemometrics applied for analysis of yogurt. Rapid fluorescence measurements applied directly on plain yogurt were used for monitoring degradation processes in yogurt during storage. The most important cause of changes in the obtained fluorescence landscapes was derived from riboflavin and ascribed to light-induced oxidation. It is demonstrated that the rapid fluorescence method has potential as a new

rapid riboflavin analysis for yogurts. We believe that the method also has the potential for determination of riboflavin in other dairy products, but with product-dependent calibrations. However, the validity of the suggested method still remains to be tested, on a larger set of samples covering a more heterogeneous collection of yogurts.

ACKNOWLEDGMENTS

This study was partly sponsored by an EU innovation programme with the acronym OPUS (IN30905I). The aim of this project was to adapt and apply advanced fluorescence measurement techniques for online analysis to traditional food industries.

REFERENCES

- Association of Official Analytical Chemists. 1990. Official Methods of Analysis. Vol. II. 15th ed. AOAC, Arlington, VA.
- Bosset, J. O., and E. Flückinger. 1986. Einfluß der licht- und gasdurchlässigkeit verschiedener packungsarten auf die qualitätserhaltung von naturyogurt. *Deutsch. Milchwirtsch.* 29:908–914.
- Bosset, J. O., and E. Flückinger. 1989. Die verpackung als mittel zur qualitätserhaltung von lebensmitteln, dargestellt am beispiel der

- lichtschutzbedürftigkeit verschiedener joghurtarten. *Lebensm. Wiss. Technol.* 22(5):292–300.
- Bosset, J. O., R. Sieber, and P. U. Gallman. 1994. Influence of light transmittance of packaging materials on the shelf life of milk and milk products—a review. Pages: 222–268 in *Food Packaging and Preservation*. Mathlouthi M. ed. Blackie Academic and Professional, Glasgow, Scotland.
- Bekbölet, M. 1990. Light effects on food. *J. Food Protect.* 53:430–440.
- Christensen, J., V. T. Povlsen, and J. Sørensen. 2002. Application of fluorescence spectroscopy and chemometrics in the evaluation of the stability of processed cheese. *J. Dairy Sci.* Accepted.
- Dufour, E., and A. Riaublanc. 1997. Potentiality of spectroscopic methods for characterisation of dairy products. I. Front-face fluorescence study of raw, heated and homogenised milks. *Lait* 77:657–670.
- Dufour, E., C. Lopez, A. Riaublanc, and N. Mouhous Riou. 1998. La spectroscopie de fluorescence frontale: une approche non invasive de la structure et des interactions entre constituants des aliments. *Agora* 10:209–215.
- Dufour, E., M. F. Devaux, and S. Herbert. 2001. Delineation of the structure of soft cheeses at the molecular level by fluorescence spectroscopy—relationship with texture. *Int. Dairy J.* 11:465–473.
- Dufour, E., G. Mazerolles, M. F. Devaux, G. Duboz, M. H. Duployer, and N. M. Riou. 2000. Phase Transition of triglycerides during semi-hard cheese ripening. *Int. Dairy J.* 10:81–93.
- Duggan, D. E., R. L. Bowman, B. B. Brodie, and S. Udenfriend. 1957. A spectrophotofluorometric study of compounds of biological interest. *Arch. Biochem. Biophys.* 68:1–14.
- Fox, J. B., and D. W. Thayer. 1998. Radical oxidation of riboflavin. *Internat. J. Vit. Nutr. Res.* 68:174–180.
- Haaland, D. M., and E. V. Thomas. 1988. Partial Least Squares Methods for Spectral Analyses. 1. Relation to Other Quantitative Calibration Methods and the Extraction of Qualitative Information. *Anal. Chem.* 60:1193–1202.
- Herbert, S., B. Bouchet, A. Riaublanc, D. J. Gallant, and E. Dufour. 1999. Fluorescence spectroscopy investigation of acid- or rennet-induced coagulation of milk. *J. Dairy Sci.* 82:2056–2062.
- Herbert, S., N. Mouhous Riou, M. F. Devaux, A. Riaublanc, B. Bouchet, D. J. Gallant, and E. Dufour. 2000. Monitoring the identity and structure of soft cheeses by fluorescence spectroscopy. *Lait* 80:621–624.
- Kristensen D., V. Orlien, G. Mortensen, P. Brockhoff, and L. H. Skibsted. 2000. Light-induced oxidation in sliced havarti cheese packaged in modified atmosphere. *Int. Dairy J.* 10:95–103.
- Martens, H., and T. Naes. 1989. *Multivariate Calibration*. John Wiley and Son, UK.
- Mazerolles, G., M-F. Devaux, G. Duboz, M-H. Duployer, N. Mouhous Riou, and E. Dufour. 2001. Infrared and fluorescence spectroscopy for monitoring protein structure and interaction changes during cheese ripening. *Lait* 81:509–527.
- Petersen, K., P. V. Nielsen, and M. B. Olsen. 2001. Physical and mechanical properties of biobased materials—starch, polylactate and polyhydroxybutyrate. *Starch/Stärke*, 53:356–361.
- Sattar, A., J. M. deMan, and J. C. Alexander. 1977. Light induced degradation of vitamins. I. Kinetic studies on riboflavin decomposition in solution. *Can. Inst. of Food Sci. Technol. J.* 10(1):61–64.
- Singleton, J. A., W. Aurand, and F. W. Lancaster. 1963. Sunlight flavor in milk. I. A study of components involved in the flavor development. *J. Dairy Sci.* 46(2):1051–1611.
- Skibsted, L. H. 2000. Light-induced changes in dairy products. *BIDFD* 346:4–9.
- Wold, J. P., K. Jørgensen, and F. Lundby. 2002. Nondestructive measurements of light-induced oxidation in dairy products by fluorescence spectroscopy and imaging. *J. Dairy Sci.* 85:1693–1704.
- Wold, S., K. Esbensen, and P. Geladi. 1987. Principal Component Analysis. *Chemometr. Intell. Lab. Syst.* 2:37–52.
- Wold, S. 1978. Cross-validated estimation of number of components in factor and principal components models. *Technometrics*, 20(4):397–405.

Paper V

**Application of Fluorescence Spectroscopy
and Chemometrics in the Evaluation of
Processed Cheese During Storage**

Jakob Christensen, Vibeke T. Povlsen and John Sørensen
Journal of Dairy Science 86 (4), 1101-1107, 2003

Application of Fluorescence Spectroscopy and Chemometrics in the Evaluation of Processed Cheese During Storage

J. Christensen*, V. T. Povlsen*, and J. Sørensen†

*Food Technology, Department of Dairy and Food Science,
The Royal Veterinary and Agricultural University,
Rolighedsvej 30, DK-1958 Frederiksberg C, Denmark

†Arla Foods Innovation, Søderupvej 26, DK-6920 Videbæk, Denmark

ABSTRACT

Front face fluorescence spectroscopy is applied for an evaluation of the stability of processed cheese during storage. Fluorescence landscapes with excitation from 240 to 360 nm and emission in the range of 275 to 475 nm were obtained from cheese samples stored in darkness and light in up to 259 d, at 5, 20 and 37°C, respectively. Parallel factor (PARAFAC) analysis of the fluorescence landscapes exhibits four fluorophores present in the cheese, all related to the storage conditions. The chemometric analysis resolves the fluorescence signal into excitation and emission profiles of the pure fluorescent compounds, which are suggested to be tryptophan, vitamin A and a compound derived from oxidation. Thus, it is concluded that fluorescence spectroscopy in combination with chemometrics has a potential as a fast method for monitoring the stability of processed cheese.

(Key words: cheese, chemometrics, fluorescence spectroscopy, PARAFAC)

Abbreviation key: GC-MS = gas chromatography-mass spectrometry, PARAFAC = parallel factor analysis.

INTRODUCTION

The development of undesirable flavor caused by lipid oxidation and nonenzymatic browning are critical quality factors during storage of processed cheese. The deterioration of the cheese product is dependent on the handling in the post manufacturing processes. Since cheese mainly consists of protein, fat, minerals and water, oxidation is reflected in the composition of these constituents. Monitoring the changes in structure and composition of the cheese constituents, especially protein and fat, will help understand the effect of stress factors

during storage. Common stress factors in the distribution retails and production are light exposure and varying temperature, which can result in reduced shelf life partly due to increased formation of free radicals. Therefore, processed cheese samples stored under different light and heat conditions are investigated in the present study.

Many methods have been developed to shed light on the degree of oxidation of dairy products, a process that consists of several stages. The early stage of lipid oxidation can form hydroperoxides, which normally are measured by HPLC or by evaluation of the peroxide value (Emmons et al., 1986). Secondary oxidation products can be analyzed by static or dynamic headspace GC-MS (Sunesen et al., 2002) or methods using thiobarbituric acid (Kristensen et al., 2001). Methods based on electron spin resonance spectrometry were recently suggested for monitoring the formation of radicals during the oxidation of processed cheese (Kristensen and Skibsted, 1999). All these methods for evaluation of the oxidative levels of dairy products have in common, that they are destructive and time consuming. In this study, the potential of front face fluorescence, measured directly on the cheese surface were investigated, as an alternative, fast and nondestructive method. Theoretically the potential of fluorescence seems sound, since the cheese product contains well known fluorescent compounds in form of aromatic amino acids, vitamin A and riboflavin (Duggan et al., 1957), which all have been reported to be affected during structural changes in cheese (Dufour et al., 2001) or during light and heat exposure (Kristensen et al., 2001; Whited et al., 2002; Wold et al., 2002).

Fluorescence spectroscopy is a sensitive, rapid and noninvasive analytical technique that can provide information on the presence of fluorescent molecules and their environment in all sorts of biological samples. The development and improvement of chemometric methods (Bro, 1996; Bro, 1997; Andersson and Bro, 2000) combined with the technical and optical development of spectrofluorometers have in recent years increased the possibilities for the use of fluorescence spectroscopy.

Received September 2, 2002.

Accepted October 25, 2003.

Corresponding author: Jakob Christensen; e-mail: jach@kvl.dk.

Thus, online monitoring sensors that enable measurements of complete excitation emission spectra (fluorescence landscapes) are now commercially available.

In the last years, a few studies have focused on the potential of using front face fluorescence of dairy products without any pretreatment of the samples. Previously heat treatment and structural changes during coagulation have successfully been investigated in milk using fluorescence spectroscopy (Dufour and Riaublanc, 1997; Birlouez-Aragon et al., 1998; Herbert et al., 1999). Changes in fat and protein composition and structure have been characterized by the means of measuring the tryptophan and vitamin A fluorescence of cheeses during ripening (Dufour et al., 2000; Mazerolles et al., 2001) and for identification of different cheeses at a molecular level (Dufour et al., 2000; Herbert et al., 2000). Wold et al. (2002) demonstrated the potential of fluorescence spectroscopy for measuring the light-induced oxidation, ascribed to the photodegradation of riboflavin.

Common to all these studies is that basic chemometric tools like Principal Component Analysis and Partial Least Squares Regression are applied for the evaluation of single excitation or emission fluorescence spectra. The multivariate approach increases the extracted information and is very useful when handling the fluorescence signal of complex food products. Even more information can be obtained, if the fluorescence measurements are not limited to single emission or excitation spectra. The possibilities when measuring whole fluorescence landscapes (excitation emission matrices) will be investigated here. New chemometric methods (Andersson and Bro, 2000) make it possible to handle fluorescence landscapes keeping the 2-dimensional data structure of each measurement. The techniques are known as N-way or multiway chemometrics, and in the case of fluorescence signals, a 3-way (samples \times excitation \times emission) data analysis is an obvious choice. The advantage of the multiway analysis is that one can utilize the original and true structure in data, which can stabilize the decomposition of the data, and potentially increase the interpretability (Bro, 1996; Bro, 1997).

In the present study Parallel Factor analysis (**PARAFAC**) (Bro, 1997) is applied on the fluorescence landscapes of processed cheese exposed to light and varying temperature during storage. PARAFAC analysis of fluorescence data is previously used with success on model system of mixtures of fluorophores and in other food applications like sugar and fish (Bro, 1999; Baunsgaard et al., 2000a; Baunsgaard et al., 2000b; Pedersen et al., 2002) to investigate the present fluorescent compounds in complex matrices. PARAFAC is based on the decomposition of the fluorescence data represented in a

three-way array, into a few spectral loadings expressing the common structure of the data. The feature of PARAFAC is that the retrieved loading spectra can be directly related to the original fluorescence characteristics of the present fluorophores, which means that the emission and excitation maximum of the loadings can be used in the interpretation and identification of the fluorophores (Bro, 1997).

Thus, the overall objective of the present investigation is to use multivariate analysis on fluorescence spectra keeping the 3-dimensional structure and extract information about the product at hand regarding age and storage conditions. This is pursued by using a non-destructive and rapid high-sensitive fluorescence method, which is simple to perform, and does not involve sample preparation.

MATERIALS AND METHODS

Processed Cheese: Product and Storage Conditions

The product and storage conditions are identical to the experimental plan used by Kristensen et al., 2001. A batch of processed cheese spread samples (density approximately 1.1 g/mL) with 65% fat in dry matter was obtained from Arla Foods aamba, Denmark. The processed cheese was produced according to standard production of processed cheese and was constituted of bovine milk, starter culture, salt and emulsifier. After production the product was filled without any headspace (140 g) in transparent glass containers and sealed with a metal lid. The samples were stored for 10 months at three temperatures 5, 20, and 37°C and were exposed by placing the samples at a distance of approx. 55 cm from a fluorescent lamp or protected from light by wrapping the glass container in tin foil. The light source was fluorescent tubes (Phillips TLD 18/83 W) with a light intensity of 2000 lx as measured by a Topcon IM-1 illumination meter (Tokyo Kogaku Kikai K.K.). Samples were taken out at the beginning of the experiment and then after 14, 28, 56, 84, 112 and 256 d. Only the 1 cm outer layer which had been in contact with the wall of the containers were used and each of the samples were taken from the glass jars by breaking the original seal prior to freezing at -80°C. The samples were frozen for a year before being thawed. Two cheese samples from each treatment were withdrawn for each analysis time.

Fluorescence Spectroscopy and Sampling

All samples were measured on a Perkin-Elmer LS 50B spectrometer equipped with a Front Surface Accessory and controlled with FLDM software. The stored cheese samples were mixed thoroughly before spread-

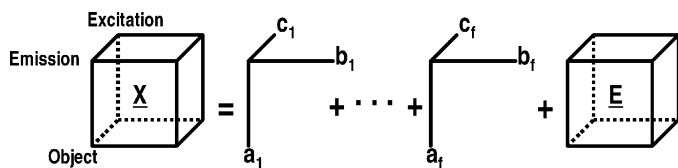


Figure 1. Illustration of the decomposition scheme into f number of components of the PARAFAC model for the data array $\underline{\mathbf{X}}$. The cube $\underline{\mathbf{E}}$ represents the residual.

ing directly onto the quartz window of a powder cell, which was then assembled and placed in the light path in an angle of around 60°. The spectral range of the experiment was selected upon an exploratory basis. A preliminary investigation measuring excitation wavelengths from 200 to 600 nm, and emission wavelengths from 220 to 800 nm on different cheeses were performed, and resulted in focusing on excitation wavelengths in the UV region. Strong fluorescence signals were obtained from the cheese samples in this area, leaving no signal from higher excitation and emission wavelengths when using this technique and set-up. The selected spectral range of the excitation wavelength was 240 to 360 nm with 20 nm intervals. Emission was obtained for every nm from 275 to 475 nm. The slit width was 6 nm for excitation and 5 nm for the emission and a 1% attenuation filter was used.

It should be noted that the selected spectral range does not cover riboflavin fluorescence, which exhibit emission around 520 nm (Duggan et al., 1957), despite it would be an obvious compound to monitor throughout storage. However, the preliminary studies on cheese samples showed that no detectable signal was obtained in this spectral area when using the described measuring set-up.

Data Analysis—PARAFAC

PARAFAC decomposes the fluorescence spectra, into tri-linear components according to the number of fluorophores present the cheese samples (objects). The number of fluorophores present in the samples is equal to the minimal number of factors ($f = 1, \dots, F$) needed to describe the fluorescence matrix $\underline{\mathbf{X}}$.

A graphical illustration of the decomposition of the data array $\underline{\mathbf{X}}$ is given in Figure 1. The object mode is expressed by the A-scores (a_1, \dots, a_f) and the two spectral loadings excitation and emission are expressed as B loadings (b_1, \dots, b_f) and C loadings (c_1, \dots, c_f), respectively. The loadings in a spectral bilinear decomposition reflect the pure spectra of the fluorophores and the true underlying spectra can be recovered in the single components.

The principle behind the PARAFAC decomposition is to minimize the sum of squares of the residual e_{ijk} , see Equation 1.

$$x_{ijk} = \sum_{f=1}^F a_{if} b_{jf} c_{kf} + e_{ijk} \quad [1]$$

$$(i = 1, \dots, I; j = 1, \dots, J; k = 1, \dots, K; f = 1, \dots, F)$$

The element x_{ijk} represents the raw fluorescence excitation/emission spectra ($\underline{\mathbf{X}}$) of the stored cheese, where i is the number of measured samples, j is the number of excitation wavelengths, k is the number of emission wavelengths and f is the number of factors. a_{if} is the object score (magnitude of the fluorophore) for factor f (first mode), b_{jf} is the excitation loading for factor f (second mode), and loading c_{kf} express the emission spectra (third mode). e_{ijk} is the residual ($\underline{\mathbf{E}}$) and contains the variation not captured by the PARAFAC model (Bro, 1997). Split half analysis is suggested for validation of PARAFAC models by Bro (1997). The idea of this strategy is to divide the data set into two halves and make a PARAFAC model on both halves. Due to the uniqueness of the PARAFAC model one will obtain the same result—same loadings in the nonsplit mode e.g., excitation and emission mode—on both datasets, if the correct number of components is chosen.

Calculating the PARAFAC Model

The following sampling was performed: 45 samples \times 2 replicates \times 2 repetitions = 190 samples. Seven samples were removed, as they were considered to be spectral outliers based on a preliminary data inspection and resulted in a total of 183 samples. The preliminary PARAFAC modelling indicated that nonnegativity constraints on all three modes (samples, excitation, and emission) were necessary. Validation of the PARAFAC modelling was performed with split half test, based on replicated samples, i.e. not splitting of the repetitions.

In addition to the split-half experiment, the residuals were inspected, and the results were judged, interpreted and compared with external knowledge.

All calculations were performed in Matlab version 6.1 (MathWorks, Inc.) with the N-way Toolbox (Andersson and Bro, 2000) and the PLS Toolbox (www.Eigen-vector.com).

RESULTS AND DISCUSSIONS

The fluorescence landscapes of two cheese samples are shown in Figure 2. The two samples represent the extremes in the experimental plan, i.e., a fresh cheese sample (a) and a cheese sample stored under the most severe conditions (b). The highest fluorescence peak for

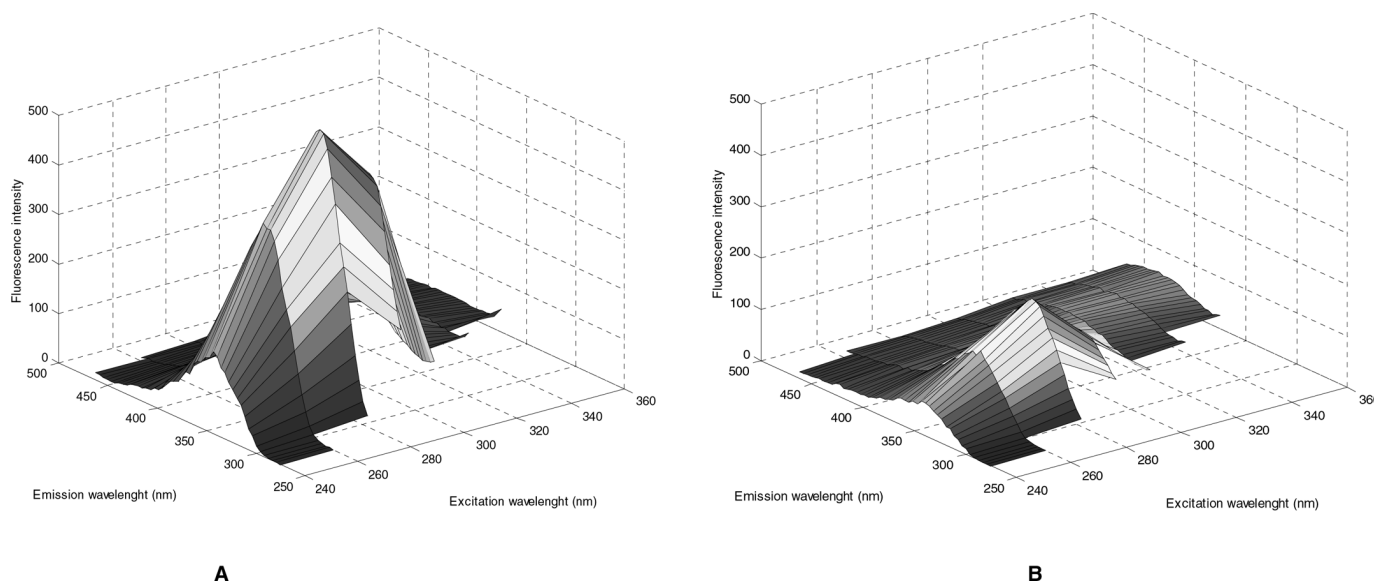


Figure 2. Three dimensional plot of fluorescence landscapes of processed cheese samples. a) fresh cheese sample, and b) cheese sample stored in 259 d at 37°C exposed to light.

both samples is seen with excitation around 280 nm and emission around 350 nm, with a significant higher and apparently broader signal from the fresh cheese. The excitation and emission characteristics indicate that the fluorescence peak corresponds to tryptophan fluorescence, which is reported to have excitation/emission wavelength maximum at 285/365 nm in pure solutions (Duggan et al., 1957), and previously measured in cheese products with excitation 290 nm and emission from 305–400 nm (Herbert et al., 2000; Dufour et al., 2001; Mazerolles et al., 2001). Apart from this major peak, a vague peak is observed in the higher wavelength region with excitation around 320 to 360 nm and emission round 400 to 460 nm, especially for the cheese sample stored for 259 d.

The aforementioned patterns in the fluorescence landscapes were investigated further by the use of PARAFAC analysis with the objective to resolve the fluorescence signal into the contributions of each of the fluorescent compounds present in the set of samples, i.e. estimate the excitation and emission profiles of fluorophores directly from the three-dimensional fluorescence landscapes. PARAFAC models of the fluorescence data were estimated with one to five components, but the four-component model was chosen based on split half analysis (Bro, 1997). A high explained variation of 99.76% is captured by the PARAFAC model, and the resulting PARAFAC components are shown in Figure 3. The model indicates that four different fluorophores are present in the cheese samples with the excitation and emission profiles shown in the figure. The excita-

tion/emission maximum for the two compounds are 300/347 nm and 280/339 nm, respectively, as listed in Table 1. The loading profiles of the second PARAFAC component corresponds quite well with the characteristics of tryptophane, whereas the excitation maximum of the first component seems a little too high for tryptophan. Having the rather low resolution of 20 nm in the excitation mode in mind, and knowing that the fluorescence properties of protein-bound amino-acids are known to be affected by the structure of protein (Lakowicz, 1999), we dare to suggest that the first PARAFAC components is also due to tryptophan fluorescence, but simply shifted due to inclusion to different protein structures.

The score values in the first column of Figure 3 represent the concentration mode for each of the fluorophores, and since the excitation and emission loadings are normalized when calculating the PARAFAC model, the contribution for each of the components can be compared to the overall variation based on the level of the scores. The score values are arranged so the development of the fluorophores easily can be caught throughout the storage time. Looking at the two proposed tryptophan components, a significant decrease is observed throughout the storage period for the samples stored at 37°C. This shows that alterations in the protein structure, monitored by the decrease in tryptophan fluorescence, somehow can reflect the conditions of the cheese samples during storage. The samples exposed to light during storage show a systematically higher tendency to be degraded throughout the storage than the samples stored in the dark. Compared with the

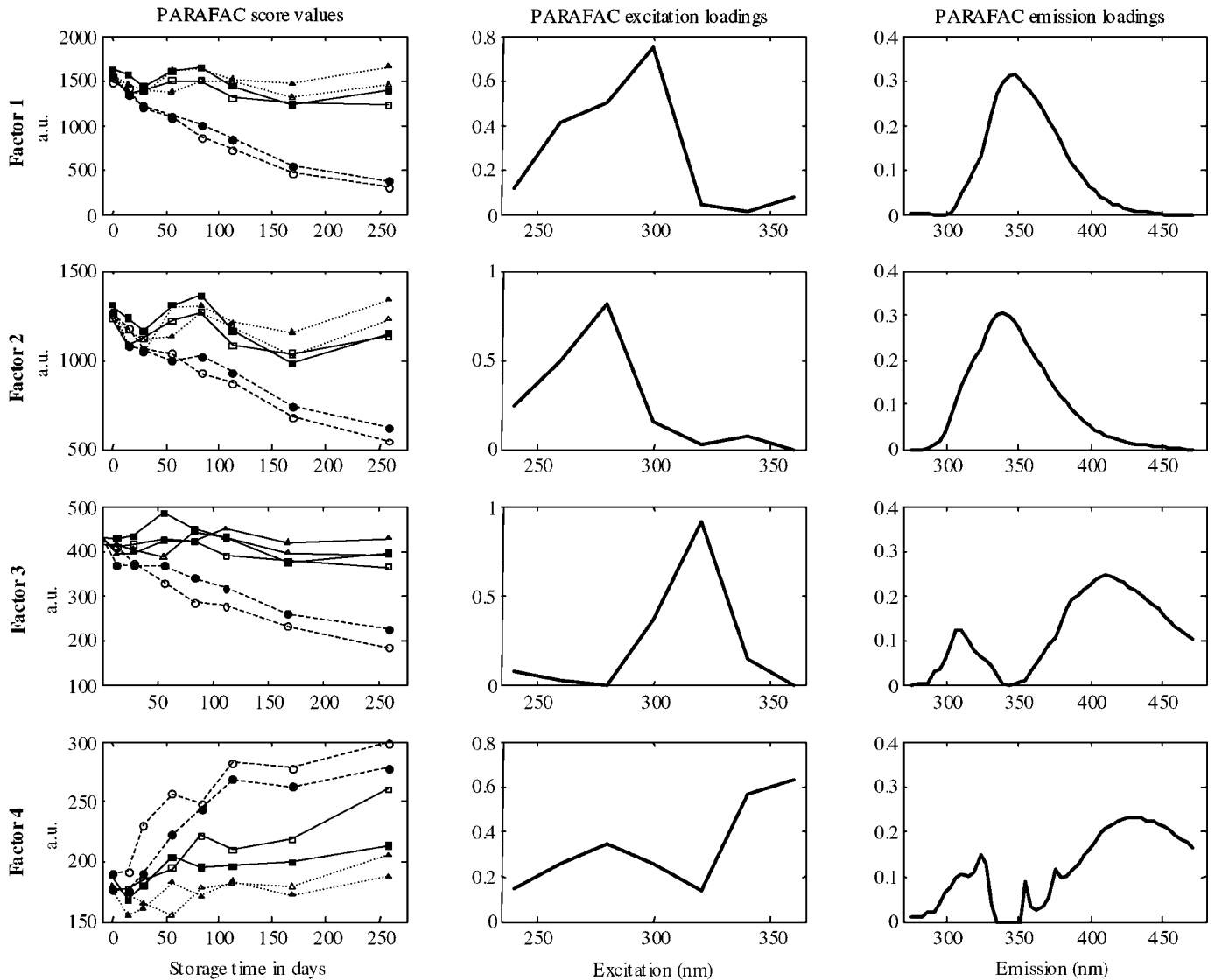


Figure 3. A- (scores), B- (excitation), and C- (emission) loadings of a four component PARAFAC model, based on the fluorescence landscapes of 183 processed cheese samples. Samples stored at 5°C are indicated with triangles, and connected with dotted line (.....). Samples stored at 20 and 37°C are shown with squares and dashed line (---) and circles connected with a full line (—), respectively. Open signs represent samples stored in light, and filled sign illustrates storage in darkness.

effect of different temperatures, the light exposure seems negligible for the two tryptophan components, though. The same storage experiment showed a similar tendency of light exposure having little, if any influence on the browning of cheese (Kristensen et al., 2001), and thereby indicate that the observed differences in the protein structure are somehow related to the browning reaction i.e. the formation of Maillard products from the protein and lipid oxidation products in cheese, even though tryptophan itself may not be part of the browning reaction scheme. As indicated by the first visual inspection of the fluorescence landscapes, the level of the score values for the two first components are much

higher than the third and fourth component, simply showing that the development in the tryptophan signal represents the major variation in the fluorescence data.

The development of the third estimated fluorophore (score values of the third PARAFAC component) shows a similar pattern as the decrease in the tryptophan signal. Thus, the cheese samples stored at 37°C contain less of this component throughout the storage, especially the samples exposed to light during storage. Comparing the fluorescence profiles seen in Figure 3 and the excitation/emission wavelength maximum of 320/411 nm (Table 1) with observed maximum of 325/470 nm in pure solution reported (Duggan et al., 1957) and

Table 1. Excitation and emission maximum of four components in the PARAFAC model of 45 different cheese samples.

Component	λ_{\max} (nm) Excitation	Emission
1	300	347
2	280	339
3	320	411
4	360	431

322/412 nm for dairy products (Dufour et al., 2001; Herbert et al., 2000), vitamin A is an obvious suggestion for the third component. This is underlined by the fact, that the observed decrease in vitamin A fluorescence signal throughout the storage period corresponds well to reported vitamin A degradation during light exposure in dairy products (Whited et al., 2000).

The fourth PARAFAC component reveals an opposite and very interesting trend in the score values, as seen in Figure 3. The level of this fluorophore increases throughout the storage period, especially for the cheese samples stored in light. The excitation and emission loadings look somewhat noisier with several small peaks, probably caused by the fact that the fluorescence signal is very low, as can be seen from the levels of the score values. Scattering effects might be the reason for the extra emission peak observed around 320 nm for both the third and the fourth component. The identification of the fourth fluorescent compound, showing an increase signal during the oxidation of the cheese samples, give rise to more doubt. Taking the increasing concentration of the fourth component throughout storage in consideration, it is obvious to suggest that the fourth component can be attributed to some kind of oxidation product. So-called "Advanced Maillard Products" in milk samples have been reported (Birlouez-Aragon et al., 1998) to excite around 350 nm with emission at 440 nm, which is almost identical to the peak observed in the fourth component. Another suggestion could be that the fourth component is a secondary oxidation product developed when carbonyl compounds produced by lipid oxidation interacts, as reported by Dillard and Tappel (1971) with a fluorescent compound from lipid peroxidation with excitation maximum at 360 nm, and emission maximum at 430 nm, which is even closer to the fluorescent characteristics of the fourth component. Finally, Stapelfeldt and Skibsted (1994), demonstrated that the reaction between secondary lipid oxidation products from milk products and β -lactoglobulin in a model system yielded a fluorescent condensation products with excitation/emission maximum at 350/410 nm, which could also form an educated guess for identification of the fourth PARAFAC component.

CONCLUSIONS

This exploratory study of processed cheese demonstrates the potential of fluorescence spectroscopy and chemometrics applied to the analysis of dairy products. The rapid fluorometric analysis reveals information at a molecular level about the stability of the cheese when exposed to manufacture handling stress like light and temperature changes. PARAFAC analysis provides a unique mathematical decomposition of four fluorescent compounds present in the cheese samples all showing a change in the fluorescence signal corresponding the storage time and the grade of oxidation.

The fluorescent signal from the processed cheese samples is suggested to derive from tryptophan, vitamin A and an oxidation product. Thus, the suggested analytical method provides a fast and simultaneous determination of the fluorescence level of all these compounds. The observed results still remain to be validated with chemical reference analyses in order to proof the identification of the fluorophores, but this investigation certainly underlines the potential of fluorescence spectroscopy in combination with chemometrics, as a fast, nondestructive innovative method, that can be applied to dairy products for monitoring oxidation, screening studies and perhaps in development of new fast quantitative analyses of vitamin A.

ACKNOWLEDGMENTS

This study is partly sponsored by an EU innovation programme, OPUS (IN30905 I), with the aim to adapt and apply advanced fluorescence measurement techniques for online analysis to traditional food industries. Povlsen wish to thank FØTEK 3 (93S-2444-Å01-00100) for financial support. Furthermore the authors wish to thank Joanna Zeppelin and Vibeke Birk from Arla Foods for making this publication possible, and for carrying out all the experimental work. Finally we are grateful to Professor Rasmus Bro for valuable discussion.

REFERENCES

- Andersson, C. A., and R. Bro. 2000. The N-way Toolbox for MATLAB. *Chemometrics Intell. Lab. Syst.* 52:1-4.
- Baunsgaard, D., C. A. Andersson, A. Arndal, and L. Munck. 2000a. Multi-way chemometrics for mathematical separation of fluorescent colorants and colour precursors from spectrofluorimetry of beet sugar and beet sugar thick juice as validated by HPLC analysis. *Food Chem.* 70:113-121.
- Baunsgaard, D., L. Munck, and L. Norgaard. 2000b. Analysis of the effect of crystal size and color distribution on fluorescence measurements of solid sugar using chemometrics. *Appl. Spec.* 54:1684-1689.
- Birlouez-Aragon, I., M. Nicolas, A. Metais, N. Marchond, J. Grenier, and D. Calvo. 1998. A rapid Fluorimetric Method to estimate the heat treatment of liquid Milk. *Int. Dairy J.* 8:771-777.

- Bro, R. 1996. Multi-way Calibration Multi-Linear PLS. *J. Chemometrics*. 10:47–62.
- Bro, R. 1997. PARAFAC. Tutorial and applications. *Chemometrics Intell. Lab. Syst.* 38:149–171.
- Bro, R. 1999. Explorative study of sugar production using fluorescence spectroscopy and PARAFAC analysis. *Chemometric Intell. Lab. Syst.* 46:133–147.
- Dillard, C. J., and A. L. Tappel. 1971. Fluorescent Products of Lipid Peroxidation of Mitochondria and Microsomes. *Lipids*. 6:715–721.
- Dufour, E., M. F. Devaux, and S. Herbert. 2001. Delineation of the structure of soft cheeses at the molecular level by fluorescence spectroscopy—relationship with texture. *Int. Dairy J.* 11:465–473.
- Dufour, E., G. Mazerolles, M. F. Devaux, G. Duboz, M. H. Duployer, and N. M. Riou. 2000. Phase Transition of triglycerides during semi-hard cheese ripening. *Int. Dairy J.* 10:81–93.
- Dufour, E., and A. Riaublanc. 1997. Potentiality of spectroscopic methods for the characterisation of dairy products. I. Front-face fluorescence study of raw, heated and homogenised milks. *Lait* 77:657–670.
- Duggan, D. E., R. L. Bowman, B. B. Brodie, and S. Udenfriend. 1957. A Spectrophotofluorometric Study of Compounds of Biological Interest. *Arch. Biochem. and Biophys.* 16:1–14.
- Emmons, D. B., G. J. Paquette, D. A. Froehlich, D. C. Beckett, H. W. Modler, G. Butler, Brackenbridge, and G. Daniels. 1986. Oxidation of butter by low intensities of fluorescent light in relation to retail stores. *J. Dairy Sci.* 69:2437–2450.
- Herbert, S., A. Riaublanc, B. Bouchet, D. J. Gallant, and E. Dufour. 1999. Fluorescence Spectroscopy Investigation of Acid- or Rennet-Induced Coagulation of Milk. *J. Dairy Sci.* 82:2056–2062.
- Herbert, S., N. M. Riou, M. F. Devaux, A. Riaublanc, B. Bouchet, D. J. Gallant, and E. Dufour. 2000. Monitoring the identity and the structure of soft cheeses by fluorescence spectroscopy. *Lait*. 80:621–634.
- Kristensen, D., E. Hansen, A. Arndal, R. A. Trinderup, and L. H. Skibsted. 2001. Influence of light and temperature on the colour and oxidative stability of processed cheese. *Int. Dairy J.* 11:837–843.
- Kristensen, D., and L. H. Skibsted. 1999. Comparison of Three Methods Based on Electron Spin Resonance Spectrometry for Evaluation of Oxidative Stability of Processed Cheese. *J. Agric. Food Chem.* 47:3099–3104.
- Lakowicz, J. R. Protein fluorescence. Pages 446–485 in *Principles of fluorescence spectroscopy*. Kluwer Academic/plenum Publishers, New York.
- Mazerolles, G., M. F. Devaux, G. Duboz, M. H. Duployer, N. M. Riou, and E. Dufour. 2001. Infrared and fluorescence spectroscopy for monitoring protein structure and interaction changes during cheese ripening. *Lait*. 81:509–527.
- Pedersen, D. K., L. Munck, and S. B. Engelsen. 2002. Screening for dioxin contamination in fish oil by PARAFAC and N-PLSR analysis of fluorescence landscapes. *J. Chemometrics*. In press.
- Stapelfeldt, H., and L. H. Skibsted. 1994. Modification of β -lactoglobulin by aliphatic aldehydes in aqueous solution. *J. Dairy Res.* 61:209–219.
- Sunesen, L. O., P. Lund, J. Sørensen, and G. Hølmer. 2002. Development of volatile compounds in processed cheese during storage. *Lebensmittel-Wissenschaft Und-Technologie*. 35:128–134.
- Whited, L. J., B. H. Hammond, K. W. Chapman, and K. J. Boer. 2002. Vitamin A Degradation and Light-Oxidized Flavor Defects in Milk. *J. Dairy Sci.* 85:351–354.
- Wold, J. P., K. Jørgensen, and F. Lundby. 2002. Nondestructive Measurement of Light-induced Oxidation in Dairy Products by Fluorescence Spectroscopy and Imaging. *J. Dairy Sci.* 85:1693–1704.